Pharmacometric modelling of haemodynamics in humans

Salma Mohamed Bahnasawy

A dissertation submitted for the degree of

Master of Pharmacy (by research only)

at the University of Otago

Department of Pharmacy, University of Otago, Dunedin, New Zealand

September 2020

ABSTRACT

Current pharmacokinetic-pharmacodynamic models describing changes to the haemodynamic system often do not include necessary feedback mechanisms. These models often provide adequate empirical description of data but may fail to adequately extrapolate to additional scenarios. This study aimed to develop a minimal model to describe the short-term changes of haemodynamics that can be used as the basis for future model development. The model was used to describe the haemodynamic effects of sodium nitroprusside (SNP) in adolescents undergoing surgery.

A minimal haemodynamic model was developed to describe the influence of drugs on blood pressure components. The model structure was defined based on known mechanisms and previously published models. The model parameters were calibrated to describe (without estimation) the heamodynamics of two antihypertensive drugs with data extracted from the literature. Structural identifiability analysis was done using various combinations of the observed variables. The model was applied to clinical data from patients receiving SNP infusion. The model was extended to accommodate the postulated mechanism of action of SNP in the literature.

The proposed model structure included mean arterial pressure (MAP), heart rate (HR), and stroke volume and was composed of four states described by differential equations. Model evaluation showed flexibility in describing haemodyanmics at different target perturbations. Overlay plots of model predictions and literature data showed a good description without data fitting. The structural identifiability analysis revealed all model parameters and initial conditions were identifiable only when HR, MAP, and cardiac output were measured together. In addition, model evaluation using SNP data suggested its mechanistic plausibility and the flexibility to describe various response patterns elicited by SNP

A minimal model of the haemodynamic system was developed and evaluated. The model accounted for short-term haemodynamic feedback processes. We propose that this model can be used as the basis for future pharmacometric analyses of drugs acting on the haemodynamic system.

Dedicated to my Dad,

I wish you could have been here. May Allah bless your soul and may you be in a better place now.

ACKNOWLEDGMENTS

All my gratitude to my creator, to *Allah* for His invaluable bounties, for guiding me to this path, and showing me the light in the tough time; *"And he to whom Allah has not granted light - for him there is no light."* **Surah An-Nur [24:40]**.

I am thankful to my supervisors Dr Hesham Al-Sallami and Professor Stephen Duffull, for making this a rich experience to change my professional path. I owe you for introducing me to this critical field of pharmacometrics, and helping me to grow up professionally and personally.

I want to acknowledge Professor Jeffrey Barrett, *Bill & Melinda Gates Medical Research Institute, Cambridge,* and Professor Nick Holford, *University of Auckland,* for providing the clinical dataset of sodium nitroprusside in paediatrics used in the current analysis, and sharing their KPD model code. I am thankful to Professor Mats Karlsson, *Uppsala University,* for contributing in the discussions on my modelling project during his sabbatical leave at the Otago Pharmacometrics group.

My deep gratitude to my lab mates at the Otago Pharmacometrics group and Dr Dan Wright. I was so lucky to have such a good company and warm environment during my stay here. I have learnt a lot from you all and enjoyed our scientific discussions, your support, coffee breaks, badminton time, and of course food. My special thanks to Qing Xi, Vijay, Sudeep, Derek, Jaydeep, Lisa, Isabelle, Sepi, Klarissa,.

I cannot express how I was blessed throughout this experience with the friends I gained who were my second family in New Zealand. I am indebted to you all for your unconditional support and opening your hearts *'before your homes'* to me. Thanks to Shaikha, Alejandra, Sharon, Izyan, Alika, Mary, Dr Adel, Mona, Dr Mohamed, Lamia, Dina, Amira.

To my friends and colleagues back home and around the world, who always teach me that distance cannot separate minds or souls. I would not have been able to see the light throughout *'not just at the end of'* the tunnel without your words. To Eman El Awady, Sara Azab, Mona Ghazy, Eman Ibrahim; thanks for being in my life. To Dr Ahmed Hamed Salem, *director of clinical pharmacology & pharmacometrics at AbbVie,* who was the first one to introduce me to the foreign word of '*Pharmacometrics*' years ago; I am thankful for your constant encouragement to pursue my career in this field.

Finally, to my little family back home, I am forever indebted to my beloved mum, who always brings life to my life and gives me the motive to be. Thank you for bringing me up to follow my intuition and to be genuinely who I am. To my wonderful sister and best friend Menna, who empowers me to keep going even when I feel like losing my track. I am blessed to have you in my life.

PUBLICATIONS

THAT HAVE ARISEN FROM WORK ASSOCIATED WITH THIS THESIS

Accepted for publication

- **Salma Bahnasawy**, Hesham Al-Sallami, Stephen Duffull. "*A minimal model to describe short-term haemodynamic changes of the cardiovascular system*". British Journal of Clinical Pharmacology (BJCP)

Oral Presentations

- **Salma Bahnasawy**, Hesham Al-Sallami, Jeffrey Barrett, Stephen Duffull. *"An ePKPD model for sodium nitroprusside in adolescents"* .The 20th annual Population Approach Group in Australia and New Zealand (PAGANZ), Auckland, New Zealand, 2019

TABLE OF CONTENTS

List Of Figures

List Of Tables

List Of Abbreviations

AAP	The American Academy of Pediatrics
ACE	Angiotensin-converting enzyme
ADH	Antidiuretic hormone
ADME	Absorption, distribution, metabolism, and excretion
BP	Blood pressure
BR	Baroreceptor reflex
BSV	Between subject variability
BTP	Blinded treatment phase
CNS	Central nervous system
CO	Cardiac output
CV	Coefficient of variation
CVS	Cardiovascular system
DBP	Diastolic blood pressure
FUP	Follow-up phase
HR	Heart rate
IPRED	Individual prediction
KPD	Kinetic-pharmacodynamic
MAP	Mean arterial pressure
NIH	National Institutes of Health
NO	Nitic oxide
ODE	Ordinary differential equation
OFV	Objective function value
OTP	Open-label treatment phase
PBPK	Physiologically based pharmacokinetic modelling
PD	Pharmacodynamics
PK	Pharmacokinetics
PKPD	Pharmacokinetics and pharmacodynamics
PP	Pulse pressure
PRA	Plasma renin activity
PRED	Population prediction
QSP	Quantitative Systems Pharmacology
RAAS	Renin-angiotensin-aldosterone system
RAP	Right atrial pressure
RSE	Relative standard error
RUV	Residual unexplained variability
SA	Sinoatrial node
SBP	Systolic blood pressure
SD	Standard deviation
SNP	Sodium nitroprusside

SV	Stroke volume
TPR	Total peripheral resistance
VPC	Visual predictive check
pcVPC	Prediction-corrected visual predictive check

Aims and structure of the thesis

The overarching aim of this thesis was to apply pharmacometric methods to quantitatively describe and predict the cardiovascular haemodynamics in humans and to show the applications of a haemodynamic model to clinical data.

The specific aims were to:

I. Develop a semi-mechanistic model to describe the haemodynamics of the cardiovascular system in humans (chapter 2).
II. Extend the developed model to model the haemodynamic effects of sodium nitroprusside in adolescents undergoing surgery (chapter 3).

The thesis has been divided into four chapters:

- Chapter 1

  This provides an introduction to the thesis. This chapter has four sections

  I. Section 1.1 includes a review of the physiology of the cardiovascular haemodynamics in humans
  II. Section 1.2 includes a review of the current state of knowledge of published models that provided a quantitative description of the haemodynamics of the cardiovascular system.
  III. Section 1.3 includes a review of the pharmacology of sodium nitroprusside and its clinical uses.
  IV. Section 1.4 includes a review of the pharmacometric methods applied in the current thesis

- Chapter 2

  This focuses on the development of a minimal model to describe haemodynamics in humans. It also covers model evaluation using published clinical data and an analysis of model identifiability.

- Chapter 3

  In this chapter, the developed model in chapter 2 is extended to model clinical data of nitroprusside when used in adolescents. The chapter includes a description of the data and the modelling steps.

- Chapter 4

This chapter provides a discussion of the results of chapters 2 and 3 in addition to concluding remarks.

CHAPTER 1: INTRODUCTION

1.1 Cardiovascular haemodynamics

Cardiovascular haemodynamics is the study of blood flow through the cardiovascular system (CVS) and the factors governing it. These factors include blood pressure (BP) and the resistance to this flow (Klabunde, 2012).

1.1.1 Blood pressure (BP)

Blood pressure (BP) is the tension within the blood vessel wall, resulting from blood flow through the lumen within the major arterial system of the body (Walker HK et al., 1990, Adelmann, 2011). BP is measured in millimetres of mercury (mmHg).

Blood flows throughout the CVS by means of the heart pumping force and pressure differences throughout the vasculature. Hence, BP is not the same in all types of blood vessels; otherwise the blood will not flow. These differences can be mainly explained by the different compliance profiles of different blood vessels (Costanzo, 2018). An illustration of the differences in BP throughout different blood vessels is represented in Figure 1 .

Each cycle of pulsation of arterial BP during systole and diastole coincides with one cardiac cycle. The arterial BP is usually described by the systolic blood pressure (SBP) and diastolic blood pressure (DBP).

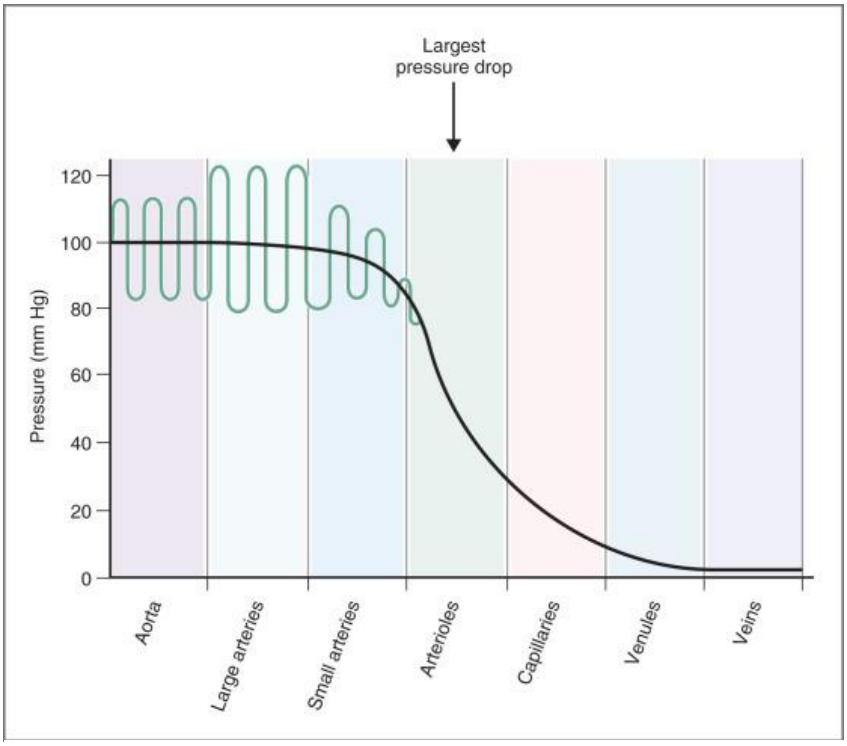

Figure 1 Blood pressure profile in the vasculature. Black line represents the mean arterial pressure, green line represents the systolic and diastolic blood pressure (Costanzo, 2018)

1.1.1.1 Systolic blood pressure (SBP)

It represents the maximum aortic blood pressure, which is achieved during cardiac contraction due to the pressure exerted on the vascular wall by the ejected stroke volume (SV).

1.1.1.2 Diastolic blood pressure (DBP)

It represents the lowest aortic blood pressure achieved after ventricular contraction when the cardiac chambers are filling. It provides the driving pressure for continuous blood flow to the peripheral tissues as the ventricles are refilled with blood for the next contraction (Cheng and Jusof, 2018, DiPiro, 2011).

1.1.1.3 Mean arterial pressure (MAP)

It represents the average arterial pressure throughout the cardiac cycle of contraction and reflect the degree of organ perfusion. It is worth noting that the mean arterial pressure (MAP) is not the BP halfway between the diastolic and systolic pressures because the duration of diastole is longer than the duration of systole in a normal cardiac cycle (Sparks and Rooke, 1987).

During a cardiac cycle, two thirds of the time is spent in diastole and one third in systole. Hence, the value for the mean pressure (geometric mean) is less than the arithmetic average of the systolic and diastolic pressures (*Figure 2*). That is why at normal resting heart rates, MAP can be calculated from the SBP and DBP using the following equation (Klabunde, 2012)

$$MAP \cong \left(\frac{1}{3} \cdot SBP\right) + \left(\frac{2}{3} \cdot DBP\right)$$

Alternatively, it can be expressed as,

$$MAP \cong DBP + \frac{1}{3}\,(SBP - DPB) \cong DBP + \frac{1}{3} \cdot PP$$

where PP is the pulse pressure.

At high heart rates (HR), MAP is more closely approximated by the arithmetic mean of SBP and DBP as the aortic pulse wave becomes shorter where the duration of diastole shortens more than does systole. Different formulas have been developed to account for HR changes for MAP calculation;

$$MAP \cong DBP + 0.01 \cdot \exp\left(4.14 - \frac{40.74}{HR}\right) \cdot PP$$ (Moran et al., 1995)

$$MAP \cong DBP + (0.33 + 0.0012 \cdot HR) \cdot PP$$ (Razminia et al., 2004)

To determine MAP with absolute accuracy, MAP can be measured using an indwelling arterial catheter. However, in normal clinical practice, SBP and DBP are more commonly measured, rather than MAP, due to the invasiveness of the used technique (Klabunde, 2012).

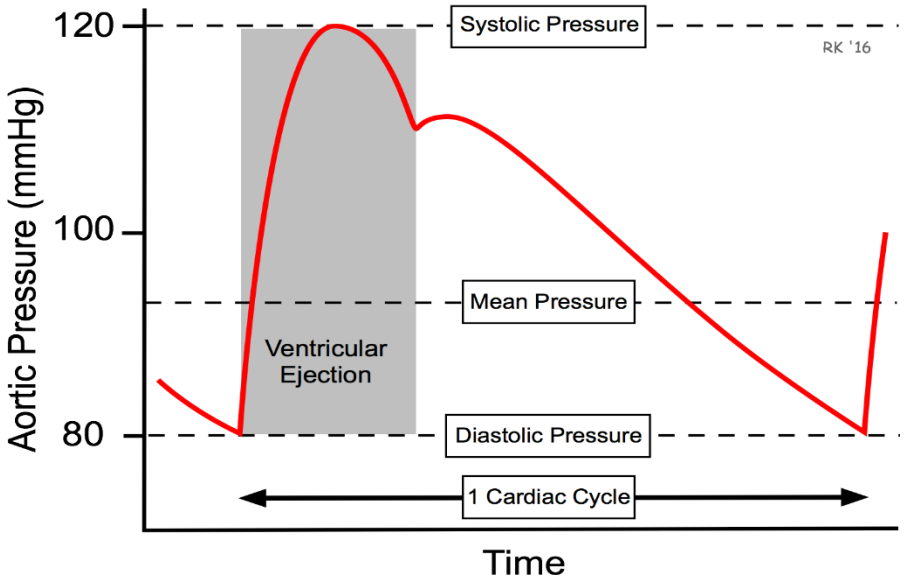

Figure 2 Aortic pulse wave during one cardiac cycle (Klabunde, 2012)

1.1.1.4 Pulse pressure

The pulse pressure (PP) reflects the pulsatile component of BP estimated by the difference between SBP and DBP. PP provides a better prognostic sensitivity in cardiovascular risk stratification and arterial stiffness at older age relative to MAP, which could show a slight change, keeping it within the normal range (Selvaraj et al., 2016). For instance, in a normal individual with BP 120/80 mmHg, the PP will be 40 mmHg, and MAP equal to 93 mmHg, while in a patient with arterial stiffness having BP 140/65 mmHg, PP is increased to 75 mmHg, whereas MAP will be 90 mmHg (Franklin and Wong, 2016).

PP can be used as an indicator of stroke volume (SV), when other factors are constant, based on the relationships between pressure, volume, and compliance expressed as,

$$C = \frac{\Delta V}{\Delta P}$$

, where C: vascular compliance, ΔV: the change in volume, ΔP: the change in pressure

Assuming that arterial compliance is constant in healthy adult, the change in arterial pressure, which is represented by *PP*, would depend on the change of blood volume in the artery at any moment in time, which is reflected by *SV* (Costanzo, 2018). Factors affecting PP are summarised in Figure 3.

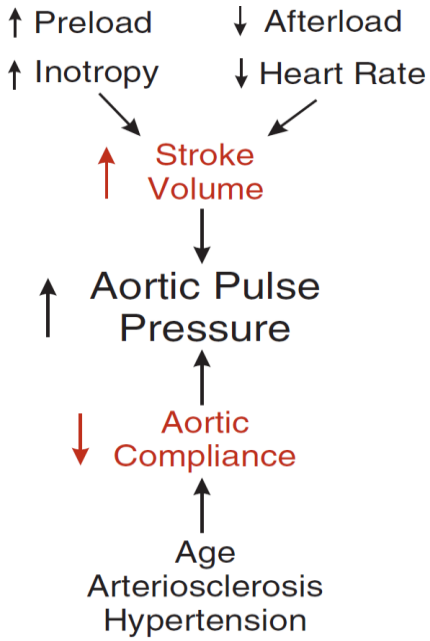

Figure 3 Factors affecting aortic pulse pressure. (Klabunde, 2012)

However, it is important to point out that although there is a strong correlation between PP and SV, it is not a linear relationship (Soltesz, 2018). Bighamian et al. reported that the relative change in arterial pulse pressure due to a left ventricular blood volume perturbation was consistently smaller than the corresponding relative change in SV, due to the nonlinear left ventricular pressure-volume relation during diastole. This in turn reduces the sensitivity of arterial PP to perturbations in the left ventricular blood volume. Therefore, arterial PP must be used with care when used as a surrogate for SV (Bighamian and Hahn, 2014).

1.1.2 Vascular compliance

Vascular compliance describes the volume of blood the vessel can hold at a given pressure and it is related to distensibility of blood vessel. This in turn implies that the higher the compliance of a vessel, the more volume it can hold at a given pressure. Figure 4 shows the compliance profile of arteries and veins where arteries are shown to have a much lower compliance than that of the veins, which is represented by lower slope of the curve**.** In other words, at a certain pressure, arteries hold much less blood than the veins. This may provide explanation why arterial pressure is much higher compared to venous pressure.

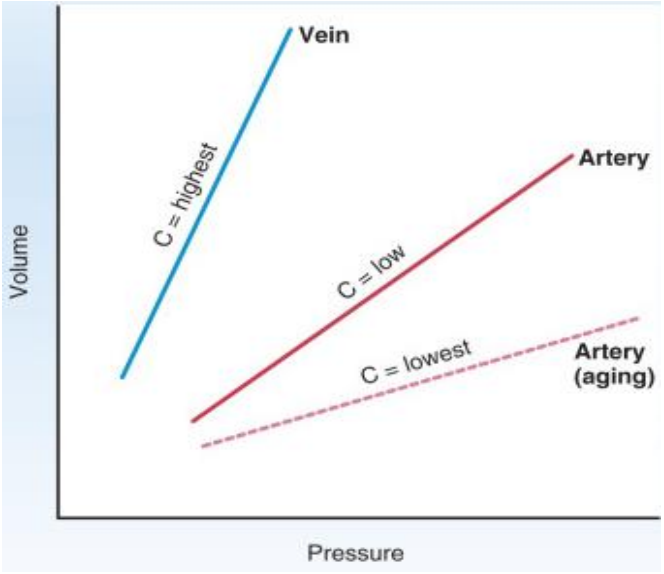

Figure 4 Vascular compliance of arteries and veins (Costanzo, 2018)

The volume of blood in veins is called the unstressed volume (large volume under low pressure). While, the arteries are much less compliant and contain the stressed volume (low volume under high pressure). The total volume of blood in the cardiovascular system is the sum of the unstressed volume plus the stressed volume (plus whatever volume is contained in the heart) (Costanzo, 2018).

1.1.3 Factors controlling blood pressure

Blood flow through a blood vessel is determined by two factors: the pressure difference between the inlet and the outlet of the vessel, and the resistance of the vessel to blood flow.

The relationship of flow, pressure, and resistance is analogous to the relationship of current (I), voltage (ΔV), and resistance (R) in electrical circuits, as expressed by Ohm's law

(Ohm's law states that $\Delta V = I \times R$ or $I = \Delta V/R$). Blood flow is analogous to current flow, the pressure difference or driving force is analogous to the voltage difference, and hydrodynamic resistance is analogous to electrical resistance. The equation for blood flow is expressed as follows:

$$Q = \frac{\Delta P}{R}$$

Where Q; flow ($mL \cdot min^{-1}$) which can be represented by cardiac output (CO), ΔP; pressure difference (mmHg) which can be represented by arterial and venous pressure, R; resistance ($mmHg \cdot mL^{-1}$ per min) which can be represented by total peripheral resistance (TPR). So, it can be written in this way

$$CO = \frac{MAP - RAP}{TPR}$$

Where CO; cardiac output ($ml \cdot min^{-1}$), MAP; mean arterial pressure (mmHg), RAP; right atrial pressure (mmHg), TPR; total peripheral resistance ($mmHg \cdot min \cdot ml^{-1}$)

Since RAP is small and does not change markedly under most conditions, the usual expression of these relations becomes

$$CO = \frac{MAP}{TPR}$$

Then, MAP can be described as

$$MAP = CO \cdot TPR$$

Hence, Arterial BP is haemodynamically generated by the interplay between the cardiac output and the resistance to blood flow (Tarazi et al., 1989).

1.1.3.1 Total peripheral resistance (TPR)

The total peripheral resistance (TPR) represents the total resistance to the blood flow throughout the vasculature because of friction within the blood and between the blood and vessel walls. Most of the TPR is caused by the arteriolar resistance, because arterioles are the primary resistance vessels (Sherwood, 2015).The diameter of blood vessels and blood viscosity are the main factors governing the TPR. The total resistance of a set of blood vessels depends on the arrangement of the blood vessels, as illustrated in Figure 5. Vasoconstriction increases resistance while vasodilation decrease the resistance (Hill et al., 2013).

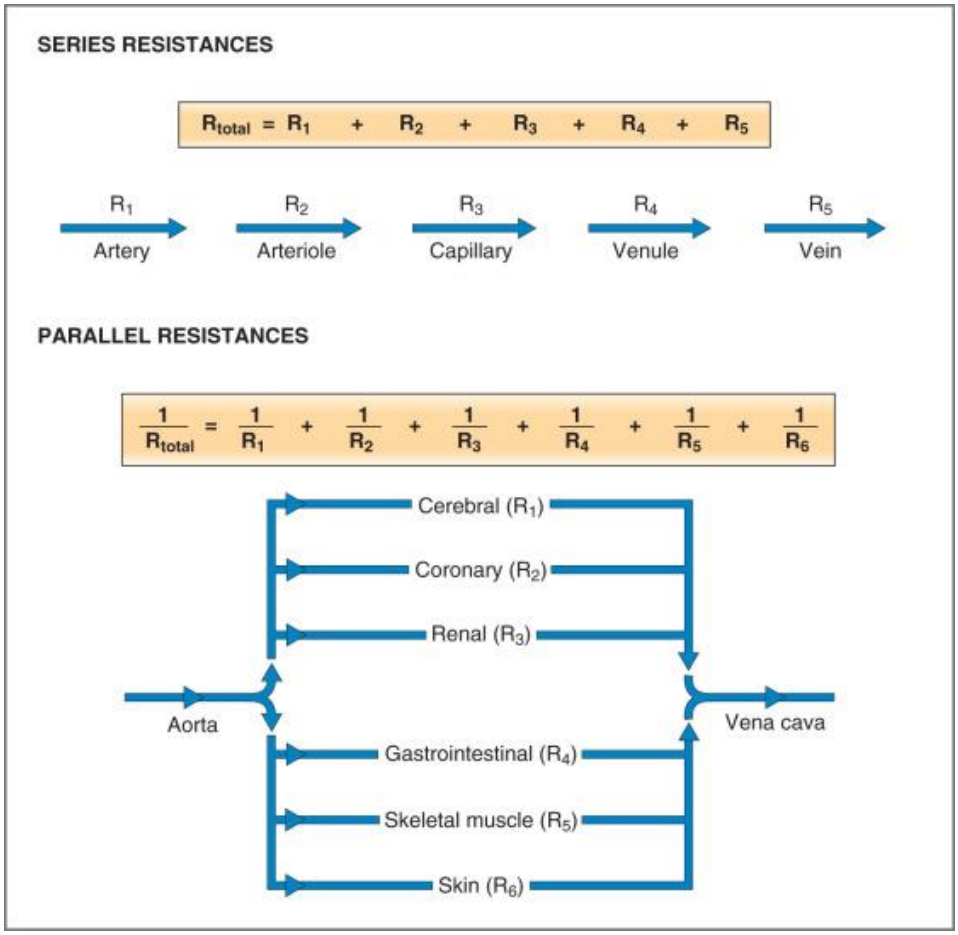

Figure 5 Resistance of blood vessels (Costanzo, 2018)

1.1.3.2 Cardiac output

The cardiac output (CO) is the total volume ejected by each ventricle per unit time. Normally, the volume of blood flowing through the pulmonary circulation is the same as the volume flowing through the systemic circulation. Hence, the CO is almost the same from the two ventricles, with minor variations.

The CO depends on the volume ejected on a single beat (stroke volume) and the number of beats per minute (heart rate) (see Figure 6). It can be represented as,

$$CO = HR \cdot SV$$

, where HR: beats per minute (beats·min^{-1}), SV: Volume ejected in one beat (mL)

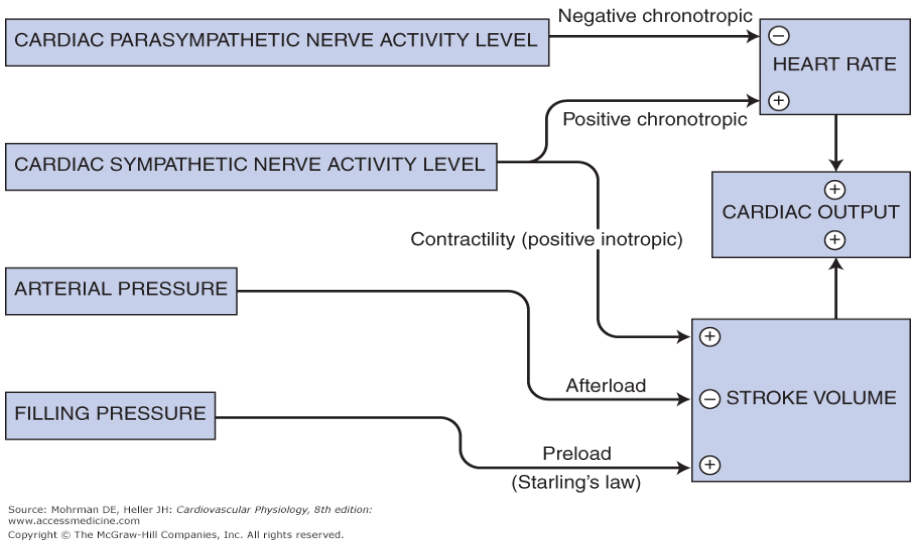

Figure 6 Summary of determinants of cardiac output (Mohrman and Heller, 2014)

1.1.3.2.1 Heart rate

The heart rate (HR) represents the number of heartbeats per minute. The average resting HR is 70 beat per minute. The HR is regulated mainly by the sinoatrial node (SA), which is considered the pacemaker of the heart. The balance between parasympathetic inhibition of the SA node through the vagal nerve and stimulation by the cardiac sympathetic nerves is the primary determinant of the HR. Concurrent increased sympathetic and decreased parasympathetic activity cause the HR to increase, whereas the HR goes down with the simultaneous rise in parasympathetic activity and decline in sympathetic activity (Sherwood, 2015).

1.1.3.2.2 Stroke volume

Stroke volume (SV) is the volume of blood ejected per beat by the left ventricle into the aorta, or from the right ventricle into the pulmonary artery. It can be estimated as the difference between the ventricular end-diastolic volume (EDV) and the end-systolic volume (ESV) which is determined by echocardiography when assessing ventricular function. Factors influencing the SV and their effects are summarised in Figure 7.

1.1.3.2.2.1 Preload

Preload is the degree of myocardial distension prior to shortening. It is best represented at the chamber level by the EDV of the left ventricle. Because volume is difficult to measure accurately and precisely in practice, preload is often estimated by left ventricle end-diastolic pressure. According to Frank-Straling law of the heart, an increase in venous return to the heart

increases the filled volume of the ventricle, which stretches the muscle fibres thereby increasing their preload. This leads to an increase in the force of ventricular contraction and enables the heart to eject the additional blood that was returned to it. Therefore, an increase in EDV results in an increase in SV. Conversely, a decrease in venous return and EDV leads to a decrease in SV by this mechanism (Braunwald et al., 2011).

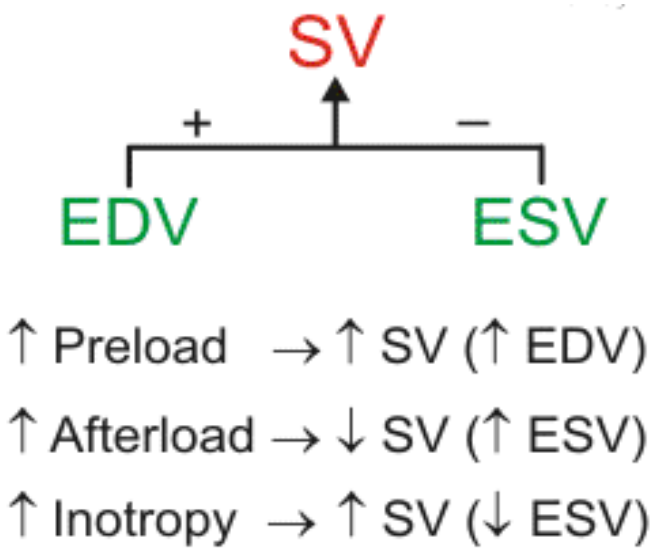

Figure 7 factors affecting stroke volume (Klabunde, 2012)

Frank-Starling law

It states that the volume of blood ejected by the ventricle depends on the volume present in the ventricle at the end of diastole. Increased preload increases sarcomere stretch inside cardiac myocytes, which generates more force during contraction, and thereby allows the heart to eject more blood. However, there is a limit to the extent that this relationship can be maintained. In failing ventricles, overstretch can limit or decrease CO. In these cases, reducing myocyte stretch to a more optimal length can improve overall cardiac function (Figure 8) (Raj, 2017).

The volume present at the end of diastole depends on the volume returned to the heart, or the venous return. Therefore SV and CO correlate directly with EDV, which correlates with venous return. The Frank-Starling relationship governs normal ventricular function and ensures that the volume the heart ejects in systole equals the volume it receives in venous return. However, If preload continues to increase, the point of overstretch is reached and eventually passed. Cardiac output plateaus and then begins to fall. The plateaued segment is called the preload independent portion.

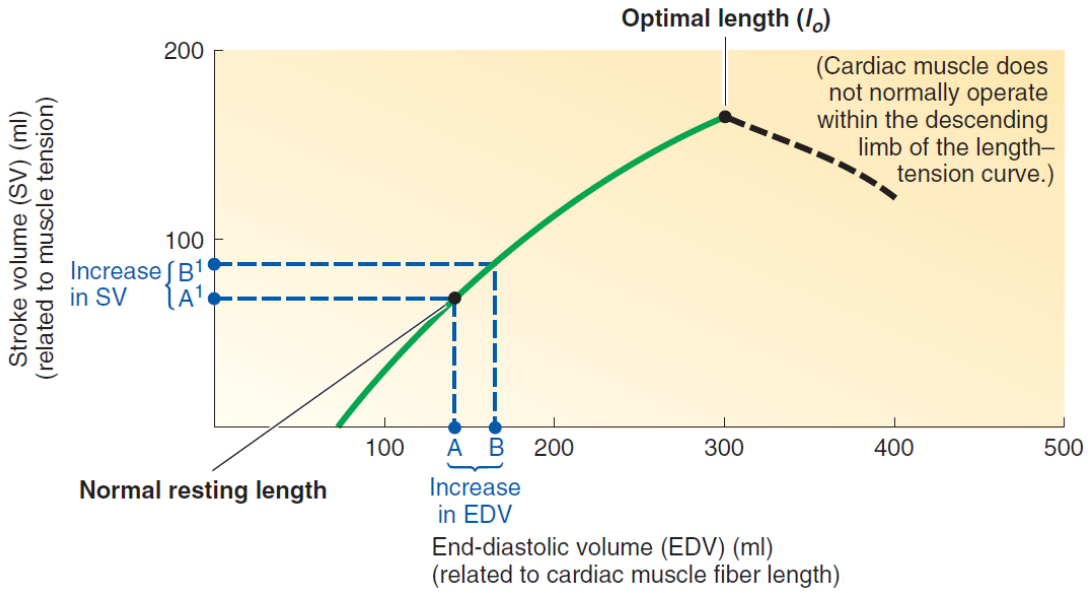

Figure 8 Frank-Starling representation of the relationship between end diastolic volume (EDV), and stroke volume (SV) (Sherwood, 2015)

1.1.3.2.2.2 Afterload

Afterload is the force against which the ventricles must act in order to eject blood, and is largely dependent on the arterial blood pressure and vascular tone. When afterload increases, the SV drops (Vincent, 2008, Braunwald et al., 2011).

1.1.3.2.2.3 Contractility

Contractility, or the inotropic state, is the inherent capacity of the myocardium to contract independently of changes in preload or afterload. Sympathetic stimulation increase the heart contractility, which is the strength of contraction at any given EDV (i.e. for the same EDV a higher SV can be obtained). This in turn, causes a left shift for the Frank-starling curve (Figure 9) (Braunwald et al., 2011).

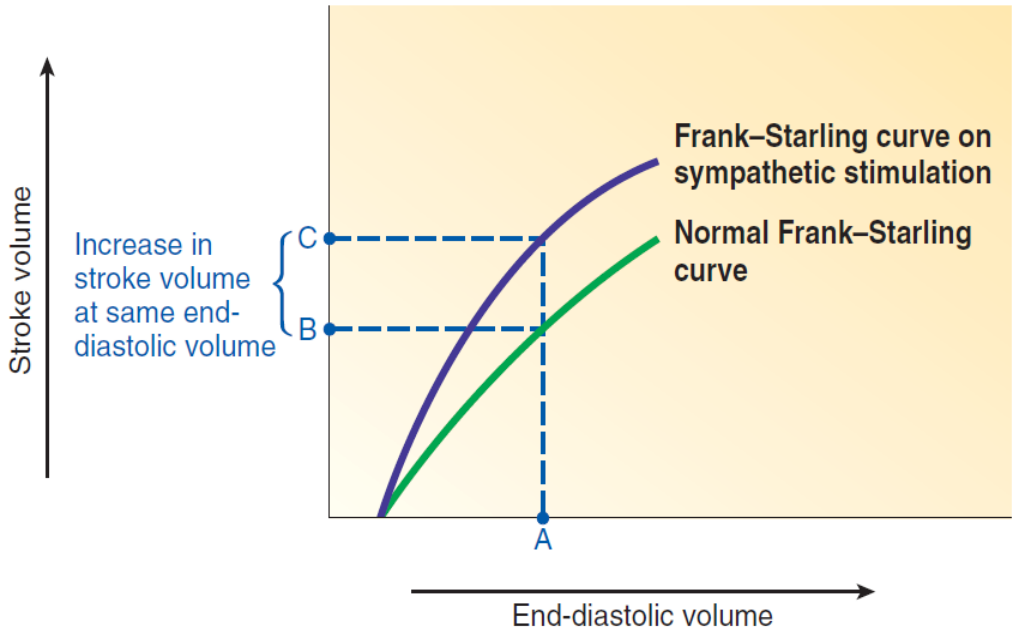

Figure 9 The influence of sympathetic stimulation on Frank-starling relationship (Sherwood, 2015).

1.1.4 Regulation of blood pressure

BP regulation is managed by short-term and long-term feedback control systems. Baroreceptor reflex is a neurally mediated short-term feedback working at a time scale of seconds to minutes to restore the BP toward its set point by altering the sympathetic, and parasympathetic signals to the CVS. The second system is the renin-angiotensin-aldosterone system (RAAS) which is hormonally mediated. It regulates BP more slowly (i.e. hours to days), primarily by its effect on blood volume.

1.1.4.1 Baroreceptor feedback regulation of blood pressure

Arterial baroreceptor, also called high-pressure baroreceptors, are the major receptors involved in the moment-to-moment regulation of blood pressure. They are located in the walls of the carotid sinus, and in the aortic arch. The carotid baroreceptors are responsive to both increases and decreases in arterial BP, whereas the aortic arch baroreceptors are primarily responsive to only increases in arterial BP (Sherwood, 2015, Armstrong M).

Other baroreceptors are termed low-pressure baroreceptors or volume receptors, because of being located within the low-pressure venous system. They are located in large systemic veins, pulmonary vessels, and the right atrium and ventricle (Stanfield, 2013). Because of the greater vascular compliance of the venous system, these type of baroreceptors

are quite sensitive to blood volume change rather than pressure changes. They respond to dropped BP by stimulating the secretion of antidiuretic hormone, renin, and aldosterone (Armstrong M).

The baroreceptor reflex functions as the major short-term negative feedback reflex that regulates arterial BP. Baroreceptors provide a dynamic signal to the brain regarding changes in BP and elicit reflex responses to maintain BP within a narrow range. They work as sensitive mechanoreceptors that stretch with increased BP by increased firing of the baroreceptors. This signal is delivered to the medullary cardiovascular centre, leading to an increase in parasympathetic outflow to the heart and a decrease in sympathetic outflow to the heart, arterioles, and veins. This induces a compensatory decrease in CO and TPR. Similarly, a decline in arterial pressure cause a decreased stretch in the baroreceptors and decreased firing rate resulting in increased cardiac output and vasoconstriction which ultimately increase BP (Armstrong M, Widmaier et al., 2019). Figure 10 summarises the baroreceptor response to decreased MAP.

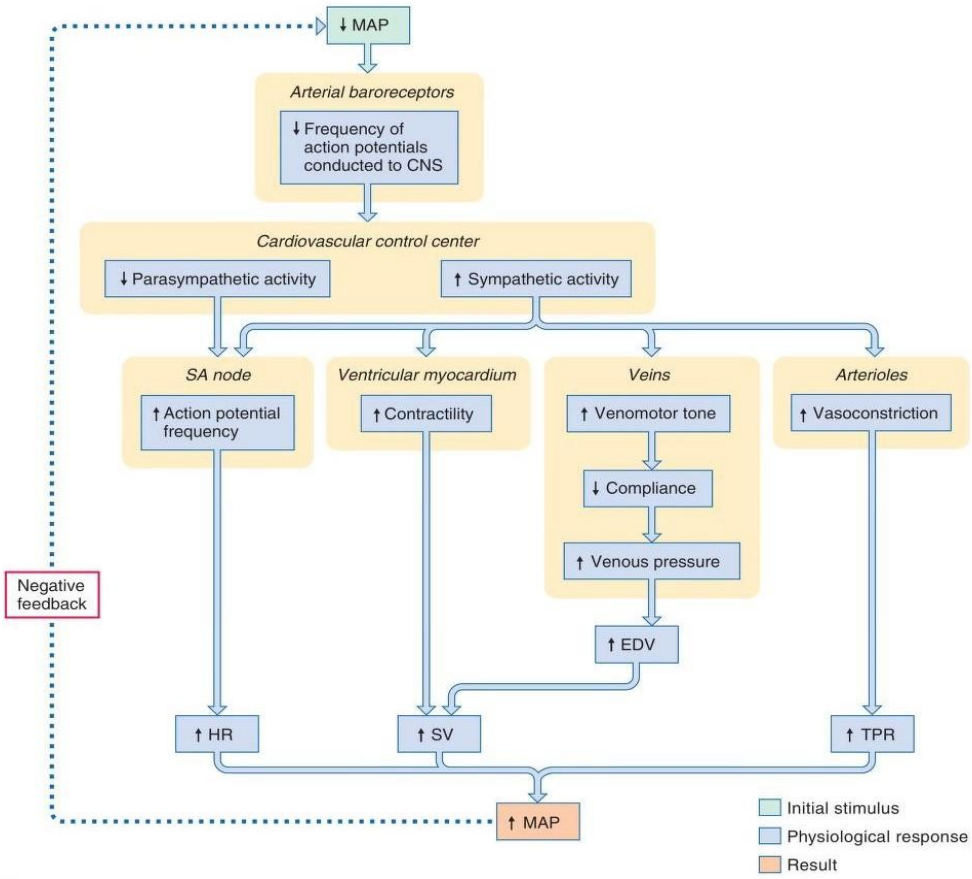

Figure 10 Arterial baroreflex to decreased mean arteria pressure. MAP: mean arterial pressure, EDV: end diastolic volume, HR: heart rate, SV: stroke volume, TPR: total peripheral resistance (Stanfield, 2013).

Baroreceptors are sensitive not only to the absolute level of pressure, but they are even more sensitive to the rate, and magnitude of changes in the BP. A rapid change in arterial BP acts as the strongest stimulus for the baroreceptors (Costanzo, 2018). Carotid baroreceptors are highly sensitive to the pulsatile profile of BP, i.e. the pulse pressure. The greater the oscillation in pressure around certain MAP, the greater the average baroreceptor activity. The role of this reflex becomes very significant during orthostasis and moderate haemorrhage, when there is a fall in PP due to the fall in SV, while having a subtle drop in MAP (Levick, 2013).

Baroreceptors can adapt to changes of MAP that can develop at different physiological (e.g. postural changes, physical exercise) and pathological conditions (e.g. hypertension). This cause a shifting of the baroreceptor function curve to a higher or lower BP by resetting the functional set point based on the new prevailing MAP (see Figure 11). This includes maintaining the sensitivity to acute changes in BP but at a different set point. The baroreceptor reflexes ac primarily to stabilise BP within a narrow range rather than maintaining a normal level of BP (Raven and Chapleau, 2014, Widmaier et al., 2019).

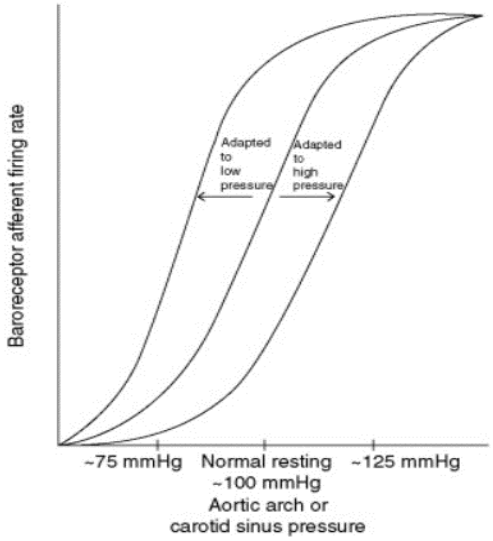

Figure 11 Baroreceptor function curve resetting in hypertension and hypotension (Sved, 2009).

1.1.4.2 Renin-Angiotensin aldosterone system

The renin angiotensin aldosterone system (RAAS) regulates BP mainly by regulating blood volume. RAAS works at a slower rate relative to the baroreflex, with a time scale of hours to days because of being hormonally, rather than neurally, mediated. A drop in BP

stimulates the RAAS with a cascade of activating several mediators to restore the BP back around the system set point (Widmaier et al., 2019).

When the BP falls, the decreased renal perfusion pressure is sensed by the mechanoreceptors in afferent arterioles of the kidney. This in turn, stimulates the secretion of renin from the juxtaglomerular cell. Renin catalyses the conversion of angiotensinogen to angiotensin I (Costanzo, 2018). Angiotensin-converting enzyme (ACE) catalyses the conversion of angiotensin I to angiotensin II. Angiotensin II has several biological activities that ends up with restoring BP:

- It stimulates the synthesis and secretion of aldosterone, which increases Na^+ reabsorption from the renal tubules, and consequently the extracellular fluid volume and blood volume.
- It has its own direct action on the kidney, independent of its actions through aldosterone. Angiotensin II stimulates Na^+-H^+ exchange in the renal proximal tubule and increases the reabsorption of Na^+ increase extracellular fluid volume.
- It also stimulates secretion of antidiuretic hormone (ADH), which increases water reabsorption in collecting ducts.
- It acts directly on the arterioles to cause vasoconstriction. The resulting increase in TPR leads to an increase in BP.

1.2 Haemodynamic models

Several attempts to develop mechanistic or semi-mechanistic models describing the CVS have been published. Some focused on describing the physiology of the CVS like Guyton's model, which consisted of hundreds of mathematical equations that provided deep insights into the long-term regulation of BP and the role of the kidney in this (Guyton et al., 1972). Guyton's model is considered a pioneer example of systems modelling approach. Other models integrated the knowledge of cardiovascular physiology with the haemodynamic effects of some drugs targeting the CVS using preclinical and clinical data (Francheteau et al., 1993, Chae et al., 2018, Snelder et al., 2014, Snelder et al., 2013).

A summary description of previously published haemodynamic models in the literature is shown in Table 1.

Table 1 Summary of previously published haemodynamic models

Reference	Short description	Described feedback control system	Comments
(Francheteau et al., 1993, Cheung et al., 2012)	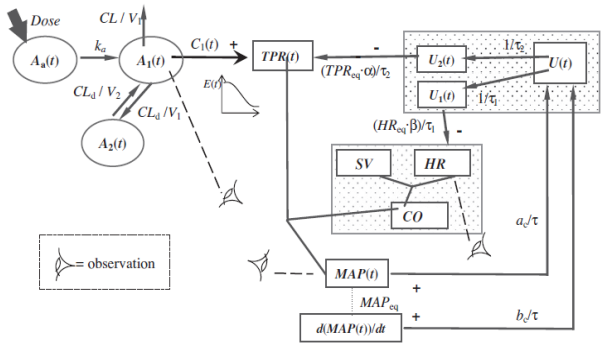 **A. Original model (Francheteau et al.) (Francheteau et al., 1993)** - Developed based on clinical data for healthy individuals receiving dihydropyridine (nicardipine and nifedipine) infusion - 3-state model (TPR, HR, U 'feedback') with a closed loop feedback control	- Considered feedback: baroreceptor reflex. - Feedback is a state variable, driven by change in MAP and the rate of this change ($\frac{dMAP}{dt}$) $\frac{dU(t)}{dt} = \frac{\left[a_c(MAP(t) + b_c\frac{dMAP(t)}{dt} - U(t)\right]}{\tau}$ -It acts on HR, TPR only	- Changes in SV are not accounted for 'SV assumed to be constant all the time' - Feedback is working on HR, TPR only 'has no effect on SV'

	- Delay between the arterial pressure change and the arterial pressure control was considered by τ, τ_1, τ_2 **B. Adapted model (Cheung et al.) (Cheung et al., 2012)** - Added a new model state for MAP - The influences of some model parameters were minimal in the model sensitivity analysis which indicates a potential unidentifability of the model - Reparametrised the model to reduce the model parameters		
(Snelder et al., 2014, Snelder et al., 2013)	**The two versions of the model were developed in rats, not validated in humans** **Snelder et al., 2013 (Snelder et al., 2013)** - Developed using data from preclinical experiments with a training set of six antihypertensive drugs acting at different targets	Considered feedback: baroreceptor reflex. **Snelder et al., 2013** - Feedback is described by 2 distinct system's parameters to be estimated (FB_1, FB_2), acting on total peripheral	- The model needs to be scaled and validated in humans as per the authors' conclusion. - The model is **locally** identifiable when HR,

	- consisted of two turnover equations cardiac output and total peripheral resistance, which were linked by negative feedback through MAP **Snelder et al., 2014 (Snelder et al., 2014)** - the turnover equation for cardiac output was replaced by two turnover equations for heart rate and stroke volume - consisted of three linked turnover equations involving TPR, HR and SV all linked by negative feedback through MAP $\frac{dHR}{dt} = K_{in_{HR}} \cdot (1 - FB \cdot MAP) - k_{out_{HR}} \cdot HR$ $\frac{dSV^*}{dt} = K_{in_{SV}} \cdot (1 - FB \cdot MAP) - k_{out_{SV}} \cdot SV^*$	resistance, cardiac output, with between subject allowed on both of them. **Snelder et al., 2014** - Feedback is a system's parameter (shared by the different variables) to be estimated with baseline MAP as covariate using a power function - It acts on HR, SV, TPR $FB = FB_0 \cdot \left(\frac{IBSL_{MAP}}{TVBSL_{MAP_{SHR}}}\right)^{FB0\_MAP}$	MAP, CO measured together

	$\frac{dTPR}{dt} = K_{in_{HR}} \cdot (1 - FB \cdot MAP) - k_{out_{TPR}} \cdot TPR$ $SV = SV^* \cdot [1 - HR_{SV} \cdot \ln\left(\frac{HR}{BSL_{HR}}\right)]$ - The link between HR and SV is considered by a log-linear relationship 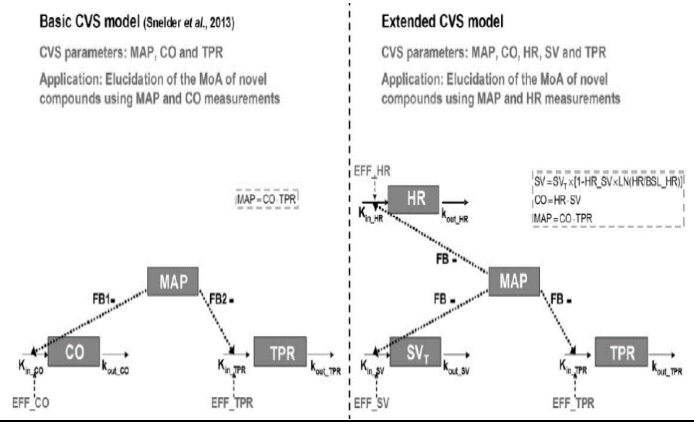		
(Chae et al., 2018)	- Based on clinical data from healthy individual upon administration of telmisartan - A four-state model (heart rate, total peripheral resistance, pulse pressure, feedback) with a negative feedback closed control loop	- Considered feedback: baroreceptor reflex.	Assumes that the set point is time varying and the system reset the baroreceptor to a

	$\frac{dHR}{dt} = k_{OUT} \cdot SP_{HR} - k_{out} \cdot HR$ $\frac{dPP}{dt} = k_{OUT} \cdot PP_0 \cdot (1 + FB) - k_{out} \cdot SV$ $\frac{dCTPR}{dt} = k_{OUT} \cdot CTPR_0 \cdot (1 - D_{EFFECT}) - k_{out} \cdot CTPR + BR$ $\frac{dFB}{dt} = k_{out} \cdot (Delta - FB)$	- Feedback is a state variable driven by the fractional change in MAP relative to the set point $Delta = \frac{MAP - SP_{MAP}}{\mathrm{SP_{MAP}}}$ - It acts on heart rate, and pulse pressure only -Baroreflex is another reflex signal acting on TPR , driven by the change in SV, HR $BR = -TPR \cdot \frac{\delta SV}{SV} - TPR \cdot \frac{\delta HR}{HR}$	direction opposing the perturbation $SP_{HR} = HR_0 \cdot (1 + FB)$ $SP_{PP} = PP_0 \cdot (1 + FB)$ $SP_{CTPR} = CTPR_0 \cdot (1 - D_{EFFECT})$ $SP_{MAP} = SP_{HR} \cdot SP_{PP} \cdot SP_{CTPR} = HR_0 \cdot \mathrm{PP_0} \cdot CTPR_0 \cdot (1 + FB)^2$ - Feedback acts on HR, and pulse pressure, while baroreflex acts on TPR. - The two feedback are distinct from each other, while working in opposite directions

(Coleman and Hall, 1992, Guyton, 1990, Hallow and Gebremichael, 2017, Hallow et al., 2014, Karaaslan et al., 2005)	- In 1972, Guyton's model was published. Further model refinement and expansions are still being published using the same core structure. - Large circulatory model of hundreds of equations mainly focused on describing the long-term regulation of blood pressure and the role of the kidney in this. - Explore the linkage between blood pressure and sodium balance and demonstrate the importance of renal salt and water balance in setting the long-term blood pressure level.	- Considered feedback: baroreceptor reflex and RAAS, , and control of arterial pressure by changes in body fluid volumes and electrolytes	Like other complex systems models, using the model for estimation purposes is a bit challenging, considering the complexity of the model structure.

1.3 Sodium nitroprusside

Sodium nitroprusside (SNP) is a potent vasodilator that has been used in clinical practice for a long time. SNP was first discovered in 1849; however, it was not until 1955 that Page et al. described the pharmacological effects of SNP in lowering the BP in severely hypertensive patients (Playfair, 1851, Page et al., 1955). In 1962, Moraca et al. investigated for the first time the clinical use and efficacy of SNP to induce deliberate hypotension during surgery in humans (Moraca et al., 1962). Since then, SNP has been introduced in perioperative settings as an effective fast-acting agent to induce intraoperative hypotension. Other indications for SNP included acute applications in hypertensive crises, heart failure, vascular surgery, and paediatric surgery (Hottinger et al., 2014).

1.3.1 Mechanism of action

1.3.1.1 Total peripheral resistance

SNP acts as a prodrug that releases nitric oxide, causing rapid vasodilation, and acutely lowering BP. SNP releases nitric oxide by interacting with the sulfhydryl groups on erythrocytes, albumin, and other proteins. This in turn stimulates a cascade of mediators ending up with vasodilation by stimulating guanyl cyclase enzyme to produce cyclic guanosine monophosphate, which causes sequestering of calcium and inhibiting cellular contraction. The net effect of nitric oxide is lowering the BP by reducing the vascular tone and the systemic vascular resistance. Sodium nitroprusside is more active on veins than on arteries (Tinker and Michenfelder, 1976).

1.3.1.2 Baroreceptor resetting

The effect of SNP on the resetting of the aortic baroreceptors has been suggested in some studies either in animals or in humans. Fritsch et al, studied the baroreceptor resetting in healthy normotensive volunteers upon infusion of SNP, and reported a significant change (resetting) of operational point (set point) toward a lower level of mean arterial pressure (Fritsch et al., 1989).

The effect of SNP on resetting of normotensive rats to hypotension, and the reversal of resetting of baroreceptors of hypertensive rats to normotension was studied by Salgado et al,. They reported that the mechanism by which SNP causes baroreceptor resetting appears to be linked to affecting baroreceptor transduction (Salgado and Krieger, 1988, Deabreu and Salgado, 1990). Similar results were presented in conscious rabbits infused with SNP, where the decrease in MAP during SNP infusion lowered the baroreflex threshold for bradycardia. As a conclusion, the authors highlighted that arterial baroreceptors are triggered by a floating

rather than a fixed set point which is determined by the prevailing blood pressure steady state (Dorward et al., 1982).

1.3.1.3 Tolerance and plasma renin activity

Development of tachyphylaxis (i.e. rapid progressive tolerance to the effect) and rebound hypertension after stopping the SNP infusion has been reported before in the literature (Amaranath and Kellermeyer, 1976, Cottrell et al., 1978, Khambatta et al., 1979, Cottrell et al., 1980, Delaney and Miller, 1980). One study was conducted on sixteen patients who were scheduled for major orthopaedic procedures. One group of the patients received SNP infusion while the others were pretreated with propranolol before SNP administration. The results of this study showed a significant increase of plasma renin activity (PRA) after 30 minutes of starting SNP infusion in patients who received SNP only, denoting that nitroprusside-induced hypotension activates the renin-angiotensin system. The PRA remained significantly elevated above the preinfusion levels after 15 minutes of SNP discontinuation. On the other hand, these changes in PRA were prevented by pretreatment with propranolol. These results showed that SNP administration triggers two opposing action: firstly, vasodilatation due to a direct action of the drug on vascular smooth muscle, and secondly, vasoconstriction which is produced by compensatory increases in PRA. Because of the very short half-life of SNP as compared to renin, this may be explaining the progressive development of tolerance and rebound hypertension that may develop upon its abrupt withdrawal of SNP by leaving the vasoconstrictor renin effects unopposed. Propranolol pretreatment attenuates activation of the renin-angiotensin system, hence decreases SNP doses required to maintain hypotension, and prevents rebound hypertension observed following withdrawal of nitroprusside (Heuser et al., 1985).

Another study in humans showed that SNP infused to induce MAP reduction caused a significant sustained elevation of PRA above control levels for 30 min after cessation of SNP infusion. This was explained by the relatively slow decline in PRA with a half-life of approximately 30 min (Cottrell et al., 1980).

1.3.2 Pharmacokinetics

The onset of action of SNP is 1–2 min. The volume of distribution is approximately the same as the extracellular space. It reacts with the sulfhydryl groups on red blood cells, releasing cyanide and nitric oxide. Because it is rapidly cleared from the bloodstream by an intraerythrocytic reaction with haemoglobin, its effects dissipate within 1–10 min following discontinuation of therapy. The drug half-life is approximately 2 minutes.

1.3.2.1 Metabolism

SNP is a water-soluble sodium salt comprised of ferrous complexed with nitric oxide and five cyanide anions. In the body, SNP is rapidly metabolised by a non-enzymatic electron transfer from the ferrous of free intracellular oxyhaemoglobin to nitroprusside yielding methaemoglobin and an unstable nitroprusside radical. This unstable radical breaks down rapidly releasing nitric oxide and five cyanide. The cyanide ions can then go through one of three pathways:

i) binding to methaemoglobin yielding cyanomethaemoglobin
ii) undergoing a reaction with thiosulfate and cobalamin in the liver catalysed by rhodanase forming thiocyanate which is excreted by the kidney
iii) cyanide not otherwise removed binds to tissue cytochrome oxidase, thus uncoupling mitochondrial oxidative phosphorylation and inhibiting cellular respiration, even in the presence of adequate oxygen stores. This is considered the main reason acute toxicity of SNP

The bioconversion of cyanide to thiocyanate is a saturable process, with the availability of sulphur-containing substrates as the limiting factor for this reaction. With prolonged administration or high doses of SNP, cyanide accumulates in the blood. The principal toxicity of SNP may be caused by the inactivation of cytochrome oxidase (Hottinger et al., 2014, Tinker and Michenfelder, 1976).

1.3.3 Toxicity

1.3.3.1 Cyanide toxicity

Occurs typically at doses ≥ 10 mcg/kg/min where the toxic effects are rapid and fatal. Manifestation of cyanide toxicity include lactic acidosis, shortness of breath, cardiac arrhythmias, tachycardia, hypertension, central nervous system (CNS) dysfunction. Cyanide blood concentrations are usually not available. Cyanide toxicity can be assessed by monitoring serum electrolytes, serum lactate, and arterial blood gases (The Food and Drug Administration (FDA), 2017b).

1.3.3.2 Thiocyanate

It is a normal physiological component of serum that is renally cleared. The half-life is doubled or tripled in renal failure. Thiocyanate is mildly neurotoxic at serum levels of 1 mmol/L and life-threatening when levels are 3 or 4 times higher. The toxicity is typically associated with high dose and prolonged infusions (e.g. >3mcg/kg/min or 1mcg/kg/min in anuric patients for >3 days). Thiocyanate levels should be closely monitored in patients with

prolonged infusions, impaired renal function, and those receiving simultaneous thiosulfate infusions (The Food and Drug Administration (FDA), 2017b).

1.3.3.3 Methaemoglobinemia

At healthy steady state, most people have less than 1% of their haemoglobin in the form of methaemoglobin. Clinically significant methaemoglobinemia (>10%) is rarely seen and it develops at exposure to very high doses of SNP. Methaemoglobinemia from excessive doses of SNP can be treated with methylene blue, which reduces methaemoglobin to haemoglobin (The Food and Drug Administration (FDA), 2017a, The Food and Drug Administration (FDA), 2017b).

1.3.4 Dosage and administration

SNP is supplied as injection for intravenous infusion. The recommended start infusion rate is 0.3 mcg/kg/min with a maximum dose of 10 mcg/kg/min. Dose titration to the desired effect is recommended by close monitoring of BP during infusion. In patients with eGFR <30 mL/min/1.73 m^2, the mean infusion rate is limited to less than 3 mcg/kg/min. In anuric patients, the mean infusion rate is limited to 1 mcg/kg/min (The Food and Drug Administration (FDA), 2017a).

1.3.5 Clinical use

SNP is a direct acting vasodilator indicated for instant reduction of BP, inducing controlled hypotension to reduce bleeding during surgery, and treatment of acute heart failure to reduce left ventricular end-diastolic pressure, peripheral vascular resistance, and mean arterial blood pressure(The Food and Drug Administration (FDA), 2017a).

1.4 Pharmacometrics

Pharmacometrics is defined as “the science of developing and applying mathematical and statistical methods to characterize, understand, and predict a drug’s pharmacokinetic (PK), pharmacodynamic (PD), and biomarker-outcomes behaviour” (Ette and Williams, 2007). Pharmacometric applications include dose individualisation for different patient subpopulations, guiding study designs and initial dose selection, and understanding disease progression and drug-disease interaction (Mould et al., 2012).

The present thesis implements pharmacometric approaches to model haemodynamics in humans and characterise the pharmacological effects of different drugs acting on the system. This section provides a brief introduction of the methods used in this thesis.

1.4.1 Models

Models are simplified version of reality. They help provide a better understanding of the modelled system. Models however are usually developed to fit the purpose of their intended use rather than to have the level of granularity of capturing the related system(s) completely. This was articulated by the British statistician George Box aphorism about models; "*Essentially, all models are wrong, but some are useful*" (Box and Draper, 1987). Quantitative modelling of drug effects and interactions with biological systems is an emerging tool in drug development (Mould et al., 2012).

1.4.1.1 PK model

PK is concerned with characterising different processes of drug in the biological system including absorption, distribution, metabolism, and excretion (ADME). PK models aim to describe and predict the time course of drug concentrations, which play an integral role in the development and clinical use of drugs (Mould et al., 2013). The complexity of PK models varies from simple empirical compartmental models to more complex mechanistic models and physiologically based PK (PBPK) models.

1.4.1.2 PKPD model

PKPD models are concerned with describing the time course of drug effect by allowing the drug PK "drug concentration" to drive the PD "drug effect". The link between the PK and PD is captured by either direct effect models "immediate response" or indirect effect models "delay models", based on the presence of lag time between having a measurable drug concentration and effect development (Upton and D, 2014).

1.4.1.3 QSP model

Despite the wide application of PKPD modelling in providing predictive guidance for dose response, having a limited biological relevance restricts its utility in extrapolating data between different physiological systems, for instance healthy and pathological (Mager et al.). Quantitative Systems Pharmacology (QSP) is an emerging modelling approach, which includes a great emphasis on the biology and physiology of the target system. QSP approaches, in comparison to other modelling approaches, are concerned with describing and quantifying the complex interaction between drugs and the human body. Moreover, they provide deeper insights into complex systems dynamics such as biological feedbacks, generate information on the mechanism of action and drug effects, and allow the assessment of disease progression(Kloft et al., 2016, Peterson and Riggs, 2015).

1.4.2 Modelling approaches.

Three approaches have been adopted in pharmacometric modelling. These include: the data driven approach, "top-down"; mechanism based approach, "bottom-up"; and middle out approach (Tylutki et al., 2016).

1.4.2.1 Top-down approach

This approach involves the development of empirical models driven by the data and achieving the parsimony of model parameters with less attention to capture the underlying physiology or pharmacology. Empirical models usually have limited application beyond the range of the input data.

1.4.2.2 Bottom-up approach

In bottom-up approach, mechanistic models are developed fully based on known mechanisms and they are generally more complex in their structure as compared to empirical models. They focus more on modelling the system information, providing deeper insight into complex physiological systems. Unlike the top-down approach, bottom-up approach allows model extrapolation to a wider range of scenarios far beyond the data limit, based on the level of complexity of the developed model.

1.4.2.3 Middle-out approach

This approach combines bottom-up and top-down approaches by allowing the observed data to inform unknown or uncertain parameters of the mechanism-based model. In the context of the current thesis, we consider QSP model and semi-mechanistic models as an application of middle out approach. This approach was applied in Chapter 2 where a minimal haemodynamic model is developed and Chapter 3 where we combined the developed model with haemodynamic data to characterise the effects of SNP.

1.4.3 Population analysis

Population analyses model individual data while accounting for the sources of variability between and within individuals in model parameters. Population models use mixed effect model estimation, which include both fixed and random effect parameters.

Fixed-effect parameters are model elements that do not vary across individuals. They reflect the typical values, or central tendencies, of the structural model parameters for the population.

Random-effect parameters are model elements that characterise the different sources of variability in the population. They include two levels: Level 1 (L1), which describes the magnitude of unexplained variability in parameters between population individuals (Between

subject variability 'BSV'); and Level 2 (L2), which quantifies the error in model predictions for multiple dependent variables (Residual unexplained variability 'RUV').

Overarching aim of the current thesis

The current thesis applies pharmacometric methods to provide a mechanistic modelling of haemodynamics in humans and to show model application to haemodynamic data from adolescents who received SNP. The motive behind this work was the lack of mechanistic haemodynamic models in humans that adequately capture the interrelationships between different haemodynamic variables while maintaining the model parsimony to allow model use for estimation purposes. This in turn served as the basis to evaluate the model performance in characterising the haemodynamic effects of SNP in adolescents by considering the different postulations about the mechanism of action of SNP.

CHAPTER 2: A MINIMAL HAEMODYNAMIC MODEL IN HUMANS

This chapter is based on the following manuscript:

Salma Bahnasawy, Hesham Al-Sallami, Stephen Duffull. "*A minimal model to describe short-term haemodynamic changes of the cardiovascular system*". Accepted for publication at the British Journal of Clinical Pharmacology (BJCP)

2.1 Introduction

Haemodynamics describes the pressure and flow of blood through the circulatory system. It is governed by cardiac output (CO) and the resistance of the blood vessels (Secomb, 2016, Klabunde, 2012). Tracking changes and the status of haemodynamics are essential parts of monitoring disease progress and the efficacy of drugs that act on the cardiovascular system (CVS) (Collins et al., 2015).

In clinical practice, blood pressure (BP), assessed by systolic (SBP), diastolic (DBP), and mean arterial pressure (MAP), and heart rate (HR) are the most commonly monitored haemodynamic variables. The fundamental relationships between these variables are well established (Levick, 2009). The haemodynamics of the CVS can be described by a closed-loop control system, where the MAP is closely regulated through adaptive changes in heart rate (HR), stroke volume (SV), total peripheral resistance (TPR), and blood volume (Raven and Chapleau, 2014). However, it remains common for many PKPD models to describe the haemodynamic variables separately without accounting for the interrelationship between these variables. While this is appropriate for descriptive models, e.g. (Caruso et al., 2014, Collins et al., 2015, Hocht et al., 2014), these models may lack the ability to accommodate extrapolation to situations that extend beyond the range of the data, e.g. the investigation of new drug targets.

Attempts to mechanistically model the cardiovascular regulation of BP date back to 1972 when Guyton and his colleagues published a large systems based circulatory model. The model focused on describing the long-term BP control with emphasis on the renal role in BP regulation (Guyton et al., 1972). This work remains a pioneer of quantitative systems analysis (Montani et al., 2009). Since then, model refinement and extended versions of the model are still being published, as a part of quantitative systems modelling, to describe the pathophysiology of hypertension and kidney disease (Hallow and Gebremichael, 2017, Hallow et al., 2014, Coleman and Hall, 1992, Guyton, 1990, Karaaslan et al., 2005). However, like other complex systems models, the focus of these models is to understand the physiology, disease progression, and drug mechanisms, while facing challenges for using such complex models for estimation purposes (Ribba et al., 2017).

There are a limited number of simpler published models with structures that account for the mechanistic interrelationships between the haemodynamic variables (i.e. MAP, HR, SV and TPR) and the feedback control loop (see (Francheteau et al., 1993, Chae et al., 2018, Snelder et al., 2014) for examples). A common feature of these models is the quantification of

the interrelationship between variables and the short-term feedback signal as represented by the baroreceptor reflex. However, different implicit model assumptions underpin these models. In Francheteau's model, SV was assumed to be constant, which could limit model application in other scenarios where significant changes in SV develop (e.g. haemorrhage, diuretics, plasma expanders) (Francheteau et al., 1993). The work of Snelder provided a simple effective control system but has not been extended beyond rats and dogs (Snelder et al., 2014, Venkatasubramanian R et al., 2016). Although Chae's model was used to describe the haemodynamics upon receiving a drug acting on TPR, the feedback control considered only cases where TPR is the site of system's perturbation, so the model may not have the flexibility to describe drugs acting on other drug targets (i.e. HR, SV) (Chae et al., 2018). Hence, to our knowledge there are no published models that accommodate the necessary features of the haemodynamic BP control for ready use in pharmacometric modelling.

The overall goal of the current work is to develop a minimal haemodynamic model that can be used by any investigator to quantify and understand the mechanistic effects of pharmacological agents on the short-term haemodynamics of the CVS in humans. It is intended that this model would be used for estimation purposes in top-down modelling applications (e.g. using NONMEM) for any situation in which BP, HR, and CO are measured either together or in isolation. This model with supporting documentation is available as an open source at GitHub (https://github.com/SalmaBahnasawy/SysModel.git).

The specific aims of the study were to: (i) build a minimal model to describe short-term haemodynamic changes, (ii) evaluate the model to characterise the haemodynamic profiles under different-target perturbations, (iii) apply the model to clinical data extracted from the literature, and (iv) check the structural identifiability of the model under different conditions for the observed variables.

2.2 Methods

2.2.1 Model development

A minimal model was developed to describe the short-term haemodynamics in humans. The model structure was adapted from Chae's model (Chae et al., 2018). This section shows the key features of the proposed model structure.

2.1.1 Interrelationship between MAP and HR, SV, and TPR

Over a period greater than one cardiac cycle the time averaged expression for cardiac output can be written, $CO = HR \cdot SV$, which yields the simple solution for MAP,

$$MAP = HR \cdot SV \cdot TPR \qquad (1)$$

The proposed minimal model does not accommodate the influence or change in arterial compliance over time and therefore does not define pulse pressure required to determine SBP and DBP. These components are generally not needed when describing the short-term haemodynamic influence of drugs over minutes to days.

2.1.2 The turnover rate of BP recovery

We use a turnover rate constant, k_{out}, to reflect the recovery rate of system to the reference BP. It is assumed to be shared by all model state variables (i.e.TPR, HR, and SV) as it is affected by a common autonomic control system. Furthermore, the current model assumes that the turnover rate of all the haemodynamic changes happens over a time scale of minutes rather than hours, so in all the subsequent simulations k_{out} was fixed to a suitably high value, reflecting a short reflex half-life of the system.

2.1.3 MAP set point

A set point for MAP is incorporated to derive the baroreceptor reflex. In this context, a set point is a reference point to which the body tries to return the BP as a part of homeostasis. This would be seen as the steady state MAP value (MAP_{SS} under no perturbation) being equal to the set point for MAP (MAP_{SP}),

$$MAP_{ss} = MAP_{SP} \ . \qquad (2)$$

If the system is started at a steady state and unperturbed initial condition then,

$$MAP_{SP} = MAP_{ss} \ . \quad (3)$$

The baroreflex feedback is driven by the relative difference of the current MAP from the reference MAP set point which is defined by the fractional change in MAP ($fcMAP$) ;

$$fcMAP = \frac{MAP - MAP_{SP}}{MAP_{SP}} . \qquad (4)$$

2.1.4 Inverse relationship between HR, SV

The current model structure considers an inverse relationship between HR and SV. This in turn, can account for the decline in SV that could develop at high HR because of the shortening of the cardiac diastolic interval and left ventricle filling time. Snelder et al described this relationship using a log-linear relationship between HR and SV (Snelder et al., 2014),

$$SV = SV_N \cdot \left[1 - \beta \cdot ln\left(\frac{HR}{HR|_{MAP=MAP_{SP}}}\right)\right] \quad (5)$$

In this equation, β is a constant that represents the magnitude of the direct effect of HR and SV, $HR|_{MAP=MAP_{SP}}$ is the HR evaluated at MAP equal to MAP_{SP} (which we term $HR|_{MAP_{ss}}$ hereafter (as per equation (3) under ideal conditions), while SV_N is the value of SV normalised to $HR|_{MAP_{ss}}$.

2.1.5 Mean arterial pressure is calculated

The SBP and DBP pressures are determined as a function of pulse pressure and MAP, where pulse pressure is a function of arterial compliance. In this work, we do not incorporate the SBP and DBP, hence have not incorporated components of pulse pressure into the calculation. In the clinical setting, it is usual to measure SBP and DBP rather than MAP, which requires an invasive technique (Klabunde, 2012). In these circumstances, MAP can be approximated from SBP and DBP (note this approximation is dependent on heart rate),

$$MAP \approx \frac{SBP + 2 \cdot DBP}{3} . \quad (6)$$

2.1.6 Feedback control defined as baroreflex

The present model structure assumes a closed-loop control structure for the system where baroreceptor reflex is a negative feedback control (i.e. system damping) acting on the three main components that drive MAP (i.e. $TPR, HR, and\ SV$). The site of system's perturbation or the primary drug target does not influence this.

2.1.7 General model structure

A turnover model, composed of four states, was used to describe the model structure. A typical representation for a generic variable (v) is

$$\frac{d(v)}{dt} = R_{in} - k_{out} \cdot v \ , \qquad (7)$$

where R_{in} is the zero-order production rate and k_out the first-order dissipation rate constant. In the context of baroreflex these concepts are empirical. At steady state

$$R_{in} = k_{out} \cdot v_{ss} \ , \qquad (8)$$

where v_{ss} is the variable at steady state.

An empirical E_{max} model was used to link the drug concentration to drug effect (D_{effect})

$$D_{effect} = \frac{E_{max} \cdot C_p}{C_{50} + C_p} \ , \qquad (9)$$

where E_{max} is the maximum fractional drug effect that could be achieved (termed as I_{max} for inhibitory drug effect), C_p is the drug plasma concentration, and C_{50} the concentration producing half of the maximum effect. Note any relevant drug effect model could be used.

The drug effect is incorporated into the general turnover model as

$$\frac{d(v)}{dt} = R_{in} \cdot (1 \pm D_{effect}) - k_{out} \cdot v \qquad (10)$$

The drug effect function could be added to affect the production or dissipation of the variable, based on its mechanism of action. Note, since dissipation is under overall system control it is perhaps unlikely to be the main site of drug action. While the dissipation of system states is somewhat complicated in a conceptual sense to consider, it is reasonable biologically. The purpose of dissipation is to allow the system to return to its set-point after perturbation (e.g. by a drug). Since the return to basal conditions is not instantaneous then the delay is considered as a parameter in the model. In the present model all changes in the system are controlled by k_{out} (the "dissipation" rate constant) which then specifies that (within the confines of normal physiology) haemodynamic processes have a delay in their response to normal physiological perturbations and to the influence of pharmacological interventions.

2.2.2 Evaluation of the model

The performance of the model was evaluated under two different simulation settings to explore its performance. All model simulations were performed in MATLAB R2017a (MATLAB, 2017).

2.2.1 System perturbation for different targets

A hypothetical scenario was simulated in which a patient with hypertension received a hypotensive drug by infusion that was stopped after one hour and the haemodynamic profiles

were tracked until return to the set point. The drug effect was simulated under three scenarios representing an inhibitory effect on $TPR, HR,$ or SV. The simulated drug followed a one-compartment PK model with a linear elimination.

The aim of the simulation was to explore the behaviour of the model performance in describing haemodynamic changes to perturbation of the system. In order to minimise the influence of drug-related changes in exposure (i.e. PK) on the system a rapidly eliminated drug was simulated. The drug parameters used for simulations are (R= 1000 mcg·hr $^{-1}$, k=10 hr $^{-1}$, V=1 L, I_{max} =0.5, C_{50}= 50 mcg·L^{-1}).

The purpose of this simulation was to evaluate the model flexibility to capture changes of different haemodynamic variables that can arise by perturbing the system at different targets. Furthermore, to explore the system's ability to stabilise the BP back around the set point after stopping the source of perturbation.

2.2.2 System perturbation when baroreceptor reflex is switched off

The model was used to simulate the effect of perturbing SV with and without baroreflex. To switch off the baroreflex signal, the rate of change of baroreflex state was assumed to be zero (i.e. $\frac{dBR}{dt} = 0$). For this simulation, only the SV was changed. No drug was added. The SV was increased over a certain interval period (0.5-1 hour) by a step function,

$$SV_0 = \begin{cases} SV|_{MAP_{ss}} & , at\ t < 0.5\ , t \geq 1 \\ SV|_{MAP_{ss}} + perturbation & , at\ 0.5 \leq\ t < 1 \end{cases}, \quad (11)$$

where $SV|_{MAP_{ss}}$ is SV evaluated at steady state MAP (equation 6).

The purpose of this simulation was to compare the haemodynamic profiles (especially of the non-directly perturbed variables) with and without the influence of feedback reflex.

2.2.4 Application of the model

Haemodynamic data were extracted from the literature using WebPlotDigitizer, 4.2 (Rohatgi). Initial conditions and the set point for MAP were calibrated to the reported initial values of the observed data assuming that the patient's baseline is the same as patient's set point (i.e. 'the system starts at steady state, $BR_0 = 0$'). Simulations were performed under the reported mean plasma concentration-time profile, with an E_{max} model linking the drug PK to the PD. To account for the variability in the reported concentrations, we simulated at the upper and lower bounds of the concentration (mean ± standard deviation). Two drug targets, HR and TPR were considered. In all cases, the simulations were overlaid on the observed data.

2.4.1 A drug inhibiting HR

The data (i.e. SBP, DBP, HR, and drug plasma concentrations) arose from a study of metoprolol, a β_1 selective adrenergic-antagonist, in fourteen female patients with mild essential hypertension. Heart rate was the primary drug target. Six patients received 80 mg and eight patients received 50 mg oral doses three times daily. Simulations were performed for the haemodynamic profiles obtained over six hours after a single oral administration under the two dosing levels using the reported mean plasma concentration (Bengtsson et al., 1975).

2.4.2 A drug inhibiting TPR

In this scenario, the haemodynamic effects of nifedipine, one of the dihydropyridine calcium channel blockers with a primary target of TPR, were simulated. Data on SBP, DBP, HR, and drug plasma concentrations were extracted from a previously published study on sublingual administration of nifedipine 10 mg to 11 patients and 20 mg to 6 patients with arterial hypertension (Pedersen and Mikkelsen, 1978). Patients with secondary hypertension were excluded. The average plasma concentrations over two hours after single dose administration were reported for the two dosing levels (seven patients on 10mg and six patients on 20 mg).

2.2.5 Structural identifiability analysis

Structural identifiability is related to the structure of the underlying mathematical model. It is concerned with whether the parameters of a model can be uniquely identified from a given experiment with perfect input-output data (Shivva et al., 2013). A structural identifiability analysis was performed to evaluate the use of the model with various combinations of data that might arise in clinical practice. The system was assumed to start at an unperturbed steady state. The MATLAB toolbox, STRIKE-GOLDD MATLAB (Villaverde et al., 2016), was used for this evaluation. An identifiability analysis was considered under four combinations of observed variable availability,

i. MAP, HR, and CO measured
ii. MAP and HR measured
iii. MAP measured only
iv. HR measured only

2.3 Results

2.3.1 Model structure

The model quantifies the interrelationships between the haemodynamic variables (HR, SV and TPR) driving the blood pressure (i.e. MAP). The current model is composed of four states capturing the changes in the haemodynamics of the CVS by a closed-loop control system, where the MAP is closely regulated through adaptive changes in HR, SV, and TPR. The short-term feedback signal is represented by the baroreceptor reflex, which is driven by the fractional change from the systems set point of MAP.

The model structure is illustrated in Figure 12 with model states shown as boxes. The model is represented by four ordinary differential equations (ODEs):

$$\frac{d(HR)}{dt} = k_{out} \cdot HR_0 \cdot (1 - BR) - k_{out} \cdot HR$$

$$\frac{d(SV_N)}{dt} = k_{out} \cdot SV_{N_0} \cdot (1 - BR) - k_{out} \cdot SV_N$$

$$\frac{d(TPR)}{dt} = k_{out} \cdot TPR_0 \cdot (1 - BR) - k_{out} \cdot TPR$$

$$\frac{d(BR)}{dt} = k_{out} \cdot (fcMAP - BR)$$

$$\mathrm{SV} = \mathrm{SV_N} \cdot \left[1 - \beta \cdot \ln\left(\frac{\mathrm{HR}}{\mathrm{HR}|_{\mathrm{MAP_{ss}}}}\right)\right]$$

$$fcMAP = \frac{MAP - MAP_{SP}}{MAP_{SP}}$$

$$MAP = CO \cdot TPR = HR \cdot SV \cdot TPR$$

The initial values were given by

$$A_0 = [HR_0, SV_{N_0}, TPR_0, BR_0]$$

When $v_0 = v|_{MAP_{SS}} \left(i.e. HR_0, SV_{N_0}, TPR_0\right)$, then the initial value for baroreflex can be fixed to zero (i.e. $BR_0 = 0$).

A description of model system parameters (k_{out}, β, MAP_{SP}) , with the values used for the model simulations, and the initial conditions ($HR_0, SV_{N_0}, TPR_0, BR_0$) is represented in Table

2. The initial conditions used for each simulation were calibrated to the data. Model calibration was done by considering the mean of initial conditions reported in the simulated datasets.

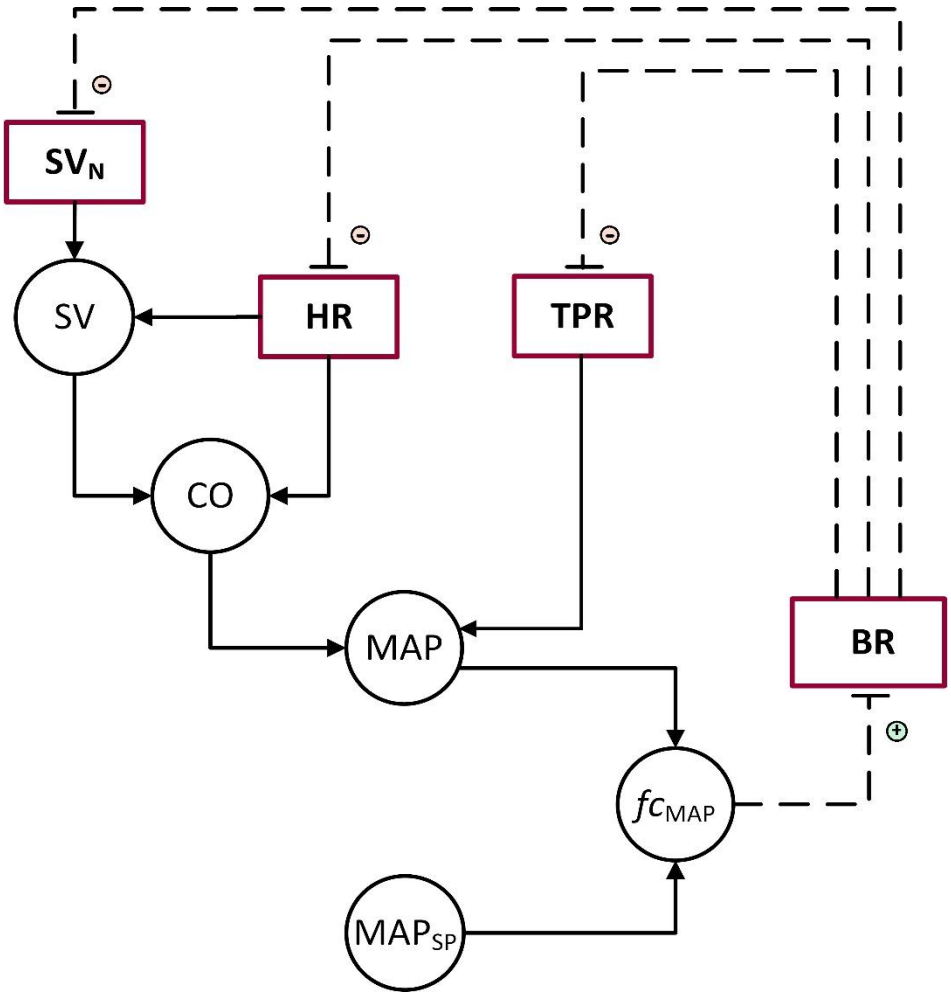

Figure 12 Model schematic. SV: stroke volume, SV_N : stroke volume normalised to a standard heart rate, HR: heart rate, TPR: total peripheral resistance, CO: cardiac output, MAP: mean arterial pressure, MAP_{SP} : MAP set point, BR: baroreflex, $fcMAP$: fractional change in MAP. Circles indicate calculated variables, while boxes indicate model states. Solid lines indicate causal calculations, dashed lines indicates a negative feedback control, positive or negative signs represent the mathematical property.

Table 2 description of model system's parameters and initial conditions

Parameters	*Units*	*Description*	*Parameter value*	*Altered in stressful physiological / pathologic conditions*	*Example use*
k_{out}	min^{-1}	1st order dissipation rate constant of the systems four state variables	$35\ h^{-1}$	Y	Pathology; baroreflex failure
β	Unitless	A scalar for the log-linear relationship of heart rate and stroke volume	0.22	Y	Pathology; heart failure, shock
MAP_{SP}	mmHg	Set point of mean arterial pressure	Calibrated to patient physiologic condition	Y	Pathology; hypertension
Initial conditions					
HR_0	$beat \cdot min^{-1}$	Heart rate initial condition		Y	Stressful physiology ; exercise, posture change
SV_{N_0}	$ml \cdot beat^{-1}$	Stroke volume initial condition		Y	
TPR_0	$mmHg \cdot min \cdot ml^{-1}$	Total peripheral resistance initial condition (usually calculated from MAP_0, HR_0, SV_{N_0}		Y	
BR_0	unitless	Baroreflex initial condition		Y	

2.3.2 Evaluation of the model

2.3.2.1 System perturbation for different targets

In the three scenarios, the profiles of primary drug targets are represented in pink and the secondary changes that developed on other haemodynamic variables are shown in purple (Figure 13). The shared feature in these scenarios is that they all show a recovery of MAP to the system set point after the source of perturbation has been discontinued. In addition, the corresponding changes in the non-directly targeted haemodynamic variables illustrate how this closed-loop control system is working at different perturbation scenarios. For instance, when a drug inhibits TPR with an overall decrease of MAP, then HR, SV and therefore CO increase as a part of the homeostasis of the baroreflex.

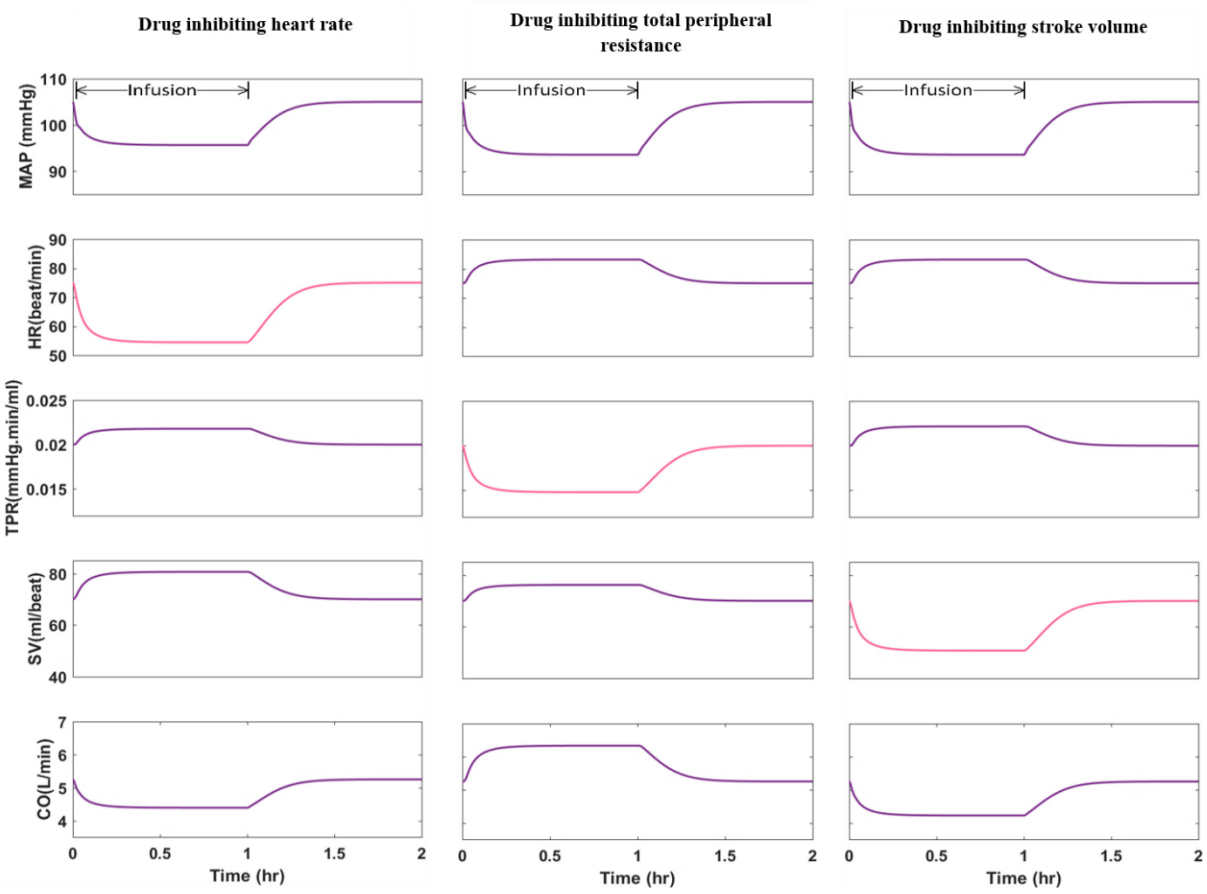

Figure 13 Simulation profiles upon one-hour infusion of a hypotensive drug in a hypertensive patient. Each column represents a simulation scenario for the drug primary target. The pink solid line represents the drug effect on the primary target; the purple line represents the secondary corresponding profiles.

2.3.2.2 System perturbation when baroreceptor reflex is switched off

Figure 14 depicts the influences of perturbing the system by a step function increase of SV while switching on/off the feedback control. A more pronounced increase in MAP, SV, CO developed when switching off the feedback (dashed line) as compared to keeping the feedback on (solid line). Moreover, while the non-targeted haemodynamic variables (i.e. HR, TPR) were inhibited as a feedback reflex (solid lines), they remained constant when the feedback was switched off (dashed line). In all the cases, the system returns back to the system set point as long as the source of perturbation is cleared (as whendrug is cleared from the body, the system return to its initial state regardless of having feedback control or not). The difference will be about the level of change in BP rather than getting back to the system set point.

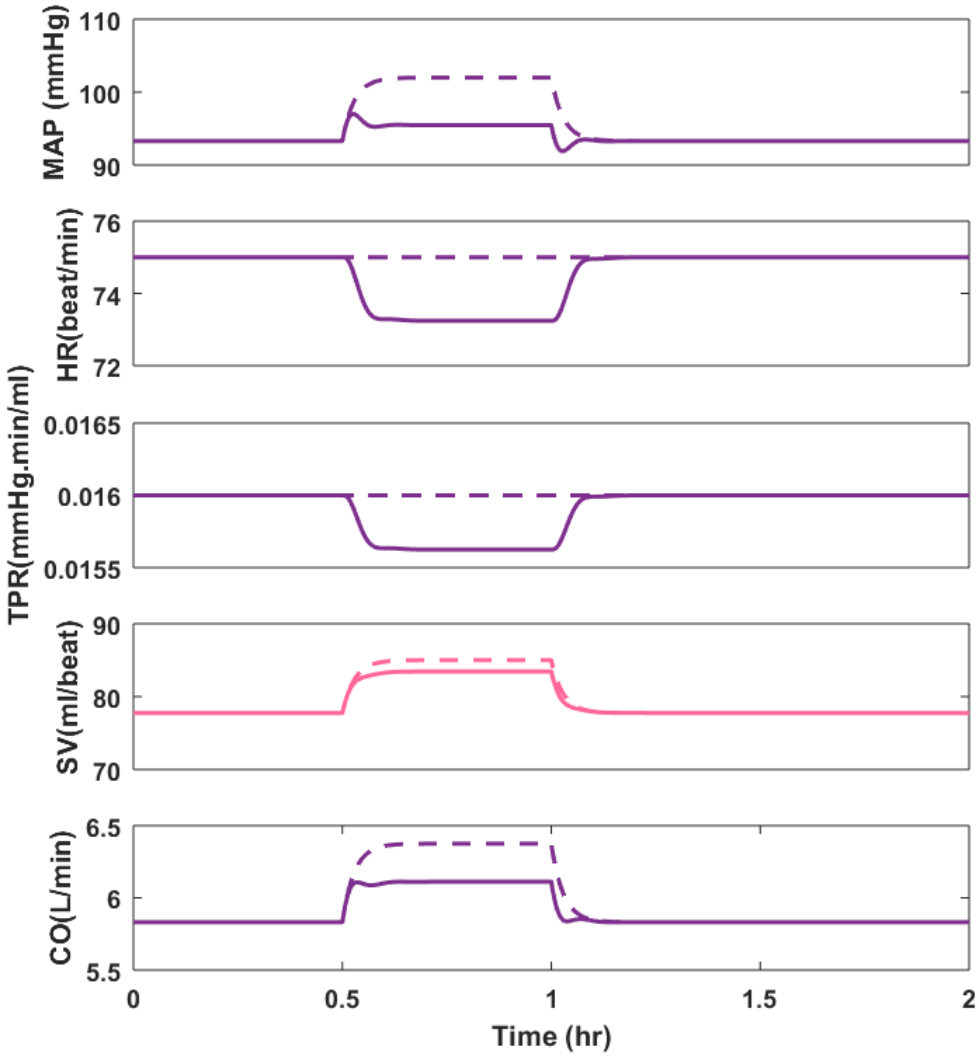

Figure 14 The haemodynamic profiles with a step function perturbing the stroke volume between 0.5-1 hour. The pink line represents the primary target perturbation; the purple line represents the secondary corresponding profiles. Solid line represents the model prediction under the baroreflex feedback control; dashed line represents the model prediction when the baroreflex is switched off.

2.3.3 Application of the model

Model application to clinical data showed an overall good description of the reported data without fitting. The overlay profiles of simulations and literature data for the different simulation scenarios (i.e. drug inhibiting HR or TPR) are shown in Figure 15 and Figure 16, respectively. The model simulations are shown using solid lines and the data are filled squares. The coloured bands represent the prediction intervals by simulating the drug effect considering the variability of reported drug concentration. For these simulations, the initial conditions and set point were calibrated to the reported data. Other system parameter were fixed based on the physiological plausibility, and reported literature estimates ($k_{out} = 35\ h^{-1},\ \beta = 0.22$). Note that these simulations represent the mechanistic structure of the model, as the parameters were not estimated.

The model use for estimation purpose in both of drug examples is shown in the Appendix 1 (Section A.1) with the model estimates, NONMEM code and overlaid plots of the simulated and estimated profiles.

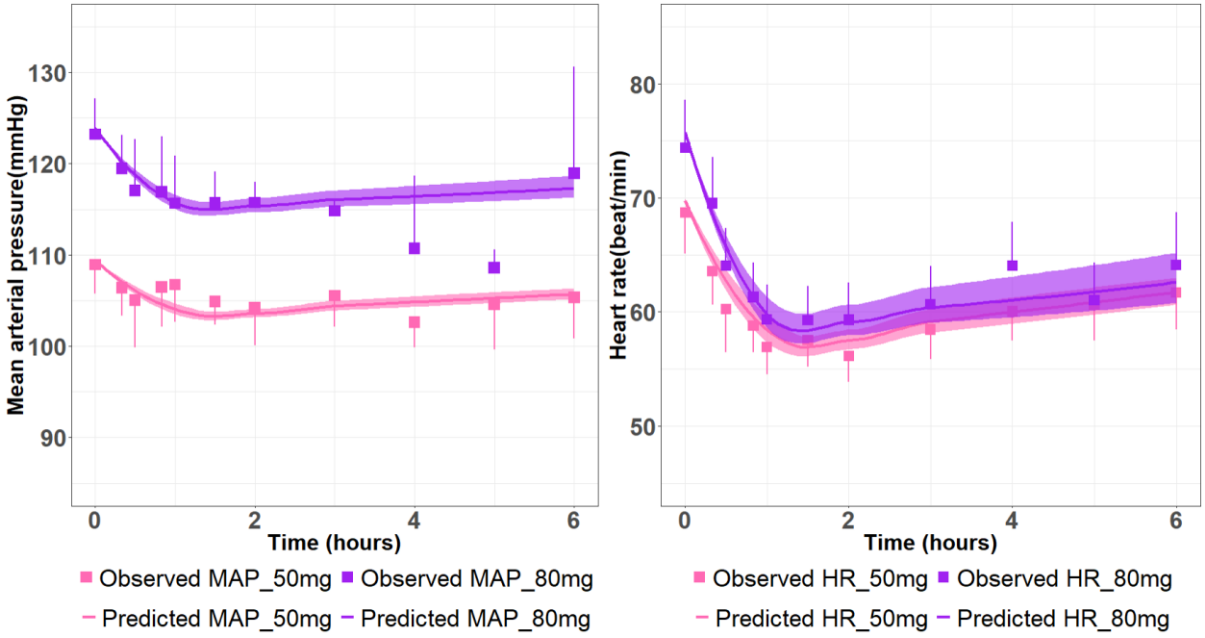

Figure 15 Overlaid haemodynamic profiles of metoprolol after a single oral dose in 14 patients with mild essential hypertension. Each data point represented by a square with bars represents the mean of the observed data ± SD (n=8 for 50mg dose, n=6 for 80mg dose). Solid lines represent the simulated profiles based on the extracted mean plasma concentration. The shaded area represents the simulated haemodynamic profiles under the reported drug plasma concentration ± SD

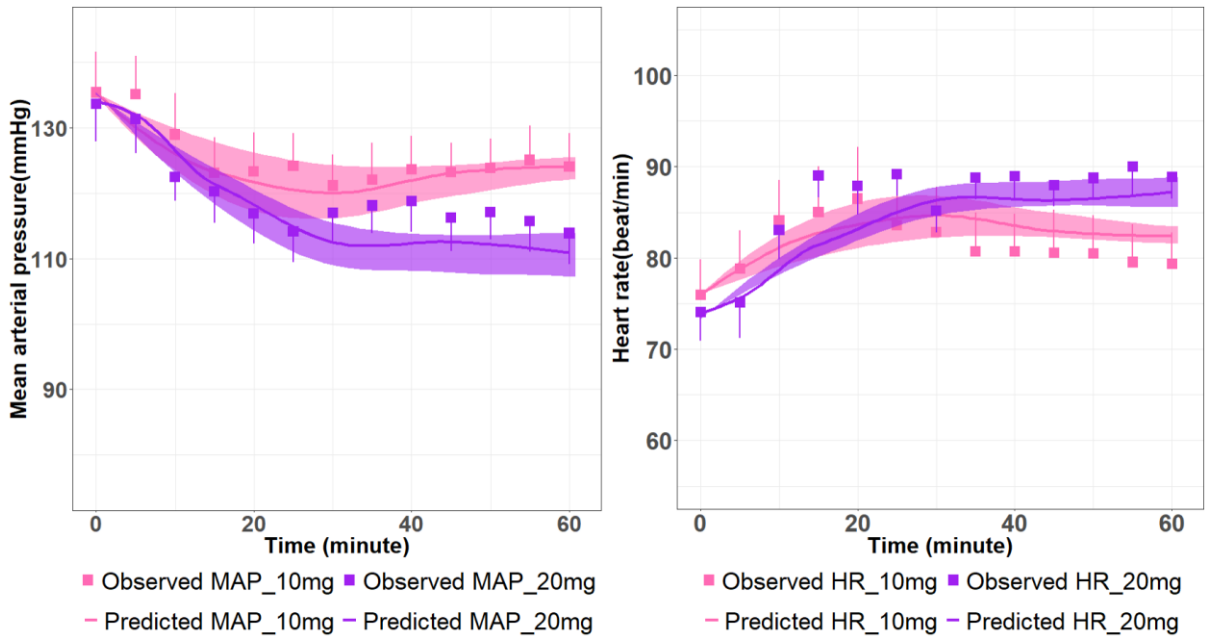

Figure 16 Overlaid haemodynamic profiles of nifedipine after a single sublingual dose in hypertensive patients. Each data point represented by a triangle with bars represents the mean of the observed data ± SD (n=11 for 10mg dose, n=6 for 20mg dose). Solid lines represent the simulated profiles based on the extracted mean plasma concentration. The shaded area represents the simulated haemodynamic profiles under the reported drug plasma concentration ± SD.

2.3.4 Structural identifiability analysis

The structural identifiability analysis revealed all model parameters and initial conditions were identifiable when HR, MAP, and CO were measured together (assuming the system to start at a non-perturbed state, i.e. $BR_0 = 0$). A summary of identifiability analysis results are represented in Table 3. It should be noted that the parameter k_{out} may be difficult to estimate if its value represents a fast dissipation of the system relative to the haemodynamic perturbation. In which case its value can be fixed to a suitably large value, (we use 35 h^{-1}, reflecting a half-life of approximately 1.2 minutes).

Table 3 Structural identifiability results

Observed variable	Identifiable parameters/ initial conditions	Parameter to be fixed
HR, MAP, and CO	$k_{out}, MAP_{SP}, \beta, HR_0, SV_{N_0}$	NA
HR, and MAP	$k_{out}, MAP_{SP}, \beta, HR_0$	SV_{N_0}
MAP only	k_{out}, MAP_{SP}, β	HR_0, SV_{N_0}
HR only	k_{out}, β, HR_0	MAP_{SP}, SV_{N_0}

2.4 Discussion

In the current work, we present a minimal model structure that can describe the short-term haemodynamic changes of the cardiovascular system. The model quantifies the interrelationship between haemodynamic variables of clinical interest (i.e. MAP, HR, SV, TPR) including describing the closed-loop control system. We define short term as control that occurs over minutes to hours rather than longer-term control (days to weeks) involving the renal system. The model was applied to MAP and HR data extracted from the literature for nifedipine and metoprolol. In both cases, the minimal model was applied with the original set of parameters (see Table 2). In this setting no parameter estimation was performed. The model with original parameter values provided an accepted description of the data. This implies the model has an appropriate level of mechanistic plausibility to capture both the scale of the data and also the necessary feedback components. Further simulations by perturbing SV provided an illustration of the flexibility of the minimal model particularly in relation to baroreceptor reflex.

We note the turnover rate constant of the recovery of BP was estimated in Chae's model in the time scale of hours reflecting a BP recovery half-life of 10.34 hour. This, in turn, means that the system reaches the steady state in about 40 hours. However, this could not accommodate rapid feedback reflex that develops upon abrupt drop in BP as in loss of blood volume, which is known to take place in a few minutes (Schadt and Ludbrook, 1991). One possible explanation for their estimated slow rate is that their model considered telmisartan–receptor interaction linked with the cardiovascular response as a single unit. It is therefore not possible to disentangle the pharmacodynamic activity of the drug from the system (Chae et al., 2018). In this case, the apparent slow turnover of the haemodynamic system would be controlled by the rate-limiting step, which might be the slow turnover rate of the mediator related to the pharmacology of the drug at the receptor site. The minimal model would provide an opportunity to consider the haemodynamic system as a separate system at which the drug exerts its action. Under this assumption, it would therefore be possible to examine the profile of the drug-receptor interaction.

The turnover model was used as a parsimonious empirical delay model (with only one parameter 'k_{out}') to describe the short delay which is under the control of the autonomic nervous system to maintain homeostasis. This provides the necessary characteristics in modulating the balance between the sympathetic and parasympathetic impulses to control the haemodynamic variables and allows return to the resting state at a defined recovery rate (governed by k_{out}). Other delay models could have been used.

The baroreceptor reflex functions as the major short-term damping control of the system that opposes the direction of system perturbation. Baroreceptors can adapt to different physiological stressors like postural change or exercise, as well as sustained pathological conditions as in hypertension. For instance, for hypertensive patients the baroreceptors continue to oppose minute to-minute changes in BP, but this occurs at a different resting value of the system, which implies that they accommodate a higher BP recovery set point (Sved, 2009, Widmaier et al., 2019). It is also possible that as the set-point shifts from the normal value (e.g. normotensive value) that the baroreceptor feedback efficiency also changes. However, we were not able to explore this in this work. Including MAP set point as a distinct component in the current model structure, gives the model the flexibility to describe the mechanism of action of some drugs that were reported to cause baroreceptor resetting (Zhang and Wang, 2001, Salgado and Krieger, 1988).

An identifiability analysis was implemented for the current model structure. All model parameters and initial conditions can be estimated when MAP, HR, and CO were measured. (Table 3). In other scenarios, some of the model parameters/initial conditions need to be fixed to keep the model identifiable. For instance, if only HR, and MAP were measured, then the initial condition of SV state needs to be fixed. This table is designed to provide guidance on how to use the model under different scenarios of the measured variables.

For model application, even though in the examples explored here, random effects were not considered as, individual level data were not available; the model is amenable to the addition of random effects to describe between-patient differences.

The baroreceptor activity response to changes in MAP is usually represented by a sigmoid curve (Sved, 2009). The carotid baroreceptors respond to pressures ranging from 60-180 mmHg. Maximal baroreceptors sensitivity occurs around the set point of MAP. Hence, small changes in MAP around this set point highly affect receptor firing so that autonomic control can be altered in such a way that the MAP remains very near to the set point (Klabunde, 2012). This could be a limitation when applying the model at extreme changes of BP, where a linear relationship may not yield appropriate response.

It is important to note that the model depends on MAP measurements to derive the haemodynamic profiles. For most clinical settings, MAP is not directly measured due to the invasiveness of the technique. Hence, usually MAP is calculated from SBP and DBP based on the knowledge that two thirds of normal cardiac cycle is spent in diastole and one third in systole. However, at high HR, MAP is more closely approximated by the arithmetic mean of SBP and DBP as the aortic pulse wave becomes shorter. Different formulas have been proposed

to account for HR changes when calculating MAP (Moran et al., 1995, Razminia et al., 2004). This could be a limitation of the model in situations of high rates of HR as in high intensity exercise where this relationship may not be constant. An extension of the model to accommodate pulse pressure and arterial compliance would accommodate this, which is the subject of future work. In addition, we anticipate the model may have a limited capacity to accommodate specific receptor level pharmacological profiles of tolerance or rebound effects. However, this could still be captured by expanding the current model structure to include other states describing the mediators that could be involved in developing such profiles based on the suggested underlying mechanisms in the literature.

2.5 Conclusions

We have described a minimal model of the haemodynamic system. Evaluation of the model suggests that its mechanistic plausibility is able to accommodate observed data profiles. It is intended that the minimal model could be used as the basis of standard pharmacokinetic-pharmacodynamic analysis of haemodynamic data in humans.

CHAPTER 3: A SEMI-MECHANISTIC MODEL OF NITROPRUSSIDE IN ADOLESCENTS

3.1 Background

Controlled hypotension is a technique that has been used to limit intraoperative blood loss, reduce the need for blood transfusions, and improve visualisation of the surgical field. It is achieved by reducing the systolic blood pressure to 80 – 90 mmHg, reducing mean arterial pressure (MAP) to 50 – 65 mmHg, or causing a 30% reduction of baseline MAP (Moraca et al., 1962).

Several drugs have been used to induce controlled hypotension in paediatric surgery. These include calcium channel blockers, beta-adrenergic antagonists, ganglionic blockers, inhalation anaesthetics, and direct-acting vasodilators such as nitroglycerin and sodium nitroprusside (Degoute, 2007, Tobias, 2002).

Sodium nitroprusside (SNP) is a direct-acting vasodilator that has been used in paediatrics to induce deliberate hypotension in perioperative settings. SNP has a potent vasodilation effect on venous and arterial smooth muscle that effectively decreases systemic vascular resistance producing its hypotensive effect (Hottinger et al., 2014). Although SNP is commonly used in paediatric patients during surgery, information about the safety and effectiveness of SNP in this population has been scant and its use had been extrapolated from clinical trials in adults.

SNP is a nitric oxide donor, which inhibits the vascular resistance with a net hypotensive effect. Moreover, some studies postulated the effect of SNP on resetting the arterial baroreceptors by shifting the set point of MAP to a hypotensive level.

In 2002, the United States Food and Drug Administration (FDA) issued a request for paediatric studies on SNP to Abbott Laboratories, as the holder of the new drug application of SNP. The approved labelling of nitroprusside use in paediatric patients for controlled hypotension lacked adequate information on dosing, pharmacokinetics, tolerability, and safety. The National Institutes of Health (NIH) in the United States issued a request in 2004 for proposals to conduct paediatric studies and awarded funds to Duke and Stanford Universities to conduct these studies. A report of the results of two paediatric studies of SNP was submitted for review to the NIH and the FDA in 2012 (Food and Drug Administration, 2014).

The first SNP study was a randomised double-blind, parallel-group, dose-ranging, effect-controlled, multicentre study and included 203 paediatric patients requiring short term SNP infusion for inducing controlled hypotension during surgery (Drover et al., 2015). The second study enrolled 63 intensive care paediatric patients who started with an open-label

prolonged SNP infusion followed by a double-blinded randomisation to either placebo or SNP (Hammer et al., 2015).

Results of the two studies provided safety and efficacy data and established a preliminary dosing guideline for paediatric SNP administration in perioperative settings. The key findings of these two studies showed the blood pressure (BP) lowering effectiveness of SNP, indicated that patients on higher doses of SNP were more likely to achieve the target MAP and at a faster rate, and suggested 0.3μg/kg/min as a reasonable starting dose of SNP in paediatric patients requiring controlled hypotension (Food and Drug Administration, 2014). However, the remaining challenges with SNP dosing were the difficulty to maintain the patient's BP within the target window since more than half of the time the BP was not within the target range, and the large unexplained variability in patient sensitivity to the drug (Drover et al., 2015).

Spielberg et al., have implemented linear regression analysis for the results of one of these two studies to explore the patient and clinical related factors that may affect BP control during deliberate hypotension in the study population. They studied several factors including the dose, dosing frequency, type of surgery, site of care, patient age, and baseline MAP. However, they reported a poor predictive capacity of the studied factors upon applying either univariate or multivariate regression model analysis for BP control. Hence, the analysis of covariates that may quantitatively predict the SNP hypotensive effect was not sufficient to reduce dose-response variability or improve BP prediction in individual patients. Most of the variability in BP control for an individual patient was due to unidentified factors and it was not feasible to predict accurately whether BP can be kept around the target MAP during deliberate hypotension (Spielberg et al., 2014).

Another analysis has been performed where a KPD model was developed to help guide the dosing of SNP in paediatrics. The model revealed that there were two subpopulations of patients having different sensitivities to SNP, but no correlations between the subpopulations and covariates were found. The model reported two C_{50} (460 and 138 μg/L) with population distributions of 70:30%, respectively. None of the investigated factors was sufficient to explain different drug sensitivities (Barrett et al., 2015). Hence, in their recommendations, they highlighted the need to work on developing a more mechanistic pharmacokinetic-pharmacodynamic characterisation to expand knowledge of SNP effects. This will in turn allow

better understanding of the variability in SNP response and provide guidance for SNP dosing for better BP control (Spielberg et al., 2014).

The developmental changes in the haemodynamic variables (e.g. SV, HR, and TPR) are linked to body size changes and physiologic maturation in children and adolescents. This has been described using different allometric power functions per each age stratum (Gillum et al., 1982, de Simone et al., 1997, Ma et al., 2012, Dewey et al., 2008). BP levels in turn are correlated with body size measurements (e.g. height, weight, and body mass index) in children and adolescents. Defining the cut-offs for normal range of BP within the different age strata helps diagnose abnormal haemodynamics (e.g. hypertension) that could develop in children and adolescents. The American Academy of Pediatrics (AAP) 2017 Guidelines for hypertension in children and adolescents define sex, age, and height percentile-adjusted SBP and DBP values in children <13 years old. However, for adolescents ≥ 13 years old, the adult blood pressure thresholds of defining hypertension have been adopted because of the closeness of the percentiles of adolescents to the adults' normal BP levels (Flynn and Falkner, 2017, Flynn et al., 2017).

The aim of the present work is to develop an extended PKPD (ePKPD) i.e. "semi-mechanistic" model that can describe the haemodynamic effects of SNP in adolescents and explain the different sensitives to the drug.

3.2 Methods

3.2.1 Data description

The data arose from a multi-centre, randomised, double-blinded, parallel group dose-ranging study to examine the safety and efficacy of SNP in paediatric patients requiring controlled reduction of blood pressure during surgery (Drover et al., 2015).

3.2.1.1 Study design

The study design involved four study phases (see Figure 17)

I. Pre-study drug administration (PRE)

- A period of up to 24 hours preceding the start of surgery.
- Patient demographics and vital signs were recorded and patients were randomly allocated to treatment groups.
- Baseline blood pressure was defined as the average of at least two pressure measurements in the preceding one minute prior to the

initiation of sodium nitroprusside after a 5-minute period of stable anaesthesia or sedation.

II. Blinded treatment phase (BTP) (not all patients completed this phase)

- After stabilisation of anaesthesia and measurement of vital signs, participants began the BTP.
- Patients were administered a blinded dose of SNP (0.3, 1, 2, and 3 µg/kg/min) for up to 30 min.
- The blinded dose was initiated at one-third of the full infusion rate for 5 min, then increased to two-thirds of the full rate for 5 additional minutes, then the dose was increased to the full rate if the target MAP was not attained.
- Followed by a washout period (BT2) until patient baseline haemodynamics are attained. Patient haemodynamics were recorded during this phase as well.
- BTP was discontinued if MAP fell below 50 mm Hg (40 mm Hg in neonates) or heart rate (HR) exceeded the age-adjusted maximum, or an adverse event occurred that was judged to be possibly related to the study drug.

III. Open-label treatment phase (OTP) (not all the patients entered this phase)

- This phase lasted at least 90 min, during which time SNP was initiated at a dose deemed appropriate by the investigator and was gradually adjusted to reach a target MAP defined by the investigator for each individual patient, in keeping with the clinical presentation and the needs of the patient.

IV. Follow-up phase (FUP)

- Started immediately after infusion of the study drug and ended after 30 days.

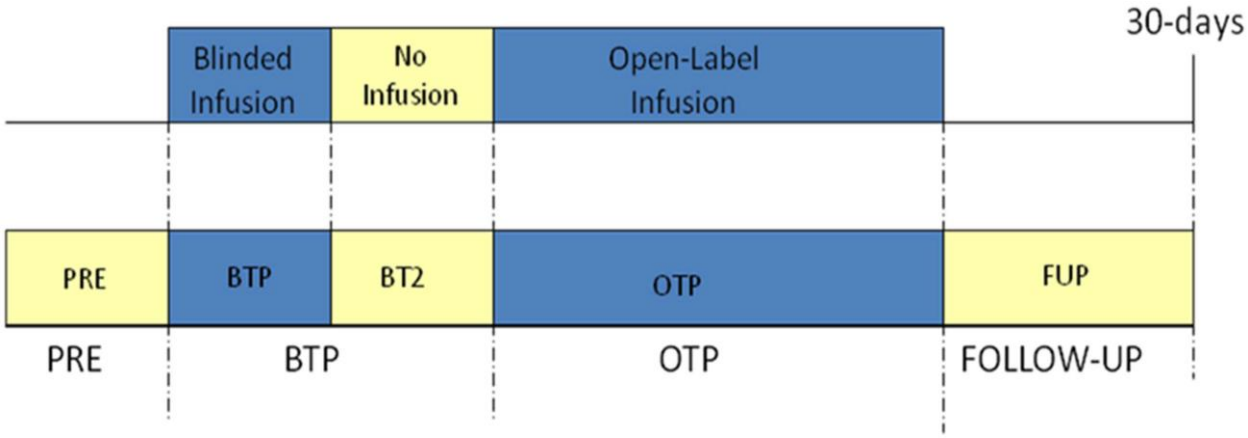

Figure 17 schematic of the study phases. PRE: pre-study drug administration period where patients were initiated and stabilised on anaesthesia; BTP: blinded treatment phase; BT2: blinded treatment phase II; OTP: open-label phase; FUP: follow-up phase (Drover et al., 2015)

3.2.1.2 Study population

The study included 203 paediatric patients who required intra-operative deliberate hypotension for at least 2 hours. Different types of surgical procedures were identified including spinal fusion, craniofacial reconstruction, coarctation of the aorta repair, and cerebral angiography. The study population age ranged from 3 days to 17 years old (see Figure 18).

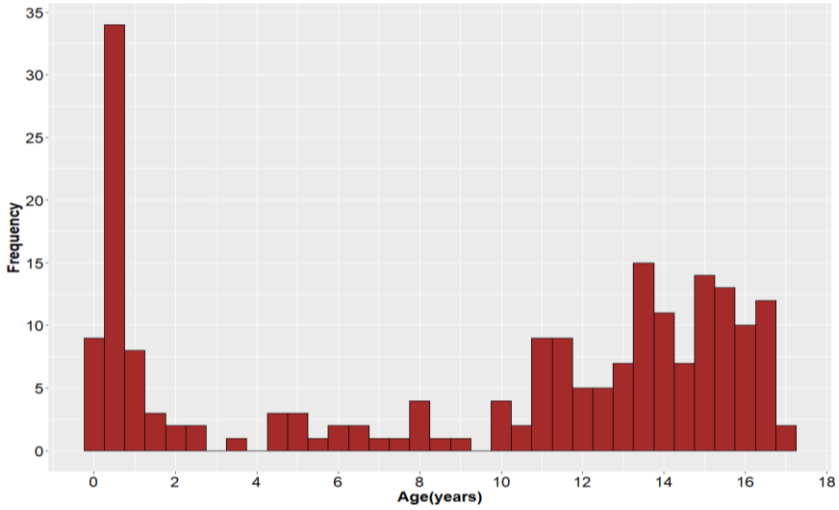

Figure 18 Histogram of age distribution of the study population

The current analysis included data from adolescents only (age ≥ 13 years old), with a total number of 86 individuals. Summary statistics of the baseline demographics of the current analysis population is shown in Table 4.

Table 4 Summary statistics of baseline demographics for adolescents ≥ 13 years old

	Treatment group dose (µg/kg/min)				***Total (N=86)***
	0.3 (N=20, 23.3%)	1 (N=21, 24.4%)	2 (N=26, 30.2%)	3 (N=19, 22%)	
Age (years)					
Mean(SD)	14.74(1.04)	14.86(1.09)	15.03(1.12)	15.10(1.15)	14.93(1.09)
Min-Max	13.11-16.75	13.03- 16.51	13.14-16.69	13.59-17.01	13.03-17
Weight (kilograms)					
Mean(SD)	51.85 (13.24)	58.78(22.42)	55.31(14.39)	54.56(14.7)	55.19(16.4)
Min-Max	29.6-73.9	28.3-112.2	28.5-93.4	34.8-84.2	28.3-112.2
Sex					
Male	3	8	11	4	26 (30.2%)
Female	17	13	15	15	60(69.76%)

3.2.1.3 Data collection

The principal method of obtaining blood pressure measurements was from an intra-arterial catheter inserted in an upper or lower extremity artery. In participants with coarctation of the thoracic aorta, a right upper extremity artery was used prior to surgical repair. In other patients, the choice of insertion sites, in order of priority, was (1) radial, (2) femoral, and (3) axillary. The MAP recorded from each of these sites is generally considered comparable.

Manual blood pressures from a non-invasive blood pressure cuff was only used prior to insertion of and during a malfunction of the arterial catheter. All blood pressure, heart rate, and oxygen saturation data were acquired electronically from a monitor when possible.

Intensive sampling of patient haemodynamic variables (MAP, HR, SBP, and DBP) was performed during BTP, with average recording frequency of 2 minutes. The plasma concentrations of SNP were not feasible to obtain because of the rapid drug metabolism, chemical instability, and short half-life.

3.2.1.4 Current analysis

The current analysis included:

- *Study population*: adolescents only (age ≥13 years). This age cut-off was chosen based on the AAP 2017 Guidelines for hypertension in children and adolescents

which adopted the adult blood pressures thresholds for all adolescents ≥ 13 years old (Flynn et al., 2017).

- *Study phase*: data from BTP phase only because the study details for this phase were available whereas not the case for OTP.
- *Dependant variables*: MAP and HR as these are the response variables included in the minimal haemodynamic model (chapter 2).

3.2.1.5 Data exploration

The haemodymaic profiles for the population (adolescents) during the blinded phase of SNP intravenous infusion is represented in Figure 19.

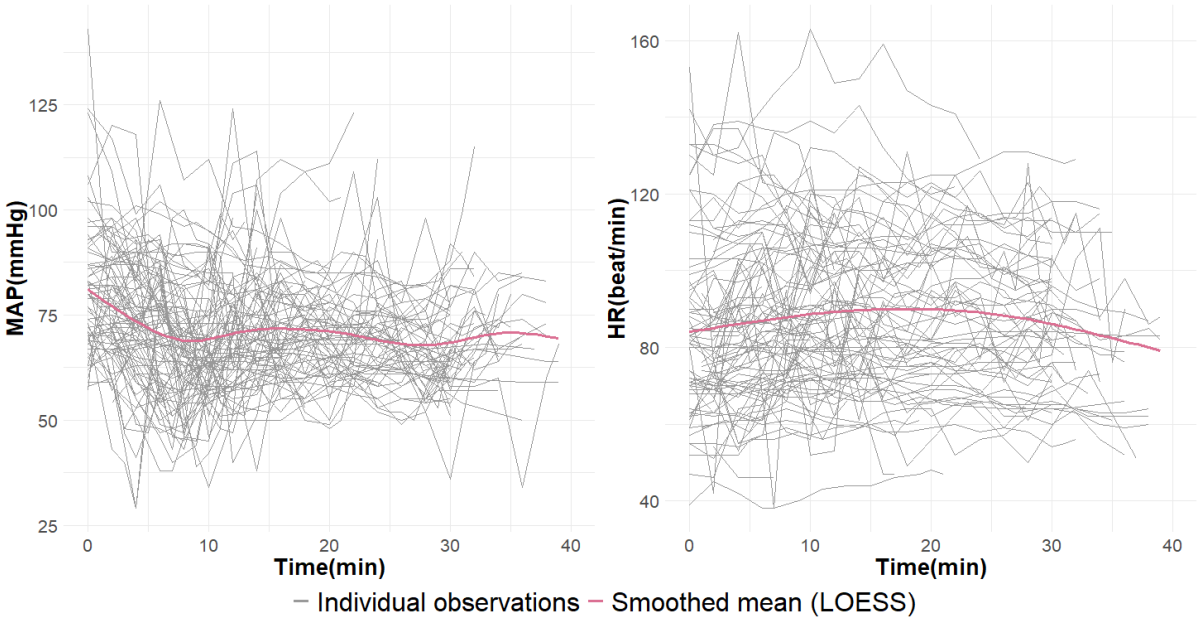

Figure 19 Spaghetti plots of individual haemodynamic profiles of adolescents during the blinded treatment phase. MAP: mean arterial pressure; HR: heart rate.

3.2.2 Model structure

3.2.2.1 Model extension

The extension of the minimal haemodynamic model developed in chapter 2 was conducted in order to describe SNP haemodynamic effect is described below. The minimal model was defined based on known mechanisms and included MAP, HR, and SV and four states described by differential equations. Model extension was informed by the postulated mechanisms for drug mechanism of action and physiologic haemodynamic response as reported in the literature.

3.2.2.1.1 Potential drug targets

3.2.2.1.1.1 Total peripheral resistance

The primary target of SNP is inhibiting total peripheral resistance (TPR) by releasing nitric oxide. This ultimately causes vasodilation of blood vessels, and consequently reduction of blood pressure. The description of SNP pharmacokinetics and pharmacodynamics is detailed in section *1.3.*

This was represented in the model by adding an E_{max} function to the TPR state, so that:

$$D_{effect} = \frac{I_{max} \cdot C_p}{C_{50} + C_p}$$

$$\frac{d(TPR)}{dt} = k_{out} \cdot TPR_0 \cdot (1 - BR) \cdot \left(1 - D_{effect}\right) - k_{out} \cdot TPR$$

where I_{max} is the maximum fractional inhibitory drug effect that could be achieved, C_p is the drug plasma concentration, and C_{50} the concentration producing half of the maximum effect.

3.2.2.1.1.2 Baroreceptor resetting

Some studies have reported the influence of SNP on the resetting of the aortic baroreceptors by affecting the baroreceptor transduction, as elaborated in section 1.3.1. The current structure accounted for the postulated mechanism of baroreceptor resetting by adding the drug effect on the baroreceptor state

$$\frac{d(BR)}{dt} = k_{out} \cdot fcMAP \cdot \left(1 - D_{effect}\right) - BR$$

, where $fcMAP$ is the fractional change in MAP

3.2.2. 1.1.3 Tolerance and plasma renin activity (PRA)

Tachyphylaxis development upon infusion of SNP has been linked to increased plasma renin activity. The detailed mechanism and supporting evidence from literature is mentioned in section 1.3.1. To account for the proposed mechanism of tachyphylaxis and rebound hypertension with SNP infusion, a new state was added to the minimal model structure shown in chapter 2. This state describes the changes in the plasma renin activity (PRA), with a turnover rate constant k_{PRA}

$$\frac{d(PRA)}{dt} = k_{PRA} \cdot (fcMAP - PRA)$$

In the current model, PRA is considered to affect the turnover of TPR, causing by opposing the direction of change in TPR;

$$\frac{d(TPR)}{dt} = k_{out} \cdot TPR_0 \cdot (1 - F_{PRA} \cdot PRA) - k_{out} \cdot TPR$$

3.2.2.1.3 Drug pharmacokinetics

There was no pharmacokinetic data available in the dataset, because of the rapid metabolism of SNP and difficulty to measure the plasma concentration of either SNP or nitric oxide, which are known to have very short half-lives as elaborated in section 1.3.3. A simple one-compartment PK model for SNP and nitric oxide representing nitroprusside metabolism was added to the model, assuming first order elimination of SNP and nitric oxide (Figure 20).

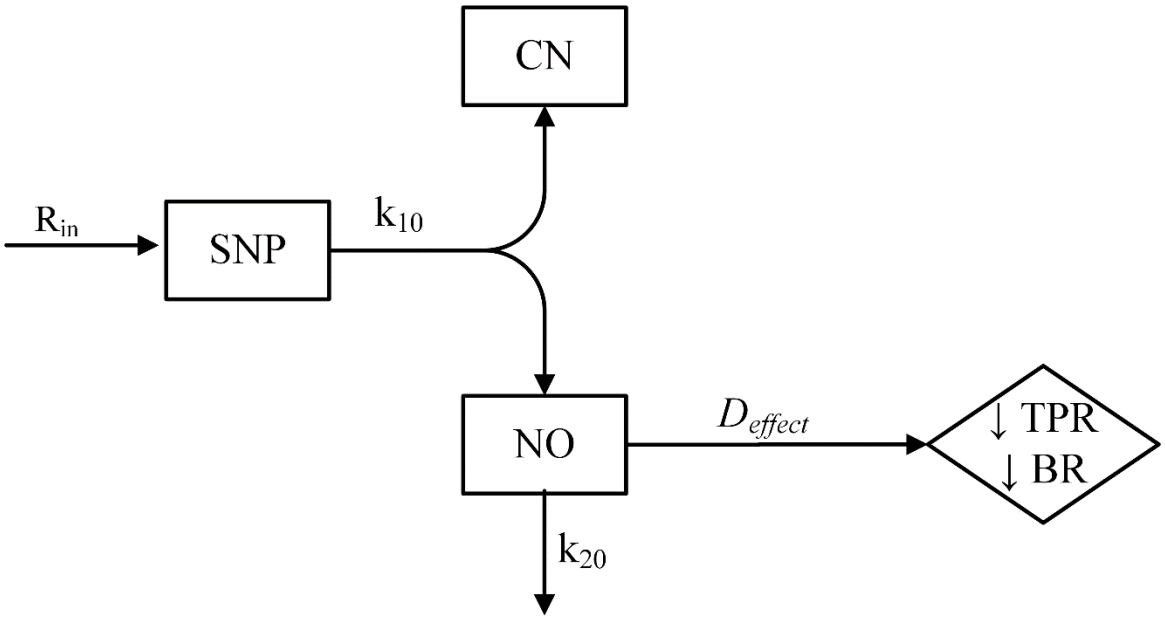

Figure 20 Pharmacokinetic model of sodium nitroprusside infusion. SNP: sodium nitroprusside, CN: cyanide, NO: nitric oxide, TPR: total peripheral resistance, BR: baroreceptor reflex

The elimination rate constants of SNP and nitric oxide were fixed in this setting based on the reported half-life of both compounds in the literature (Hakim et al., 1996, Simmonds et al., 2014, Ivankovich et al., 1978), while the volume of distribution was assumed to be 1 L.

$$\frac{d(SNP)}{dt} = R_{in} - k_{10} \cdot (SNP)$$

$$\frac{d(NO)}{dt} = k_{10} \cdot (SNP) - k_{20} \cdot (NO)$$

$$D_{effect} = \frac{I_{max} \cdot C_{p(NO)}}{C_{50} + C_{p(NO)}}$$

where, R_{in} is the infusion rate of SNP, k_{10} is the first order elimination rate constant of SNP, k_{20} is the first order elimination rate constant of nitric oxide

3.2.3 Model simulation and calibration

The simulations were conducted in MATLAB R2017a (MATLAB, 2017). Only deterministic simulation was considered without accounting for between-subject variability. The parameter values were calibrated based on the physiological plausibility and reported literature estimates.

In this simulation, a single dose of a 30-minute infusion of SNP was added to the system. The different haemodynamic profiles were simulated under two conditions, considering the suggested increased renin activity and assuming no significant changes develop in the renin activity. To switch off the PRA signal, the rate of PRA state change was assumed to be zero (i.e. $\frac{dPRA}{dt} = 0$).

The aim of this simulation was to obtain the signature profile of different haemodynamic variables that can arise with and without considering the increased PRA, and to calibrate the initial parameter estimates that provided a reasonable starting position for estimation. For this simulation, the drug parameters used are (R= 4000 mcg·h^{-1}, k_{10}=20.8h^{-1}, k_{20}=1250h^{-1}, V=1 L, I_{max} =1, C_{50}= 3 mcg·L^{-1}). The MATLAB simulation code is provided in Appendix 2 (section A.2.1).

3.2.4 Model estimation

Model estimation was performed using a nonlinear mixed-effects model framework in NONMEM version 7.3.0 (ICON Development Solutions, Ellicott City, MD, United States). First-order conditional estimation method with interaction (FOCE-I) was used for model fitting. Model runs were executed using Perl-Speaks-NONMEM 4.5.0 (PsN), Pirana 2.9.0 and Xpose 0.4.8. An exponential model was used to describe the between-subject variability (BSV) and an additive residual error model (RUV) was used. For these estimations, model parameters were relaxed one at a time in a stepwise manner, where the run that causes the highest drop in the objective function value is selected. For nested models, the likelihood ratio test (LRT) was used whereby a reduction in OFV of ≥ 3.84 represents a statistically significant difference for one degree of freedom. The BSV parameters (ω^2) were tested to be added to eligible

parameters one at a time in the same manner. Model selection was informed by the minimum objective function value, goodness of fit plots, and parameter value biological plausibility. Model evaluation was based on the visual inspection of goodness of fit of individual plots.

Two different scenarios for SNP mechanism of action were considered in model estimation based on the reported mechanisms in literature as elaborated in section 1.3.1 ; (a) affecting TPR only, (b) affecting both TPR and baroreceptors (i.e. combined mechanism).

3.3 Results

3.3.1 Model structure

The final model structure used to describe the haemodynamic effects of SNP consisted of seven states (two states describing the PK of SNP and five states describing the changes in haemodynamic variables of concern and the feedback signals). The model schematic is shown in Figure 21.

$$\frac{d(SNP)}{dt} = R_{in} - k_{10} \cdot [SNP]$$

$$\frac{d(NO)}{dt} = k_{10} \cdot [SNP] - k_{20} \cdot [NO]$$

$$\frac{d(HR)}{dt} = k_{out} \cdot HR_0 \cdot (1 - BR) - k_{out} \cdot HR$$

$$\frac{d(SV_N)}{dt} = k_{out} \cdot SV_{N_0} \cdot (1 - BR) - k_{out} \cdot SV_N$$

$$\frac{d(TPR)}{dt} = k_{out} \cdot TPR_0 \cdot (1 - BR) \cdot \left(1 - D_{effect}\right) \cdot (1 - F_{PRA} \cdot PRA) - k_{out} \cdot TPR$$

$$\frac{d(BR)}{dt} = k_{out} \cdot fcMAP \cdot \left(1 - D_{effect}\right) - BR$$

$$\frac{d(PRA)}{dt} = k_{PRA} \cdot (fcMAP - PRA)$$

$$D_{effect} = \frac{I_{max} \cdot C_{p(NO)}}{IC_{50} + C_{p(NO)}}$$

$$SV = SV_N \cdot \left[1 - \beta \cdot ln\left(\frac{HR}{HR|_{MAP_{ss}}}\right)\right]$$

$$fcMAP = \frac{MAP - MAP_{SP}}{MAP_{SP}}$$

$$MAP = CO \cdot TPR = HR \cdot SV \cdot TPR$$

The initial values were given by

$A_0 = [SNP_0, NO_0, HR_0, SV_{N_0}, TPR_0, BR_0, PRA_0]$

When $v_0 = v|_{MAP_{SS}}$ $(i.e. HR_0, SV_{N_0}, TPR_0)$, then the initial value for baroreflex and plasma renin activity can be fixed to zero (i.e.$BR_0 = 0, PRA_0 = 0$).

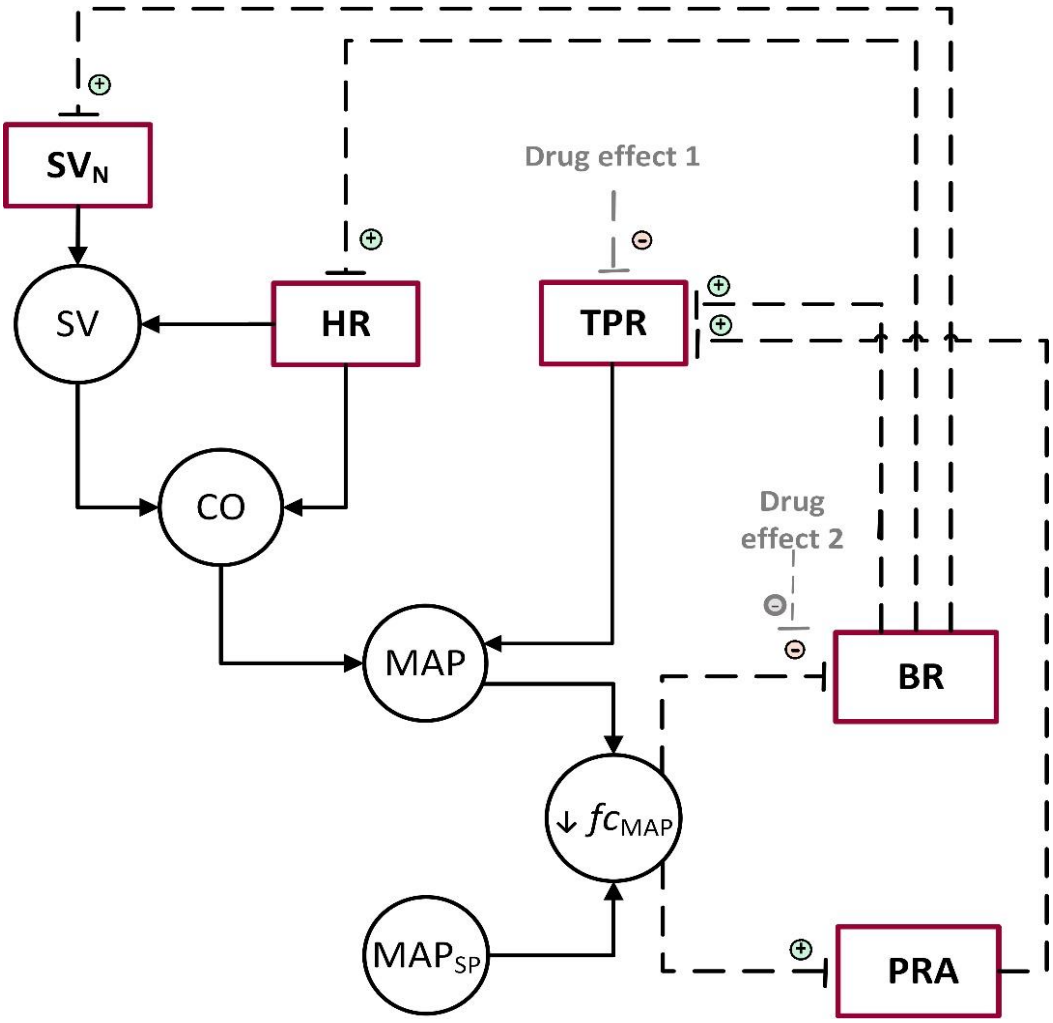

Figure 21 Haemodynamic model for sodium nitroprusside considering the drug affecting both total peripheral resistance and baroreceptors.SV: stroke volume, SV_N : stroke volume normalised to a standard heart rate, HR: heart rate, CO: cardiac output, TPR: total peripheral resistance, MAP: mean arterial pressure, MAP_{SP}: MAP set point, fcMAP: fractional change in MAP, BR: baroreceptor, PRA: plasma renin activity. Circles indicate calculated variables, while boxes indicate model states. Solid lines indicate causal calculations, dashed lines indicates a negative feedback control, positive or negative signs represent the mathematical property.

3.3.2 Model simulation and calibration

Figure 22 depicts the haemodynamic effects of SNP infusion on the different variables with and without considering the possibility of increasing the PRA. It is noted that a resistance

to the effect of SNP on MAP starts to develop over the infusion window (without a corresponding change in SNP level) when the PRA state is considered (solid line), as compared to switching off this state (dashed line). In addition, when the PRA state is considered (solid line), upon stopping the infusion, the TPR and MAP get back to a higher than baseline level and gradually return to the baseline level. This corresponds to the increased level of PRA that does not instantly get back to normal with stopping the infusion (solid line). The same behaviour is observed with the non-directly targeted haemodynamic variables (SV, HR), but in the opposite direction, where they drop to lower than baseline levels and return gradually to the baseline levels.

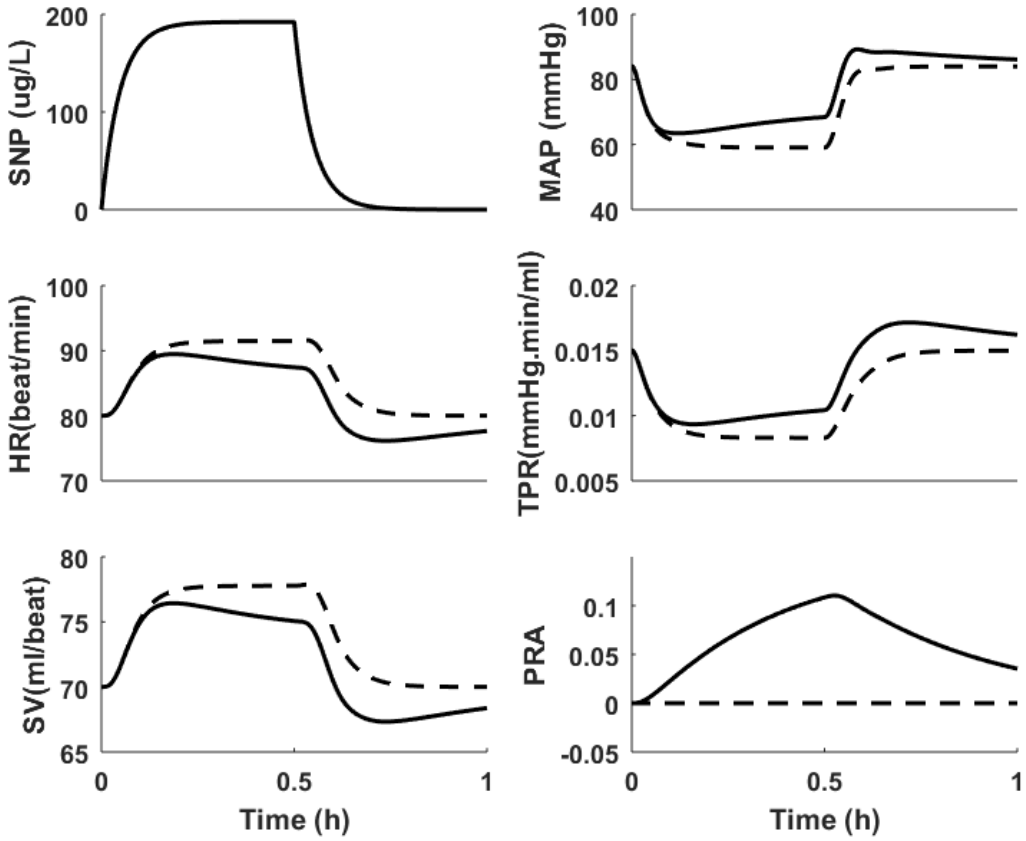

Figure 22 Signature profile of different haemodynamic variables upon a 30-minute infusion of sodium nitroprusside. Solid line represents the model prediction under the PRA feedback control; dashed line represents the model prediction when the PRA is switched off. SNP: sodium nitroprusside, MAP: mean arterial pressure, HR: heart rate, TPR: total peripheral resistance, SV: stroke volume, PRA: plasma renin activity

3.3.3 Model estimation

The final model was developed based on the data from 86 patient with 2617 observations of the dependent variables MAP and HR. In the final model, it was considered that SNP has a dual effect on both peripheral resistance and resetting of the baroreceptors (i.e. a combined mechanism), since it provided a better model fit compared to affecting peripheral resistance only. A single E_{max} function was used to account for this dual effect, since it was

revealed by different model runs that considering two E_{max} functions for the two targets has no benefits on either model fitting or stability.

Because the two dependent variables were measured at the same time points (every two minutes), part of the measurement error (e.g. sample record time) is expected to be correlated across the dependent variables. To account for this correlation arising between the RUV items, correlation in the level-two (L2) data item was considered by adding L2 data item in the dataset and modelling a full sigma matrix for the RUV. In NONMEM, the L2 data item is used to group together observations that have the same realisation of the residual unidentified variability.

Standard residual variability models assume the same residual variability magnitude for all individuals; however, this assumption can be violated with rich data because of the presence of outliers. Allowing between-subject variability on the magnitude of residual variability provides weighting across individuals. Because of the rich sampling schedule in the current study, outliers were accounted for by adding BSV on the RUV.

The differences in patients sensitivities to SNP (e.g. some patients developed tachyphylaxis or were resistant to SNP) were considered by assuming a system parameter for the fraction of plasma renin activity (F_{PRA}). There were two patient subpopulations for drug sensitivity with differences in PRA elicited by SNP infusion (i.e. two F_{PRA}, with population contribution of 67:33%).

In the current analysis, the drug related pharmacokinetic parameters (since there is no PK data) and system parameters (because of model stability issues) were fixed during the estimation runs based on the reported values in the literature, and the physiological plausibility. Only drug related PD parameters, initial conditions and BSV parameters were allowed to be estimated. The final parameter estimates are shown in Table 5. The NONMEM estimation code and model building table is provided in Appendix 2 (section A.2.2).

Table 5 Final parameter estimates of the extended PKPD model.

Parameter /initial condition (unit)	***Description***	***Final estimate***	***BSV CV% [η_{sh}%]***
PK parameters			
$k_{10}\ (h^{-1})$	The first order elimination rate constant of nitroprusside	20.8*	
$k_{20}\ (h^{-1})$	The first order elimination rate constant of nitric oxide	1250 *	
$V(L)$	Volume of distribution of nitric oxide	1 *	
Initial conditions			
$SV_0(ml \cdot beat^{-1})$	Stroke volume initial condition	70 *	
$HR_0(beat \cdot min^{-1})$	Heart rate initial condition	81.4	22 [4%]
$MAP_0\ (mmHg)$	Mean arterial initial condition	79.1	13.9[5%]
System- related parameters			
$k_{out}(h^{-1})$	The first order dissipation rate constant of the systems four state variables	25 *	
$k_{PRA}(h^{-1})$	The first order dissipation rate constant of plasma renin activity	1.5 *	
β (uniteless)	A scalar for the log-linear relationship of heart rate and stroke volume	0.212 *	
Drug PD parameters			
I_{max} ***(uniteless)***	The maximum inhibitory fractional drug effect that could be achieved	1 *	
$C_{50}\ (\mu g \cdot L^{-1})$	The nitric oxide concentration producing half of the maximum inhibitory effect.	2.99	131[12%]
Probability of low PRA		0.692	
F_{PRA} ***– low (uniteless)***	The fraction of plasma renin activity for the subpopulation with low plasma renin activity	0.01 *	

$F_{PRA} - high$ ***(uniteless)***	The fraction of plasma renin activity for the subpopulation with high plasma renin activity	10.7	
RUV parameters			
$\sigma^2_{add_{MAP}}$ [ε_{sh}%]	Additive RUV on mean arterial pressure	58.7[1%]	47.2[8%]
$\sigma^2_{add_{HR}}$ [ε_{sh}%]	Additive RUV on heart rate	47.4[1%]	57.9[4%]
cov_{σ} ($corr$%)	Covariance between the L2 data item	5.35(10.3%)	

****Fixed parameter***

CV; Coefficient of variation

3.3.4 Model evaluation

Individual plots for MAP and HR were plotted considering the infusion rate (black solid line) as a secondary y-axis to give an indication of how the haemodynamic response was influenced by the change in infusion rate. In addition, the target predetermined MAP for each patient was added to the plots as a guide to elaborate how the decision to up titrate or terminate the infusion rate was taken.

For most patients, there was a general alignment between observations and the model individual predictions (IPRED). However, predictions at the population level (PRED) were generally not well aligned with observations. Some patients (e.g. ID 31, ID 56, and ID 177) could not be described by even IPRED, since they showed unexplained haemodynamic response (e.g. increased MAP upon SNP infusion) which is not supported by the mechanistic underlying of the model as shown in Figure 24.

Some patients showed a development of resistance (i.e. tachyphylaxis) to the effects of SNP, exhibiting an initial drop in MAP followed by a gradual increase in MAP with no change of SNP infusion rate. Figure 23 shows the individual plots for patients developing tachyphylaxis, and how the IPRED provides a good description for this pattern of response.

A sample of individual plots for some patients for MAP and HR are shown in Figure 25 and Figure 26. The individual plots for all the patients is provided in Appendix 2 (Section A.2.3)

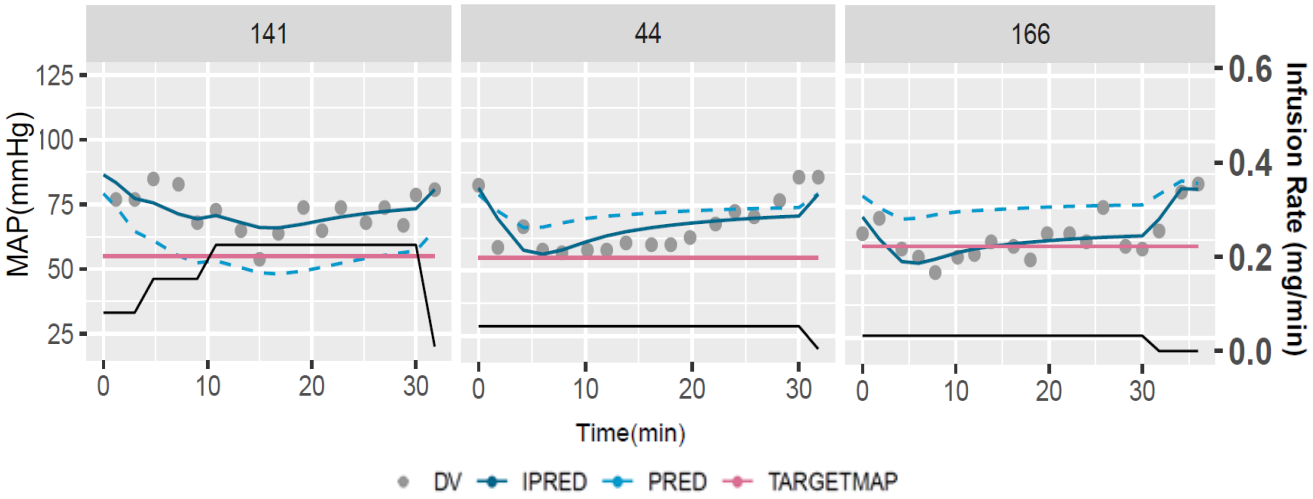

Figure 23 individual plots of some patients showing tachyphylaxis upon infusion of nitroprusside. The black solid line represents the infusion rate of nitroprusside.

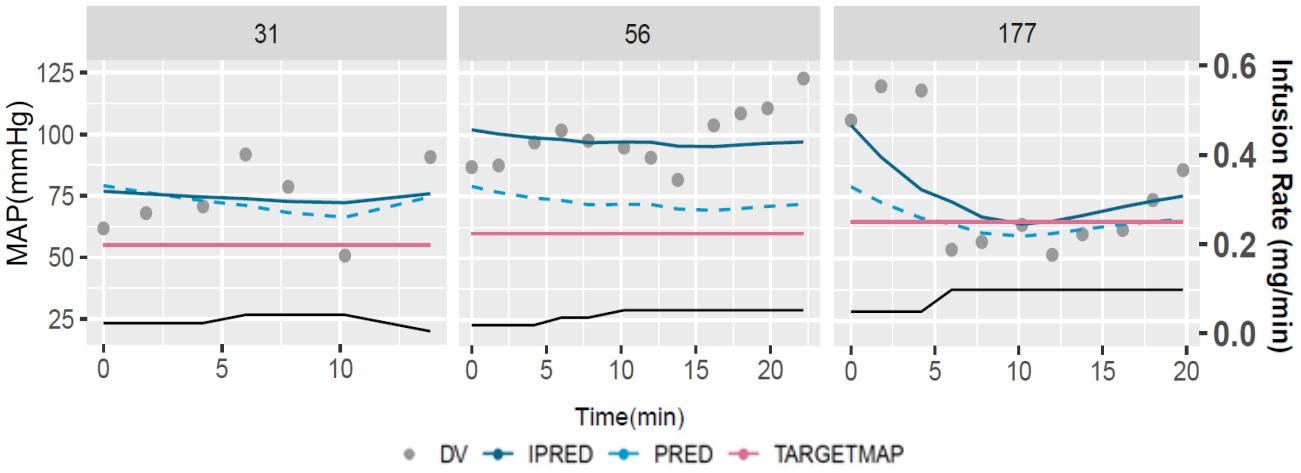

Figure 24 individual plots of patients who showed increased mean arterial pressure upon infusion of nitroprusside. The black solid line represents the infusion rate of nitroprusside.

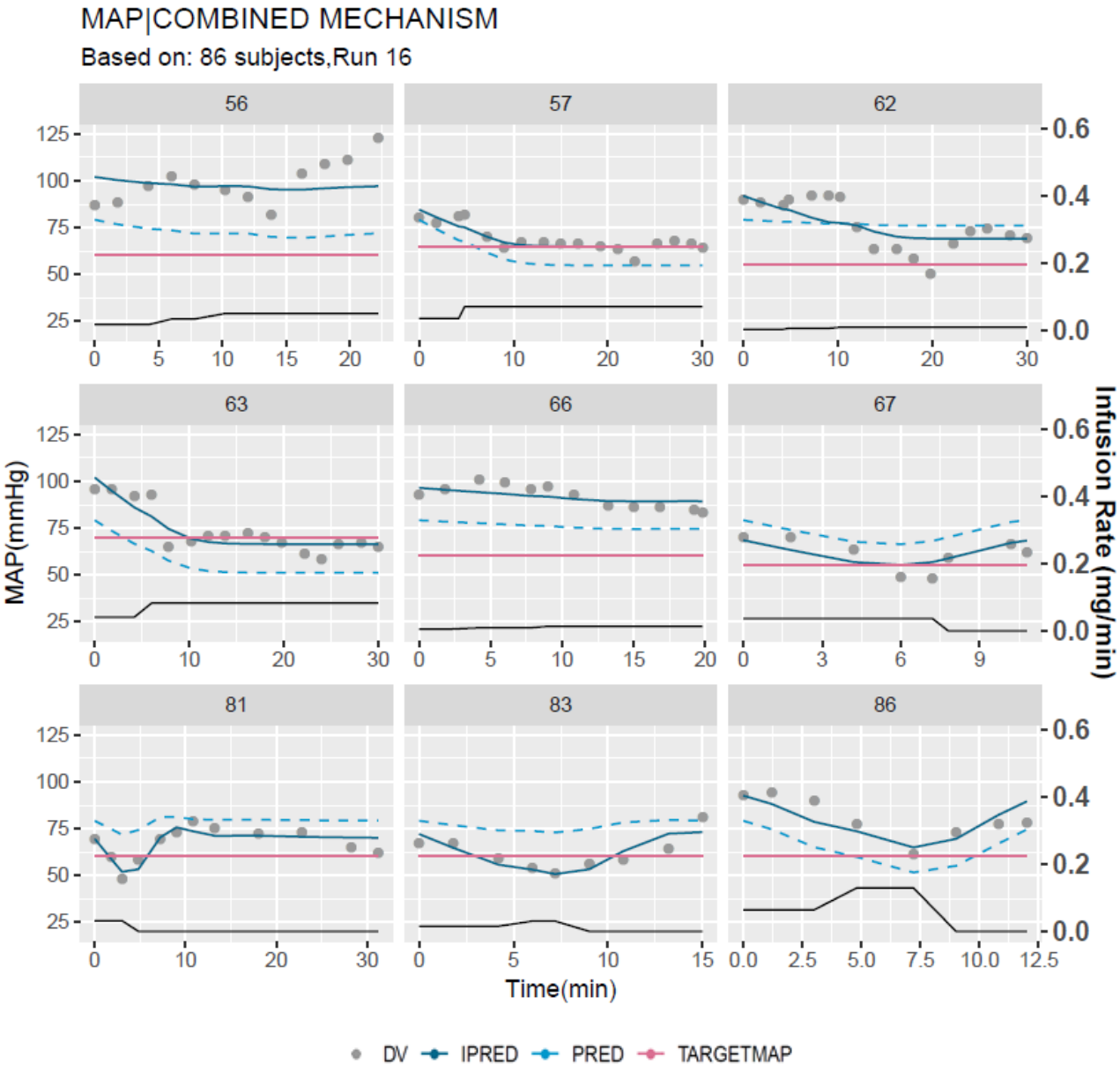

Figure 25 A sample of individual plots of mean arterial pressure versus time. The black solid line represents the infusion rate of nitroprusside.

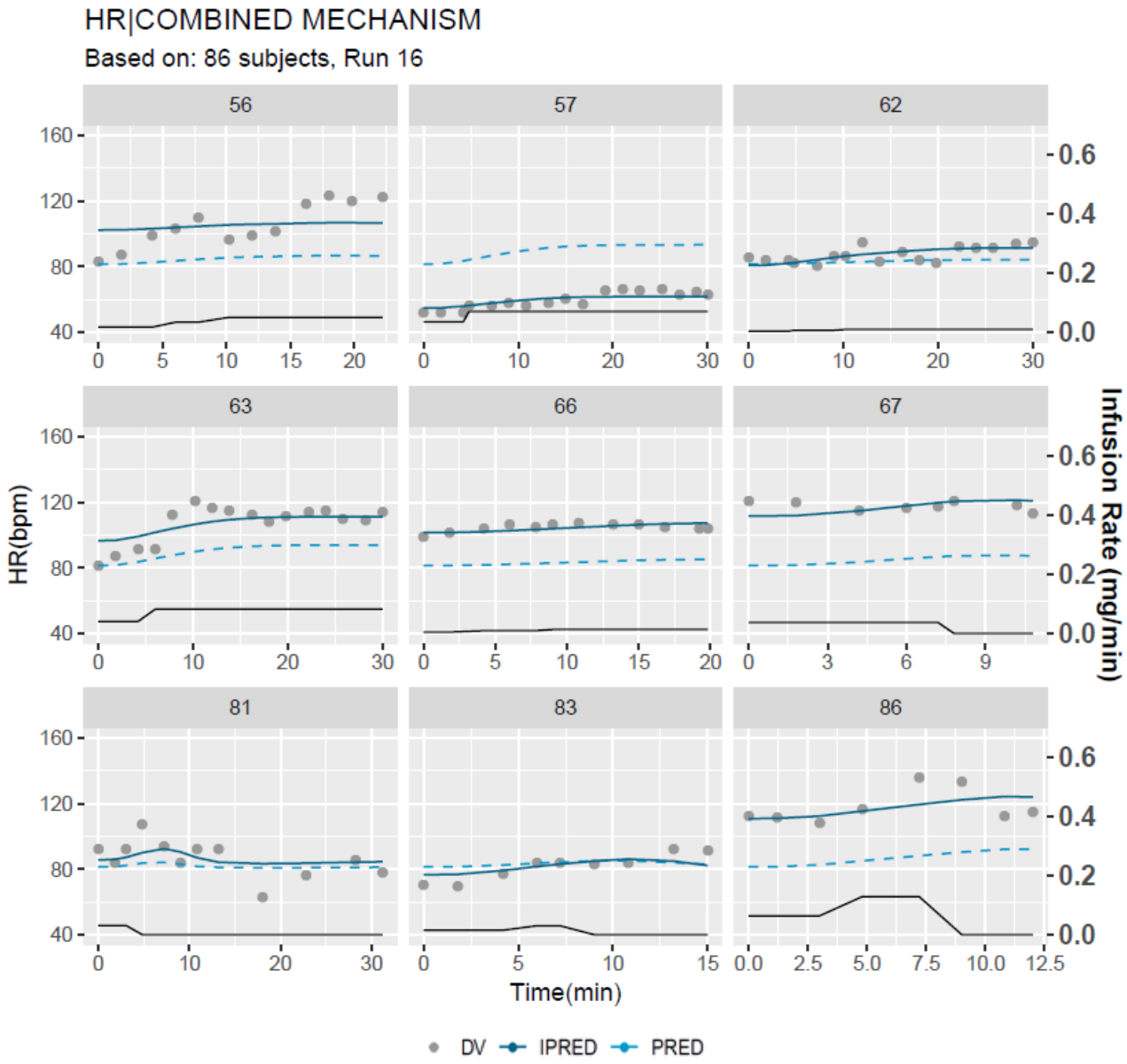

Figure 26 A sample of individual plots of heart rate versus time. The black solid line represents the infusion rate of nitroprusside.

3.4 Discussion

The current work presents an evaluation of the minimal haemodynamic model developed in chapter 2. An extended PKPD (i.e. semi-mechanistic) model to describe the haemodynamic effects of sodium nitroprusside in adolescents undergoing surgery was developed. The model structure was adapted from the minimal haemodynamic model and extended based on the postulated drug mechanisms of action and haemodynamic physiologic responses reported in the literature. The model was fitted to haemodynamic data and provided a good description for MAP and HR changes, based on the individual prediction plots.

A mixture KPD model was previously developed by modelling the full range of age of individuals participated in the study used in the current analysis (Barrett et al., 2015). However, in their work, only MAP measurements were considered when modelling the data, and the whole age range for the study population (3 days-17 years old) was included in their analysis (203 patients). The model provided good prediction for the data, but could not provide an explanation for the two levels of drug sensitivity exhibited by the study participants. This is why a mixture model was used with two patient subpopulations having different C_{50} estimates.

In the present work, we tried to implement a mechanistic approach to characterise the SNP haemodynamic effects and to provide a deeper insight into the underlying mechanism of different drug sensitivities and tachyphylaxis that may emerge upon the administration of SNP.

The previously developed minimal haemodynamic model was extended by adding a state describing the changes in PRA, as guided by the proposed mechanism to explain the development of tachyphylaxis in some individuals by increased PRA (Abukhres et al., 1979, Amaranath and Kellermeyer, 1976, Bush and Vollmer, 1984, Cottrell et al., 1980, Cottrell et al., 1978, Lagerkranser et al., 1985, Miller et al., 1977). Model simulations with and without accounting for the possibility of increased PRA upon SNP infusion (see Figure 22) show how accounting for PRA (solid line) adds model flexibility to describe the gradual resistance development in some individuals, and the rebound hypertension that can develop upon stopping SNP infusion. The individual plots further confirmed this as illustrated in Figure 23, which gives an example of the model ability to capture the haemodynamic profile of patients developing tachyphylaxis.

It was noted that the population predictions (PRED) did not provide a sufficient description for the data. This can be explained by the fact that the current model does not have any covariates as part of the model. This aligns with the previously published analyses on the

same study data using either the blinded phase or open-labelled phase, which could not correlate any of the investigated factors such as age, baseline MAP, surgery type, and dose adjustment frequency or magnitude as an eligible covariate to predict the haemodynamic response (Barrett et al., 2015, Spielberg et al., 2014). On the other hand, the individual model predictions (IPRED) showed an overall good description for most individual profiles. By looking at the eta-shrinkage for the final parameter estimates (see Table 5), none of the values exceed 20%, which allows a reasonable diagnosis of the IPRED fitting for the individual data.

The model could not explain some of the haemodynamic profiles (see Figure 24), where an increased MAP was developed upon the infusion of SNP. The mechanistic assumption underlying the model is that SNP decreases MAP by inhibiting the TPR and resetting the baroreceptor reflex, which contradicts the observed profiles. However, these profiles can be explainable if we considered several factors that may affect blood pressure other than SNP administration in this study setting. For example, pain, anaesthesia, other administered medications, and excitement, which all are known to affect blood pressure; however, these factors were not recorded and therefore are not accounted for in the model.

Although visual predictive check (VPC) is a widely used simulation based tool to diagnose model bias with respect to both the fixed and random effects, it was not feasible to generate it for our final model. The current study design was based on adaptive dosing, where the individual infusion rate is adjusted to the response (i.e. achieving the predefined target MAP). In this case generating prediction corrected VPC (pcVPC), is advised where it requires implementing the adaptive dosing algorithm when simulating the original dataset (Bergstrand et al., 2011). The study protocol stated that in each of the four doing groups, the patients will be initiated at one-third the full infusion rate for 5 minutes, then increased to two-thirds the full rate for 5 additional minutes, then the dose was increased to the full rate if the target MAP was not attained. In addition, termination of the infusion was advised in case of MAP drop below the target MAP. However, observing the data records showed inconsistencies in following the study protocol for most of the individuals, which makes it hard to implement adaptive dosing algorithm to simulate the data and generate a pcVPC. Generated pcVPC without accounting for adaptive dosing is provided in Appendix 2 (Section A.2.4)

The model provided a good description to the data, nevertheless there are some limitations related to the study design and the data collection that may not support drawing inference to other clinical settings. First, the patients received other medications affecting the haemodynamics including anesthetic agents, plasma expanders; however, we cannot backtrack

what happened to these patients, and we do not have access to the exact timing for administering these medications. Secondly, although the model provided a mechanistic description of the tachyphyalxis as explained by increased PRA, it was still not possible to provide an explanation for the high variability in PRA, which required implementing a mixture model. As compared to the previously published mixture KPD model on the same data (Barrett et al., 2015), the final model was not able to further our understanding of why some patients show to a higher sensitivity to the drug than the others (i.e. belong to a high C_{50}, or low a PRA subpopulation). Moreover, the current model parameter estimates were assessed based on data in adolescents undergoing surgery under anaesthesia, hence they could vary in other settings.

3.5 Conclusions

We have developed an extended/semi-mechanistic PKPD model to describe the haemodynamic effects of sodium nitroprusside intravenous infusion in adolescents undergoing surgery. SNP was shown to exhibit a combined mechanism by inhibiting TPR and resetting baroreceptor reflex, with an ultimate hypotensive effect. The model fitted most of the data well suggesting its mechanistic plausibility and the flexibility to describe the different response patterns elicited by SNP.

CHAPTER 4: DISCUSSION AND CONCLUSIONS

4.1 Discussion

The scope of the present thesis was implementing pharmacometric methods in the modelling of haemodynamics in humans. We presented a minimal haemodynamic model and showed model application to clinical data from the literature on drugs targeting different aspects of the cardiovascular system. The model was intended to be used for estimation purpose in top-down modelling. The model was developed based on the cardiovascular physiology reported in literature and previously published models describing the haemodynamic variables. The final model is composed of four states and three parameters and can be used to quantify and understand the mechanistic effects of pharmacological agents on the short-term haemodynamics of the CVS in humans.

The minimal model was evaluated using clinical data from the literature for drugs targeting HR and total TPR. HR and MAP data from clinical studies on patients who received either metoprolol or nifedepine were digitised and superimposed with predictions from the minimal model. The results of model evaluation show model flexibility to characterise the different haemodynamic profiles at different perturbation sites without data fitting. Moreover, a hypothetical scenario of model simulation with and without considering the baroreceptor reflex shows that the current closed-loop structure is able to capture the changes in other system's states that may not be the primary perturbation site. Compared to published PKPD models, which usually describe the haemodynamic variables separately without accounting for the interrelationship between these variables, the current model can accommodate extrapolation to situations beyond the range of the data.

The developed minimal haemodynamic model was applied to clinical data from adolescents who received intravenous infusion of SNP during surgery in order to induce hypotension. Controlled hypotension is an intraoperative technique used to lower the BP during surgery and keep it within a certain predefined window to limit intraoperative blood loss, reduce the need for blood transfusions, and improve visualisation of the surgical field. The minimal model was extended to accommodate the postulated mechanism of action of SNP in literature.

The hypotensive effect of SNP has been explained in the literature by being a nitric oxide donor having a direct action on vascular smooth muscle inhibiting TPR and causing vasodilation (Tinker and Michenfelder, 1976). Some studies postulated the effect of SNP on the resetting of the aortic baroreceptors with shifting of the system's set point toward a lower level of MAP (Fritsch et al., 1989, Salgado and Krieger, 1988, Deabreu and Salgado, 1990).

The current model application supports a combined mechanism for SNP by inhibiting TPR and resetting baroreceptor reflex, with an ultimate hypotensive effect. Several studies have reported rapid progressive tolerance development upon infusion of SNP and linked this to increased plasma renin activity (PRA) resulting in an opposing vasoconstrictive effect (Heuser et al., 1985, Cottrell et al., 1980, Amaranath and Kellermeyer, 1976, Cottrell et al., 1978, Khambatta et al., 1979, Delaney and Miller, 1980). Tachyphylaxis development was explained in the model by the PRA, which was added as a new model state to link the changes in PRA to the progressive tolerance that develops in some patients. Due to lack of PK data of SNP, a simple one-compartment PK model for SNP and nitric oxide was added to the model, assuming first order elimination of SNP and nitric oxide.

Observed MAP and HR data in these patients were superimposed with predictions from the model. The individual model predictions (IPRED) fitted most of the data well, while having low shrinkage estimate, suggesting its mechanistic plausibility and the flexibility to describe the different response patterns elicited by SNP. However, the population predictions (PRED) did not provide a sufficient description for the data which is justified by the lack of covariates in the current model. This aligns with the previously published analyses on the same study data (including other study phases and age groups in the analysis), which could not correlate any of the investigated factors such as age, baseline MAP, surgery type, and dose adjustment frequency or magnitude as an eligible covariate to predict the haemodynamic response (Barrett et al., 2015, Spielberg et al., 2014).

Previously, Barrett et al. developed a mixture KPD model for SNP using the data from all the age range of the study used in the current analysis (Barrett et al., 2015). The model could not provide an explanation for the two levels of drug sensitivity exhibited by the study participants. The current model provided a mechanistic description for the development of tachyphylaxis by linking increased PRA to tachyphylaxis development. This was explained by the relatively slow decline in PRA with a half-life of approximately 30 min (Cottrell et al., 1980). Nevertheless, due to limitations pertaining to the lack of adequate record for probable confounding factors (e.g. administration of other medication affecting haemodynamics, pain, and excitement), the model was not able to fully explain the mechanistic underlying of different patient sensitivities to SNP.

4.2 Limitations and future perspectives

The proposed model does not account for the circadian variability on the autonomic function. This could be a potential for a future work to expand the utility of the current model to situations when the influence circadian variability is evident. On the other hand, the model depends on MAP measurements to derive the haemodynamic profiles. Nevertheless, in the clinical setting, BP is usually assessed by SBP and DBP rather than MAP, which requires an invasive technique to be measured, so MAP is approximately calculated from SBP and DBP (Klabunde, 2012). However, at high HR, the formula used to calculate MAP from SBP and DBP may not hold anymore because of the change in the length of cardiac cycle and distribution between systole and diastole (Moran et al., 1995, Razminia et al., 2004). This limits the model application to situations of a significant increase in HR such as in high intensity exercise where this relationship may not be constant.

Furthermore, extending the current minimal model structure to include arterial compliance and pulse pressure (PP) will allow SBP and DBP to be modelled separately apart from MAP. PP gives a better description of the pulsatile components of BP (i.e. SBP, DBP) compared to MAP that describe the static component of BP (i.e. indicates tissue perfusion). PP is highly affected by the compliance of blood vessels, hence it provides a better prognostic sensitivity in cardiovascular risk stratification and arterial stiffness at older age relative to MAP, which could show a slight change, keeping it within the normal range (Selvaraj et al., 2016). Adding these components to the model could in turn enhance the model capacity to describe the influence of aging and arterial stiffness on haemodynamics. However, this require further clinical data to support and evaluate model extension.

Although the model application supports the possible combined mechanism of SNP (i.e. inhibiting TPR, and resetting of baroreceptor), further clinical studies need to be conducted in different settings to provide an evidence for this postulation. On the other hand, the current model was evaluated using SNP data in adolescents. The developmental changes in the haemodynamic variables (e.g. SV, HR, and TPR) are linked to body size changes and physiologic maturation in children and adolescents. This has been described using different allometric power functions per each age stratum (Gillum et al., 1982, de Simone et al., 1997, Ma et al., 2012, Dewey et al., 2008). Model scaling to other age groups could enhance the model application to paediatrics. Further clinical data is needed to evaluate model application to paediatrics.

4.3 Conclusions

In conclusion, in the present thesis pharmacometric methods were implemented to develop a minimal haemodynamic model and to apply it to clinical data of SNP in adolescents undergoing surgery. The minimal model was provided as an open access source through GitHub to be used as a generic platform to characterise the short-term haemodynamic changes in humans (https://github.com/SalmaBahnasawy/SysModel.git). Model extension to mechanistically describe the haemodynamic effects of SNP showed the mechanistic plausibility of the proposed model.

APPENDIX 1: APPENDIX TO CHAPTER 2

A.1 Minimal haemodynmic model use for estimation

Two data sets extracted from literature were used to evaluate the model use for estimation purposes. The following points were considered in the current analysis

1. The extracted data were reported as mean ± SD:
   a. PK (drug plasma concentration)
   b. PD(systolic blood pressure, diastolic blood pressure, heart rate)
2. For model estimation, only PD data were modelled. PK data were used as covariate to link PK to PD using Emax model. This is to minimise the variability/error arising from having the summary statistics of the PK to propagate to the PD, which is the main scope of the model.
3. Data sets in the NONMEM format were created using R:
   a. 2 DVs (MAP, HR), with DVID column as a flag
   b. Concentration entries were added in a separate column as a covariate.
   c. The different dose levels were considered as different individuals (e.g. 2 dosing levels→ 2 IDs), with BSV allowed on the initial conditions (i.e.MAP_0, HR_0)
4. For the nifedipine dataset
   a. PD data are intensely sampled (every 5 minutes for 60 minutes, 13 record) while the PK data are more sparsely sampled (6 records over 60min). Linear interpolation was implemented to impute the missed PK measurement using $FINEDATA utility in NONMEM, and checked the resulting PK profile graphically before using the resulting full data set with imputed concentrations.
   b. The reported summary PK, PD are not matching in the number of patients (for the 10 mg dose: PD is the mean of 11 patients, while PK is the mean of 7 patients).

Results

i.Model estimates

a. Metoprolol dataset

Model.no	Description	OFV	θ_{SV0}	θ_{HR0} (RSE%)	θ_{MAP0}(RSE%)	θ_{kout}	θ_{β}	θ_{Imax}(RSE%)	θ_{c50} (RSE%)	ω_{HR0} (RSE%) [$\eta_{sh\%}$]	ω_{MAP0} (RSE%) [$\eta_{sh\%}$]	σ_{addMAP} (RSE%) [$\varepsilon_{sh\%}$]	σ_{addMAP} (RSE%) [$\varepsilon_{sh\%}$]
run1	metoprolol dataset with BSV on HR_0, MAP_0	111.828	90	70.1(1.5%)	115(3. 3%)	35	0.212	0.279 (34.7%)	32.9(122.5%)	0.0016(50.6%) [5%]	0.00267(10%)[0%]	5.67(51.1%)[5%]	1.9(8.6%)[5%]

a. Nifedipine dataset

Model.no	Description	OFV	θ_{SV0}	θ_{HR0} (RSE%)	θ_{MAP0}(RSE%)	θ_{kout}	θ_{β}	θ_{Imax}(RSE%)	θ_{c50} (RSE%)	ω_{HR0} (RSE%) [$\eta_{sh\%}$]	ω_{MAP0} (RSE%) [$\eta_{sh\%}$]	σ_{addMAP} (RSE%) [$\varepsilon_{sh\%}$]	σ_{addMAP} (RSE%) [$\varepsilon_{sh\%}$]
run1	Nifedipine dataset with BSV on HR_0, MAP_0	132.662	90	76.2(0.8%)	136(0.3%)	35	0.212	0.57 (12.6%)	52.1(40.7%)	0.0002 (40%) [0%]	0.0001 (66.7%) [0%]	3.25 (6.1%) [3%]	5.22 (1%) [3%]

*Fixed

A. Metoprolol

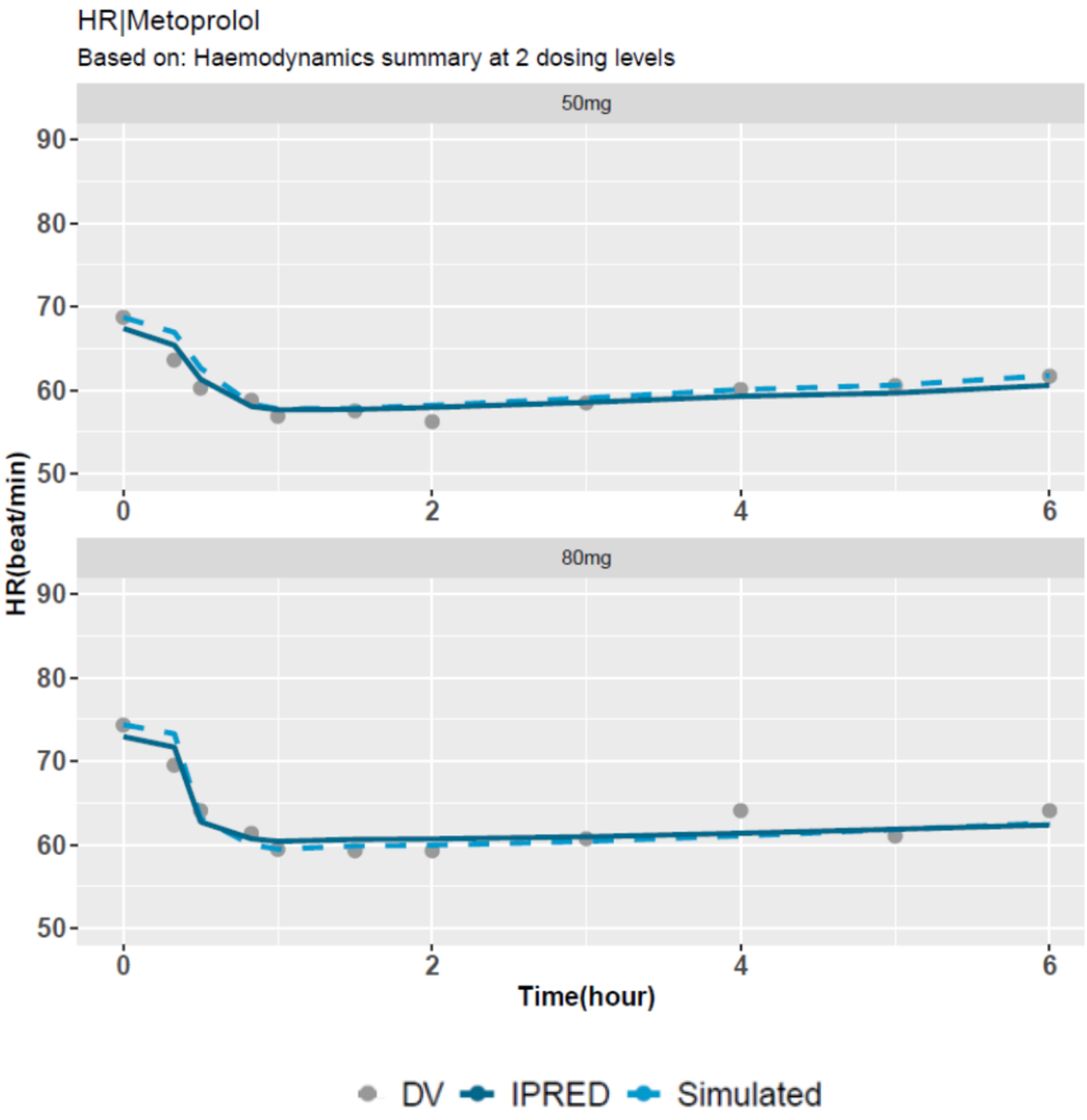

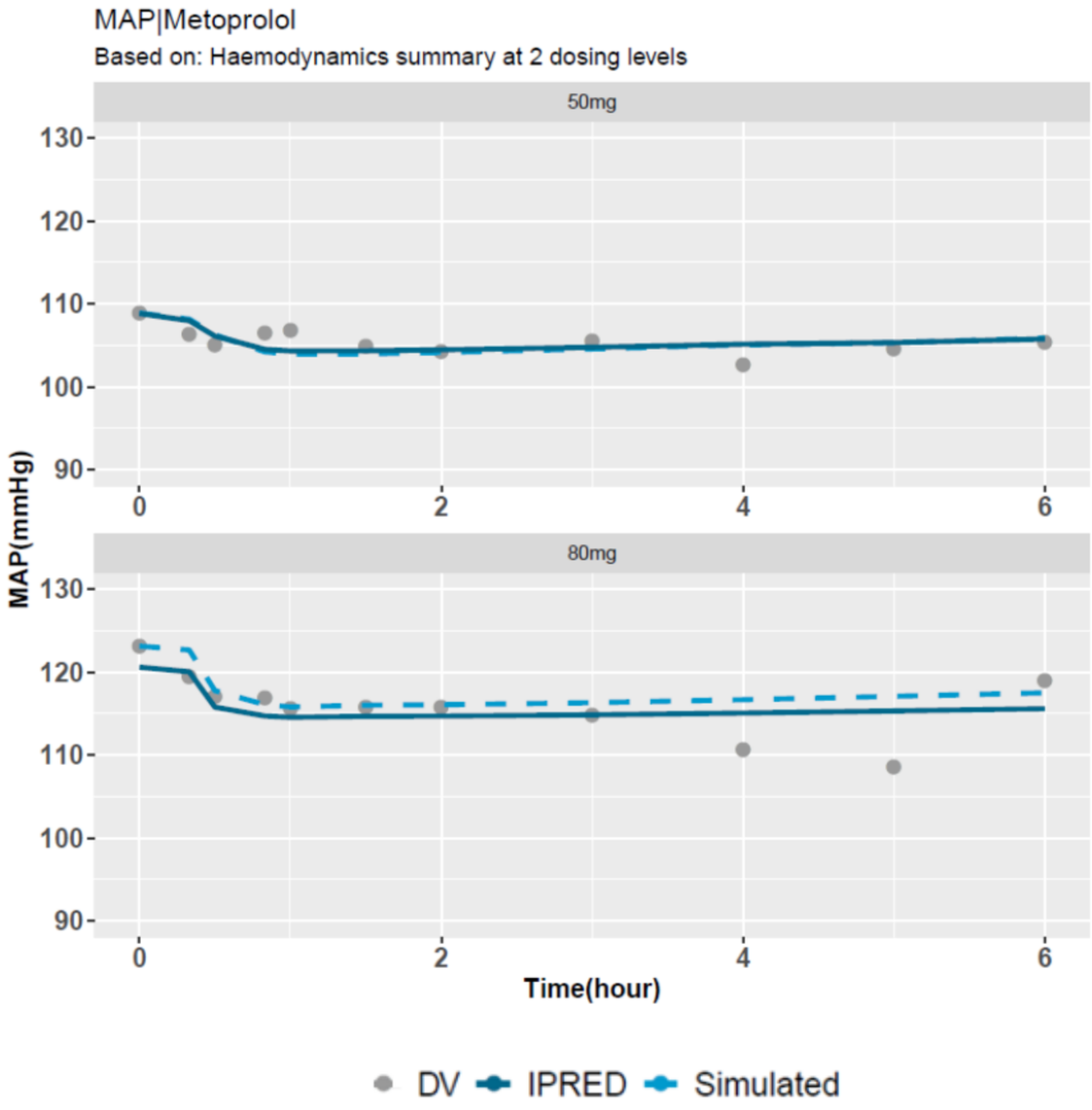

B. Nifedipine

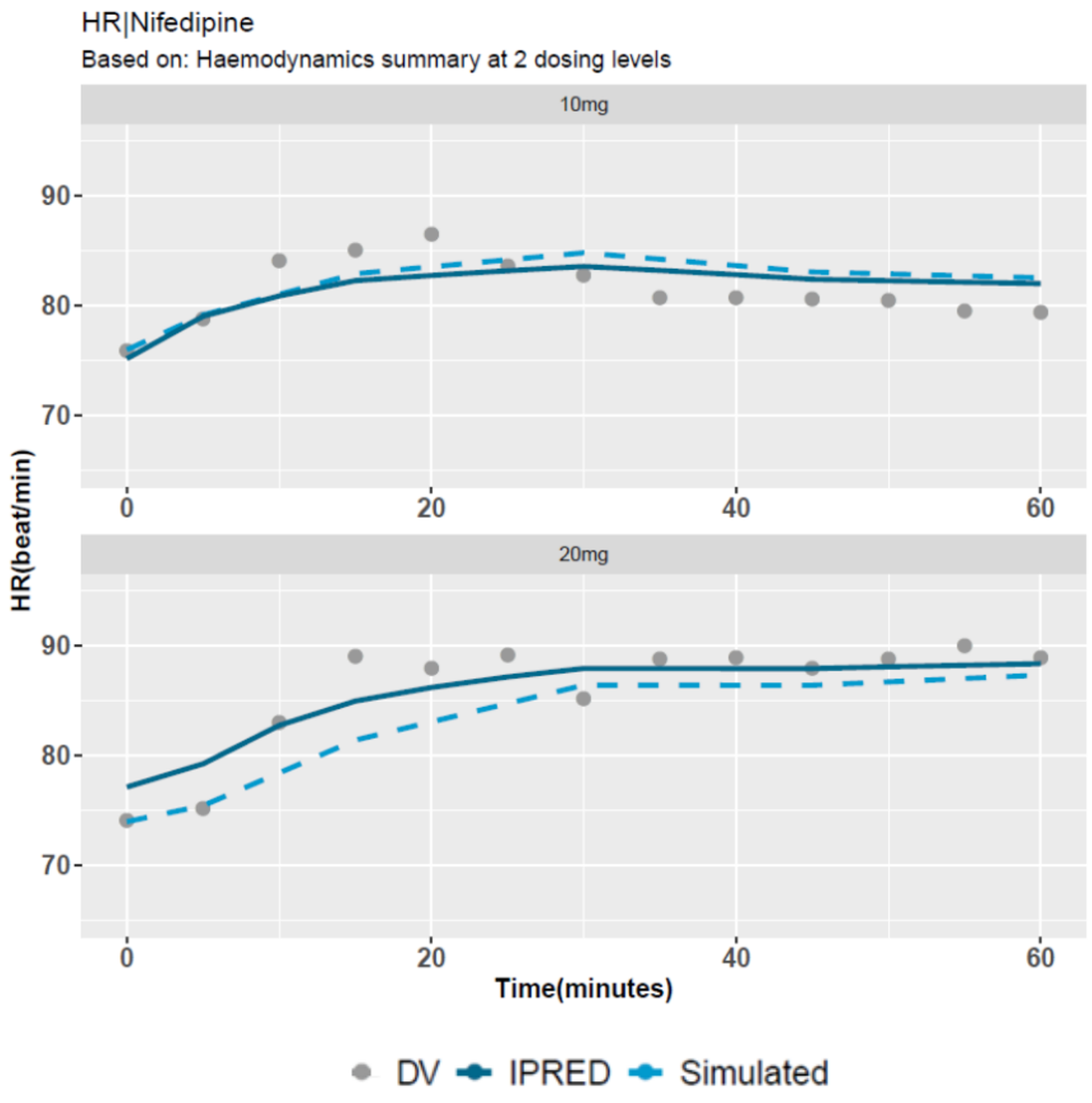

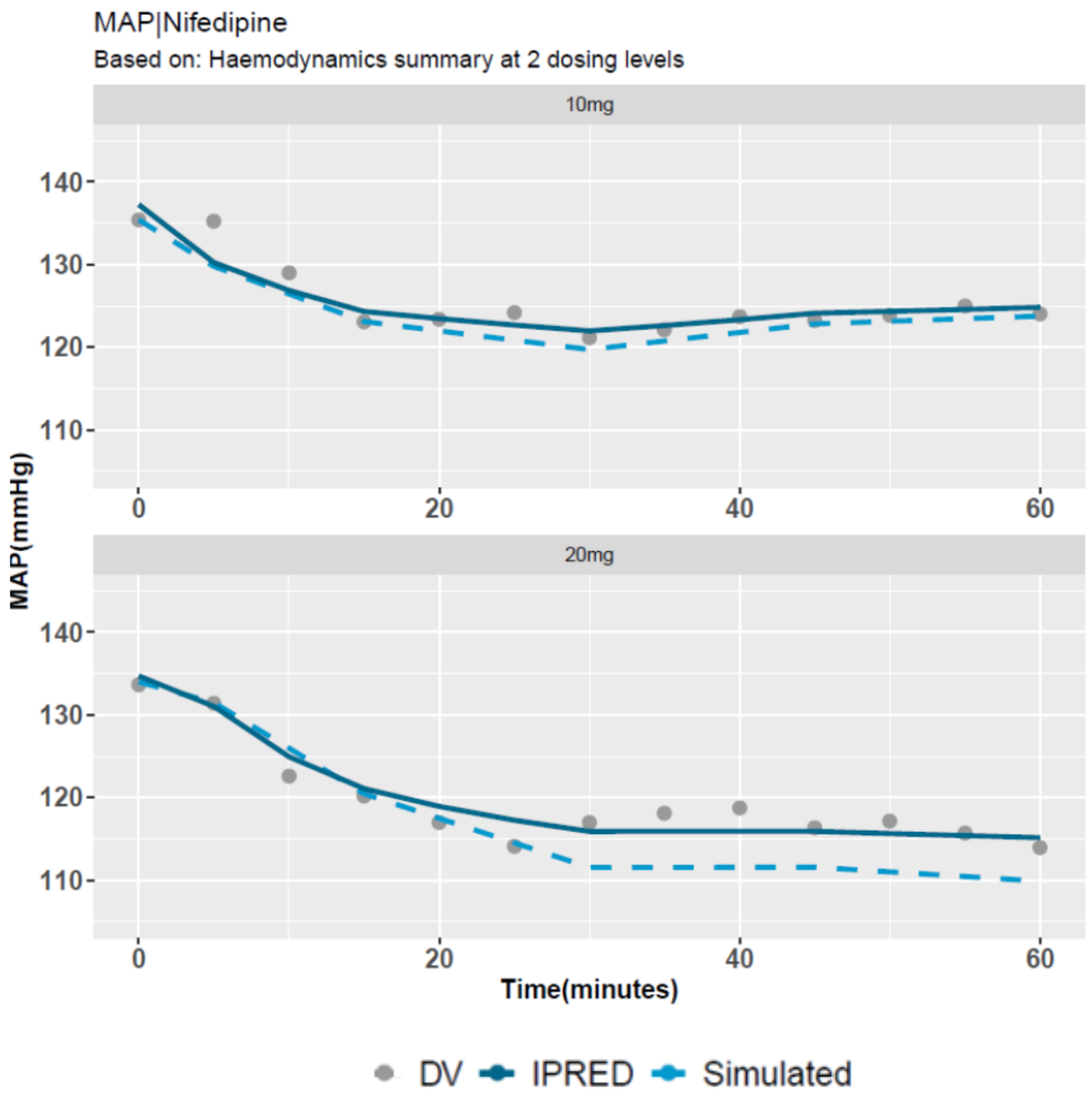

NONMEM code for estimation of nifedipine dataset

```
$PROBLEM ESTIMATION OF Nifedipine dataset
$INPUT ID TIME DOSE=DROP DV DVID CONC CMT
$DATA Nifefull.csv
IGNORE=#
$SUBROUTINE ADVAN6 TOL=4

$MODEL
COMP(SV)
COMP(HR)
COMP(TPR)
COMP(BR)

$PK
; PD model
SV0= THETA(1)
HR0= THETA(2)*EXP(ETA(1))
MAP0= THETA(3)*EXP(ETA(2))
KOUT=THETA(4)
BET=THETA(5)
Imax= THETA(6)
C50= THETA(7)
```

```
; specify initial conditions
TPR0=MAP0/(HR0*SV0)
A_0(1)= SV0
A_0(2)= HR0
A_0(3)= TPR0
A_0(4)= 0

$DES
; Specify drug effect model
I = (Imax*CONC)/(C50+CONC) ;drug effect on TPR

; set points & MAP
MAP_SP=MAP0
SV=A(1)*(1-BET*LOG(A(2)/HR0))
MAP = A(2)*A(3)*SV
DELTA = (MAP-MAP_SP)/MAP_SP                    ;change in
  blood pressure

; specify ODEs of differnet cmt
DADT(1)= KOUT*SV0*(1 - A(4)) -  KOUT*A(1)      ;SV
DADT(2)= KOUT*HR0*(1 - A(4)) - KOUT*A(2)       ;HR
DADT(3)= KOUT*TPR0*(1- A(4))*(1-I) - KOUT*A(3) ;TPR with the drug
  effect
DADT(4)= KOUT*DELTA - KOUT*A(4)                ;delta BR
```

```
$ERROR
SV2=A(1)*(1-BET*LOG(A(2)/HR0))
HR=A(2)
TPR=A(3)
BR=A(4)
IMAP= SV2*HR*TPR

IF (DVID.EQ.1) THEN
IPRED=IMAP
Y=IPRED+EPS(1)
ENDIF

IF (DVID.EQ.2) THEN
IPRED=HR
Y=IPRED+EPS(2)
ENDIF

$THETA
 90 FIX ;SV0
 (60, 75, 140) ; HR0
 (90,130,150) ; MAP0
 (10, 35, 100)  FIX ; KOUT
 (0, 0.22, 0.9) FIX;BETA
 (0.01,0.6, 1) ; Imax
 (20,120,150) ; C50
```

```
$OMEGA
 0.01  ;PPVHR
 0.01  ;PPVMAP

$SIGMA
 5 ;ADDMAP
 5 ;ADDPHR

$EST MAXEVALS=9999 NSIG=3 NOABORT PRINT=20 METHOD=COND
  INTER
$COV
$TABLE ID TIME CMT DV DVID PRED IPRED RES CWRES NOAPPEND
  ONEHEADER NOPRINT FILE=sdtab1
$TABLE ID TIME ETA(1) ETA(2) NOAPPEND ONEHEADER NOPRINT
  FILE=patab1
```

APPENDIX 2: APPENDIX TO CHAPTER 3

A.2.1 MATLAB simulation code for model

Run file (PD_run.m)

```
%% SNP Model simulation w/out PRA

clear all % clears variable cache
clc  % clears screen

%% Parameter input
PD_parameters
T=[];
Y=[];
%% Set initial conditions & run simulation
get_initials
options = odeset('RelTol',1E-7);

[t, A]= ode15s(@PD_ODEs_PRA,[0 1], A0, options,  K0, K10,  K20,
 V, Imax, IC50, SP_MAP0, SV0,HR0, TPR0, KOUT,k);
VEC
Time=t;
output_PRA=table(Time, SNP,MAP, HR,TPR,SV,PRA);

[t, A]= ode15s(@PD_ODEs_noPRA,[0 1], A0, options,  K0, K10,
 K20, V, Imax, IC50, SP_MAP0, SV0,HR0, TPR0, KOUT,k);
VEC
Time=t;
output_noPRA=table(Time, SNP,MAP, HR,TPR,SV,PRA);

%% Output visualisation
% PD_profile
overlaidPlot
```

Model Parameters (PD_parameters.m)

```
%% PK parameters
```

```
V=1;
K0=4000; %infusion rate (ug/hr)
K10 = 20.8; %hr-1 SN
K20= 1250; %hr-1 T0.5=2sec

%% system parameters
k=1.5;
KOUT=35;

%% Drug parameters
%DRUG EEFFECT
 Imax= 1;
 IC50=3;
```

Model Parameters (PD_parameters.m)

```
%% initial conditions
HR0= 80;
SV0=70;
TPR0= 0.015;
MAP0=HR0*SV0*TPR0;
SP_MAP0=MAP0;
A0 = [0 0 SV0 HR0 TPR0 0 0];
```

Model ODE with PRA(PD_ODEs_PRA.m)

```
%% model ode's drug effect with PRA included
function dAdt = PD_ODEs(t, A, K0, K10,  K20, V, Imax, IC50,
 SP_MAP0, SV0,HR0, TPR0, KOUT,k)



% Stop the infusion after 1 hour
if t>=0.5
   K0=0;
end
```

```
%% Specify drug effect
CP = A(2)/V;
I1 = (Imax*CP)/(IC50+CP);
%% Set point
SP_MAP = SP_MAP0;
SV=A(3)*(1-0.212*log(A(4)/HR0));
MAP = A(5)*A(4)*SV;
DELTA = (SP_MAP-MAP)/SP_MAP; %change in MAP relative to MAP set
 point
%% ODEs matrix
dAdt(1) = K0  - K10*A(1);                              %d(SNP)/dt
dAdt(2) = K10*A(1) - K20*A(2);                         %d(NO)/dt
dAdt(3)=KOUT* SV0*(1 + A(6)) -  KOUT*A(3);            %d(SV)/dt
dAdt(4)= KOUT*HR0*(1 + A(6)) - KOUT*A(4);              %d(HR)/dt
dAdt(5)=KOUT*TPR0*(1-I1)*(1 + A(6))*(1+3*A(7)) - KOUT*A(5);
 %d(TPR)/dt
dAdt(6)=KOUT*DELTA*(1-I1) - KOUT*A(6);                 %d(BR)/dt
dAdt(7)=k*(DELTA-A(7));                                %d(PRA)/dt
dAdt=[dAdt(1);dAdt(2);dAdt(3);dAdt(4);dAdt(5);dAdt(6);dAdt(7)];
end
%%
```

Model ODE w/out PRA(PD_ODEs_noPRA.m)

```
%% model ode's drug effect
function dAdt = PD_ODEs(t, A, K0, K10,  K20, V, Imax, IC50,
 SP_MAP0, SV0,HR0, TPR0, KOUT,k)

% Stop the infusion after 1 hour
if t>=0.5
   K0=0;
end
%% Specify drug effect
CP = A(2)/V;
I1 = (Imax*CP)/(IC50+CP); %drug effect on DELTA BAROREFLEX
```

```
%% Set point
SP_MAP = SP_MAP0;
SV=A(3)*(1-0.212*log(A(4)/HR0));
MAP = A(5)*A(4)*SV;
DELTA = (SP_MAP-MAP)/SP_MAP; %change in MAP relative to MAP set
 point
%% ODEs matrix
dAdt(1) = K0  - K10*A(1);                          %d(SNP)/dt
dAdt(2) = K10*A(1) - K20*A(2);                      %d(NO)/dt
dAdt(3)=KOUT* SV0*(1 + A(6)) -  KOUT*A(3);          %d(SV)/dt
dAdt(4)= KOUT*HR0*(1 + A(6)) - KOUT*A(4);          %d(HR)/dt
dAdt(5)=KOUT*TPR0*(1-I1)*(1 + A(6))*(1+3*A(7)) - KOUT*A(5);
 %d(TPR)/dt
dAdt(6)=KOUT*DELTA*(1-I1) - KOUT*A(6);             %d(BR)/dt
dAdt(7)=0;                                         %d(PRA/dt
dAdt=[dAdt(1);dAdt(2);dAdt(3);dAdt(4);dAdt(5);dAdt(6);dAdt(7)];
end
%%
```

Save output (VEC.m)

```
%% Define variables from algebric equations as vectors
SNP=A(:,1)/V;
CP=A(:,2)/V;
EDRUG = (Imax*CP)./(IC50+CP);

SV=A(:,3).*(1-0.212*log(A(:,4)./HR0));
MAP = A(:,5).*A(:,4).*SV ;
HR=A(:,4);
PRA=A(:,7);
TPR=A(:,5);
```

Get plots (overlaidPlot.m)

```
figure (1);

subplot(3, 2,1)
```

```
hold on
plot(output_PRA.Time,output_PRA.SNP,'Color','black','LineWidth'
 ,1.5)
plot(output_noPRA.Time, output_noPRA.SNP,'--'
 ,'Color','black','LineWidth',1.5)
ylabel('SNP (ug/L)')
set(gca,'FontSize',9,'FontWeight','bold','xtick',[])

subplot(3, 2,2)
hold on
plot(output_PRA.Time,output_PRA.MAP,'Color','black','LineWidth'
 ,1.5)
plot(output_noPRA.Time, output_noPRA.MAP,'--
 ','Color','black','LineWidth',1.5)
ylabel('MAP (mmHg)')
set(gca,'FontSize',9,'FontWeight','bold','xtick',[])

subplot(3, 2,3);
hold on
plot(output_PRA.Time,
 output_PRA.HR,'Color','black','LineWidth',1.5)
plot(output_noPRA.Time, output_noPRA.HR,'--
 ','Color','black','LineWidth',1.5)
ylabel('HR(beat/min)')
set(gca,'FontSize',9,'FontWeight','bold','xtick',[])

subplot(3, 2,4);
hold on
plot(output_PRA.Time,
 output_PRA.TPR,'Color','black','LineWidth',1.5)
plot(output_noPRA.Time, output_noPRA.TPR,'--
 ','Color','black','LineWidth',1.5)
ylabel('TPR(mmHg.min/ml)')
set(gca,'FontSize',9,'FontWeight','bold','xtick',[])
```

```
subplot(3, 2,5);
hold on
plot(output_PRA.Time,output_PRA.SV,'Color','black','LineWidth',
 1.5)
plot(output_noPRA.Time, output_noPRA.SV,'--
 ','Color','black','LineWidth',1.5)
ylabel('SV(ml/beat)')
xlabel('Time (h)')
set(gca,'FontSize',9,'FontWeight','bold')

subplot(3, 2,6);
hold on
plot(output_PRA.Time,output_PRA.PRA,'Color','black','LineWidth'
 ,1.5)
plot(output_noPRA.Time, output_noPRA.PRA,'--
 ','Color','black','LineWidth',1.5)
xlabel('Time (h)')
ylabel('PRA')
ylim([-0.05 0.15])
set(gca,'FontSize',9,'FontWeight','bold')
```

A.2.2 NONMEM code for SNP model estimation

```
;; 1. Based on: run15
;; 2. Description: run15 Mixture model no bsv

;; x1. Author: Salma Bahnasawy

$PROBLEM ePKPD
$INPUT
ID
DAT1=DROP
TIME
PHAS ; PHASE OF STUDY 1 = PRE-OPERATIVE, 2 = BLINDED TREATMENT PHASE, 3 = OPEN LABEL
TREATMENT, 4 = FOLLOW UP
DPHASE=DROP
GTX ; RANDOMIZED TREATMENT GROUP MCG/MIN/KG
TBD ;Time before infusion
TAD
DOSE=DROP ; MCG LOCF
AMT ; MCG
DURN ; INFUSION DURATION MINUTES
RATE ; MCG/H
RINF; Infusion rate at time
DV ; HR MAP PP SBP DBP
DVID ; DV TYPE 0=DOSE, 1=HR, 2=MAP, 3=PP, 4=SBP,5=DBP
DVT=DROP
CMT
MDV
TARGETMA
SEX ; 1=MALE; 2=FEMALE
AGE
AGED=DROP
```

```
WT ; WEIGHT KG

RACE ; RACE 1 = AMERICAN INDIAN OR ALASKAN NATIVE, 2 = ASIAN, 3 = BLACK OR AFRICAN
AMERICAN, 4 = NATIVE HAWAIIAN OR PACIFIC ISLANDER, 5 = WHITE OR CAUCASIAN, 6 = OTHER

ETHN; ETHNICITY 1= HISPANIC; 2 = NON HISPANIC

L2

$DATA Full_rR.csv

IGNORE=#

IGNORE (PHAS.NE.2)

IGNORE (AGE.LT.13)

IGNORE (DVID.GT.2)

IGNORE (ID.EQ.156)

$SUBROUTINE ADVAN13 TOL=6

$MODEL

COMP(INF, DEFDOSE)

COMP(NO, DEFOBS)

COMP(SV)

COMP(HR)

COMP(TPR)

COMP(FB)

COMP(PRA)

$MIX

NSPOP=2

P(1)=THETA(14)

P(2)=1-THETA(14)

$PK

; simple pk model of NP

K10= THETA(1) ;elimination rate const of SNP

K20= THETA(2) ;elimination rate const of NO

V= THETA(3)

; PD model

SV0= THETA(4)
```

```
HR0= THETA(5)*EXP(ETA(1))
MAP0= THETA(6)*EXP(ETA(2))
KOUT=THETA(7)
Imax= THETA(8)
IC50= THETA(9)*EXP(ETA(5))
kpra=THETA(10)

IF (MIXNUM.EQ.1) THEN
FPRA=THETA(11);*EXP(ETA(6))
END IF

IF (MIXNUM.EQ.2) THEN
FPRA=THETA(12);*EXP(ETA(7))
ENDIF
BET=THETA(13)

; specify initial conditions
TPR0=MAP0/(SV0*HR0)
A_0(1)= 0
A_0(2)= 0
A_0(3)= SV0
A_0(4)= HR0
A_0(5)= TPR0
A_0(6)= 0
A_0(7)= 0


$DES
; Specify drug effect model
CP=A(2)/V
I1 = (Imax*CP)/(IC50+CP)
```

```
; set points & MAP;
SV=A(3)*(1-BET*LOG(A(4)/HR0))
MAP = A(5)*A(4)*SV
MAP_SP=MAP0
DELTA = (MAP-MAP_SP)/MAP_SP                    ;change in blood pressure

; specify ODEs of differnet cmt
DADT(1)= -K10*A(1)                                          ;SNP
DADT(2)= K10*A(1) - K20*A(2)                                ;NO
DADT(3)= KOUT*SV0*(1 - A(6)) -  KOUT*A(3)                   ;SV
DADT(4)= KOUT*HR0*(1 - A(6)) - KOUT*A(4)                    ;HR
DADT(5)= KOUT*TPR0*(1-I1)*(1-A(6))*(1-FPRA*A(7)) - KOUT*A(5)  ;TPR
DADT(6)= KOUT*DELTA*(1-I1)- KOUT*A(6)                       ;delta BR
DADT(7)= kpra*(DELTA-A(7))                                  ;Delta PRA

$ERROR
C1=A(1)/V
C2=A(2)/V
SV2=A(3)*(1-BET*LOG(A(4)/HR0))
HR=A(4)
TPR=A(5)
BR=A(6)
PRA=A(7)
IMAP= SV2*HR*TPR

IF (DVID.EQ.1) THEN
IPRED=IMAP
Y=IPRED+EPS(1)*EXP(ETA(3))
ENDIF
IF (DVID.EQ.2) THEN
IPRED=HR
```

```
Y=IPRED+EPS(2)*EXP(ETA(4))
ENDIF

$THETA
(0.001, 20.8) FIX ;K10= THETA(1)
(0.001, 1250) FIX ;K20= THETA(2)
(1) FIX ;V= THETA(3)
(70) FIX ;SV0= THETA(4)
(60, 85,140) ;HR0= THETA(5)
(50, 80,120) ;MAP0= THETA(6)
(0.001, 25) FIX ;KOUT=THETA(8)
(0.01,1) FIX  ;Imax= THETA(9)
(0.001, 3) ;C50= THETA(10)
(0.001, 1.5) FIX ;kpra
( 0.01)FIX ;FPRA1
(0.0001, 5) ;FPRA2
(0, 0.212,1) FIX ;BETA
(0,0.5,1);P
$OMEGA BLOCK(2)
 0.04  ;PPVHR
 0.01 0.01  ;PPVMAP

$OMEGA BLOCK(2)
 0.1  ;PPVRUVMAP
 0.01 0.2 ;PPVRUVHR
$OMEGA
0.1 ;PPVC50
;0.1 ;PPVFPRA
;0.1 ;PPVFPRA2
$SIGMA BLOCK(2)
 89.5 ;ADDMAP
```

5 55.6 ;ADDPHR

$EST MAXEVALS=9999 NSIG=3 NOABORT PRINT=0 METHOD=COND INTER MSFO=msfo16.msf

$COV

$TABLE ID PHAS TIME MDV CMT RINF MAP_SP DV DVID PRED IPRED SV2 PRA HR RES TARGETMA CWRES NOAPPEND ONEHEADER NOPRINT FILE=sdtab16

$TABLE ID ETA(1) ETA(2) TIME ETHN RACE NOAPPEND ONEHEADER NOPRINT FILE=patab16

$TABLE ID WT AGE NOAPPEND ONEHEADER NOPRINT FILE=cotab16

$TABLE ID ETHN RACE NOAPPEND ONEHEADER NOPRINT FILE=catab16

Model	Refer	Description	OFV	ΔOFV	θ_{k10}	θ_{k20}	θ_V	θ_{SV0}	θ_{HR0}	θ_{MAP0}	θ_{kout}	θ_{Imax}	θ_{c50}	θ_{k_PRA}	θ_β	θ_{FPRA}	θ_{FPRA2}	θ_{Mix_prop}
run0		Combined mechanism; MAXEVAL=	16750.02		20.8	1250	1	70	80	78	25	0.5	4	1.5	0.21	2		
run1	run0	run1;MAXEVAL=9999, relax MAP0;	15287.47	-1462	20.8	1250	1	70	83.7	73.5	25	0.5	4	1.5	0.21	2		
run2	run1	run1; BSV on RUV	14757.64	-531	20.8	1250	1	70	83.5	73.3	25	0.5	4	1.5	0.21	2		
run3	run2	run2; relax Imax	14693.21	-65.4	20.8	1250	1	70	82.6	75.5	25	0.79	4	1.5	0.21	2		
run4	run2	run2; relax c50	14656.08	-103	20.8	1250	1	70	81.5	77.4	25	0.5	0.86	1.5	0.21	2		
run5	run2	run2; relax fpra	14728.72	-28.3	20.8	1250	1	70	82.9	73.7	25	0.5	4	1.5	0.21	0.02		
run6	run4	run2; relax Imax	14647.06	-9.02	20.8	1250	1	70	81.4	77.8	25	0.58	1.16	1.5	0.21	2		
run7	run4	run2; relax fpra	14645.21	-10.9	20.8	1250	1	70	81.3	78.5	25	0.5	0.89	1.5	0.21	0.5		
run8	run7	run2; relax Imax	14537.48	-108	20.8	1250	1	70	79.6	78	25	0.54	1.04	1.5	0.21	0.91		
run9	run8	run8; BSV on Imax	14431.88	-106	20.8	1250	1	70	81.1	79.5	25	0.6	1.05	1.5	0.21	0.01		
run10	run8	run8; BSV on C50	14400.41	-137	20.8	1250	1	70	80.8	78.8	25	0.8	2.67	1.5	0.21	0.08		
run11	run8	run8; BSV FPRA	14483.77	-53.7	20.8	1250	1	70	81	78.9	25	0.55	0.85	1.5	0.21	0.6		
run12	run10	run10 BSV on FPRA	14372.46	-28	20.8	1250	1	70	81.2	79.3	25	0.94	2.78	1.5	0.21	1		
run13	run12	run12 L2 data item considered	14364.74	-7.7	20.8	1250	1	70	80.8	79.1	25	0.97	2.97	1.5	0.21	1.02		
run14	run13	run13 FIX Imax	14364.86	0.12	20.8	1250	1	70	81.4	79.3	25	1	3.12	1.5	0.21	1		
run15	run14	run14 Mixture model for F_{PRA}	14346.28	-18.6	20.8	1250	1	70	80.4	78.9	25	1	2.96	1.5	0.21	0.01	10.2	0.687
run16	run15	run15 Mixture model fix θ_{FPRA}	14345.89	-0.39	20.8	1250	1	70	81.4	79.1	25	1	2.99	1.5	0.21	0.01	10.7	0.692
run17	run14	run16 Mixture model with BSV on	14346.6	0.71	20.8	1250	1	70	80.1	78.4	25	1	3.08	1.5	0.21	0.01	10.6	0.692

Model	ω_{HR0} [η_{shk}]	ω_{MAP0} [η_{shk}]	cov_{HR0_MAP0}	ω_{RUVMAP} [η_{shk}]	ω_{RUVHR} [η_{shk}]	cov_{RUV} (corr%)	ωc_{50} [η_{shk}]	ω_{logit} [η_{shk}]	ω_{F_PRA} [η_{shk}]	ω_{F_PRA2} [η_{shk}]	σ_{addMAP} [ε_{shk}]	σ_{addHR} [ε_{shk}]	cov_σ (corr%)
run0	0.05	0.02	0.01								60	30	
run1	0.0477[1%]	0.013[6%]	0.01(44%)								126[3%]	85.7[3%]	
run2	0.0475[0%]	0.0223[4%]	0.01(42%)	0.125[2%]	0.244[2%]	0.172(100%)					98.6[0%]	56.2[3%]	
run3	0.048[0%]	0.0169[3%]	0.0112(39%)	0.122[2%]	0.233[2%]	0.172(100%)					92.7[1%]	54.5[0%]	
run4	0.0475[0%]	0.0163[4%]	0.0123(44%)	0.131[2%]	0.23[2%]	0.174(100%)					92.1[1%]	55.7[0%]	
run5	0.0485[0%]	0.0141[4%]	0.0108(41%)	0.124[2%]	0.239[2%]	0.172(100%)					96.8[0%]	55.7[0%]	
run6	0.0474[0%]	0.0178[3%]	0.0122(42%)	0.122[2%]	0.225[2%]	0.172(100%)					89.1[0%]	54.7[0%]	
run7	0.0474[0%]	0.0174[3%]	0.0122(42%)	0.128[2%]	0.221[2%]	0.171(100%)					89.5[0%]	55.6[0%]	
run8	0.0496[2%]	0.0178[3%]	0.0174(43%)	0.174[7%]	0.28[4%]	0.125(57%)					76.9[0%]	49.4[0%]	
run9	0.0472[0%]	0.0214[3%]	0.0142(45%)	0.184[5%]	0.298[3%]	0.129(55%)		2.65[23%]			64.5[1%]	49.1[0%]	
run10	0.0475[0%]	0.0193[3%]	0.0126(42%)	0.203[5%]	0.29[3%]	0.14(58%)	1.43[12%]				61.7[1%]	49[0%]	
run11	0.047[0%]	0.0198[5%]	0.0129(42%)	0.181[5%]	0.303[3%]	0.152(65%)				7.27[39%%]	74.9[0%]	49[0%]	
run12	0.0474[0%]	0.02[0%]	0.0136(44%)	0.185[4%]	0.298[3%]	0.136(58%)	1.04[11%]		3.69[38%]		58.4[1%]	48.5[0%]	
run13	0.0474[0%]	0.02[0%]	0.0136(44%)	0.186[5%]	0.291[3%]	0.136(58%)	0.984[9%]		3.63[37%]		58.6[1%]	48.1[1%]	5.02(9.6%)
run14	0.0473[0%]	0.0201[0%]	0.0136(44%)	0.185[5%]	0.291[3%]	0.136(58%)	0.97[8%]		3.66[36%]		58.4[1%]	48.1[1%]	5.05(9.7%)
run15	0.0484[3%]	0.0195[5%]	0.0128(42%)	0.2[8%]	0.289[4%]	0.135[56%]	0.996[12%]				58.6[1%]	47.4[1%]	5.32(10.2%)
run16	0.0482[4%]	0.0194[5%]	0.0132(43%)	0.201[8%]	0.289[4%]	0.135[56%]	1[12%]				58.7[1%]	47.4[1%]	5.35(10.3%)
run17	0.0492[4%]	0.0194[5%]	0.0132 (43%	0.203[8%]	0.289[4%]	0.135[56%]	1.01[12%]		0.277[100%]	0.00252[100%	58[1%]	46.7[1%]	5.4(10.4)

Fixed estimate

Selected model run

A.2.3 Individual plots of the final model

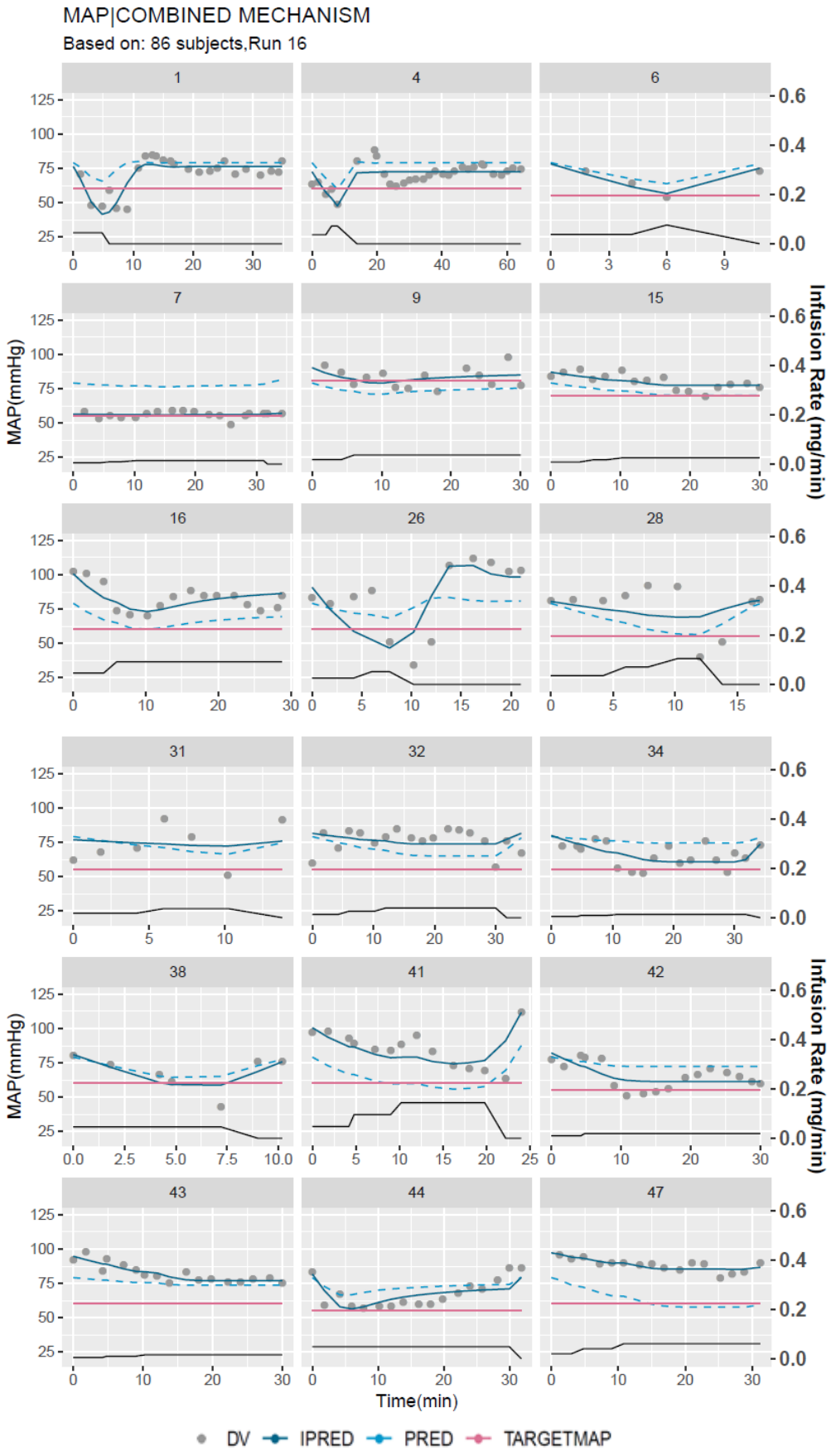

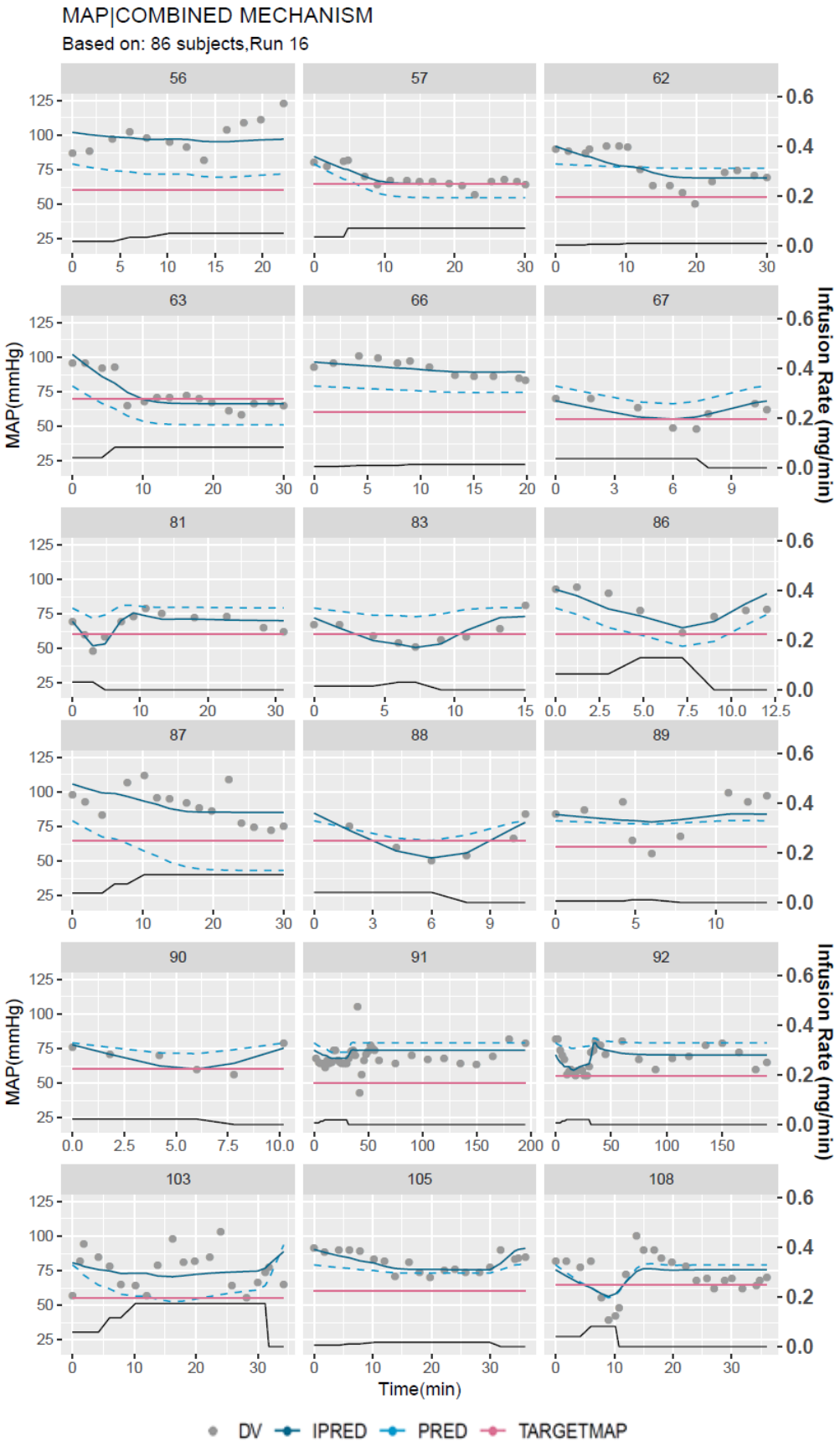
MAP|COMBINED MECHANISM
Based on: 86 subjects,Run 16
56
57
62
63
66
67
81
83
86
87
88
89
90
91
92
103
105
108
MAP(mmHg)
Infusion Rate (mg/min)
Time(min)
DV
IPRED
PRED
TARGETMAP

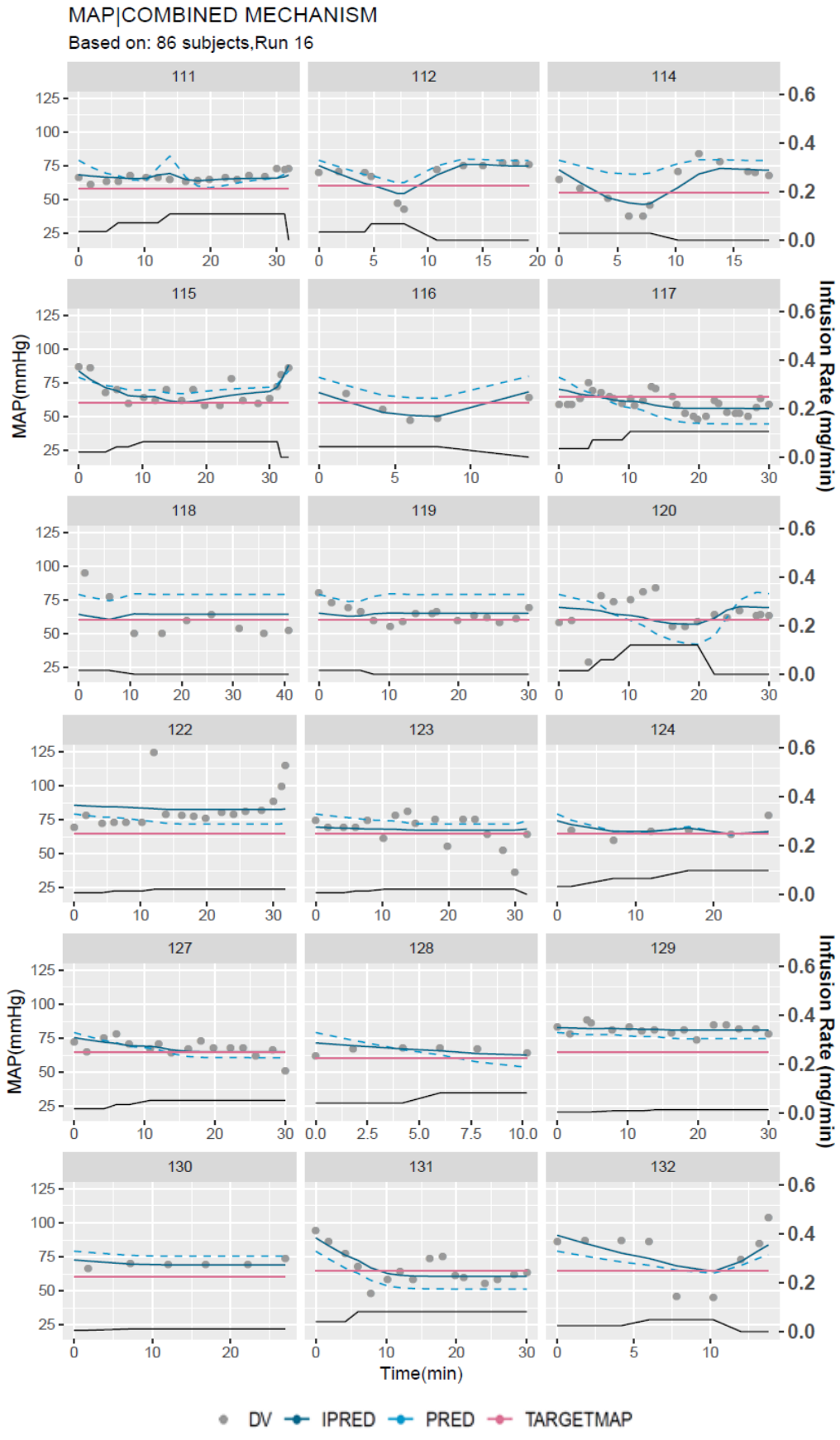
MAP|COMBINED MECHANISM
Based on: 86 subjects,Run 16
111
112
114
115
116
117
118
119
120
122
123
124
127
128
129
130
131
132
MAP(mmHg)
Infusion Rate (mg/min)
Time(min)
DV
IPRED
PRED
TARGETMAP

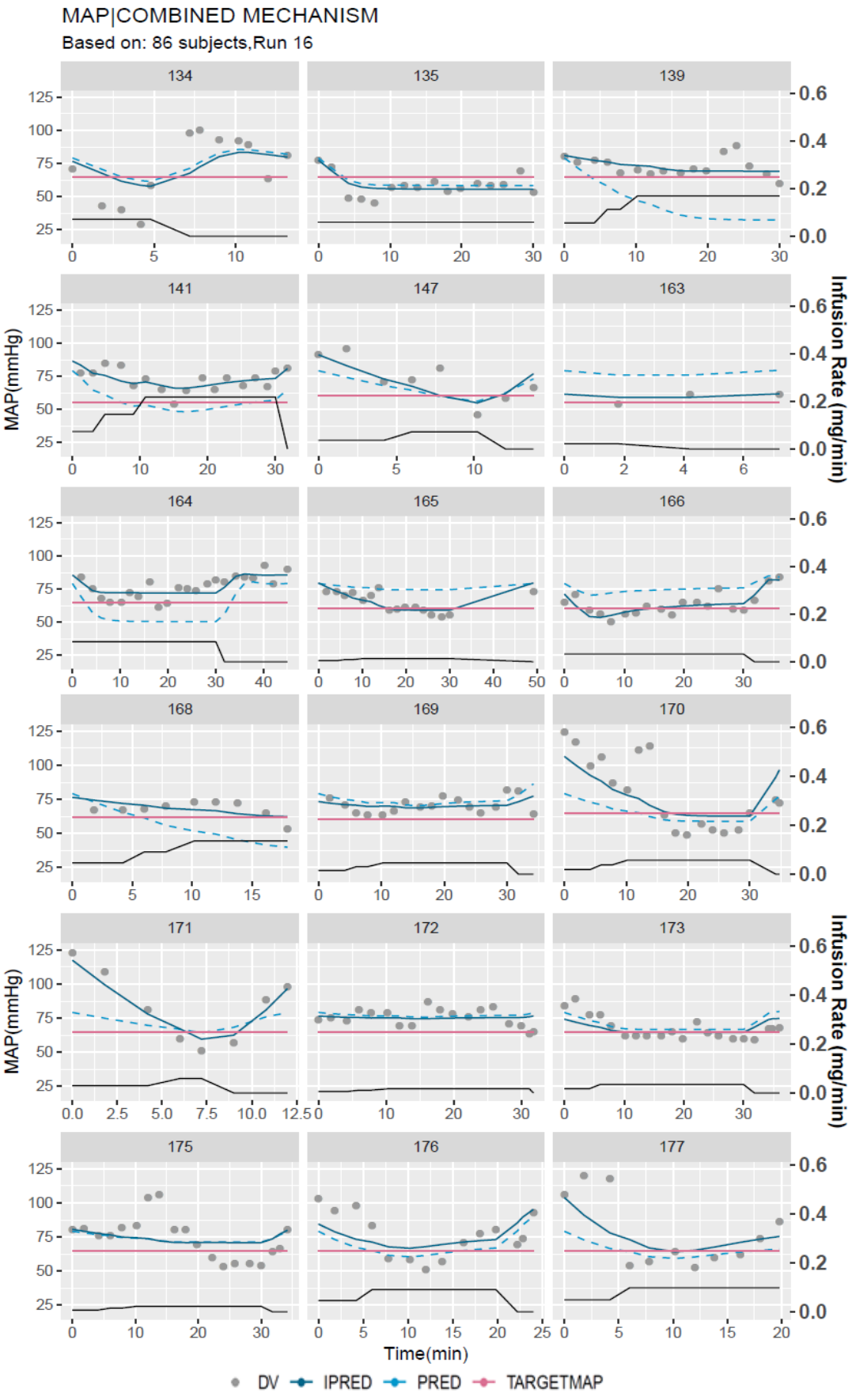
MAP|COMBINED MECHANISM
Based on: 86 subjects,Run 16
134
135
139
141
147
163
164
165
166
168
169
170
171
172
173
175
176
177
MAP(mmHg)
Infusion Rate (mg/min)
Time(min)
DV
IPRED
PRED
TARGETMAP

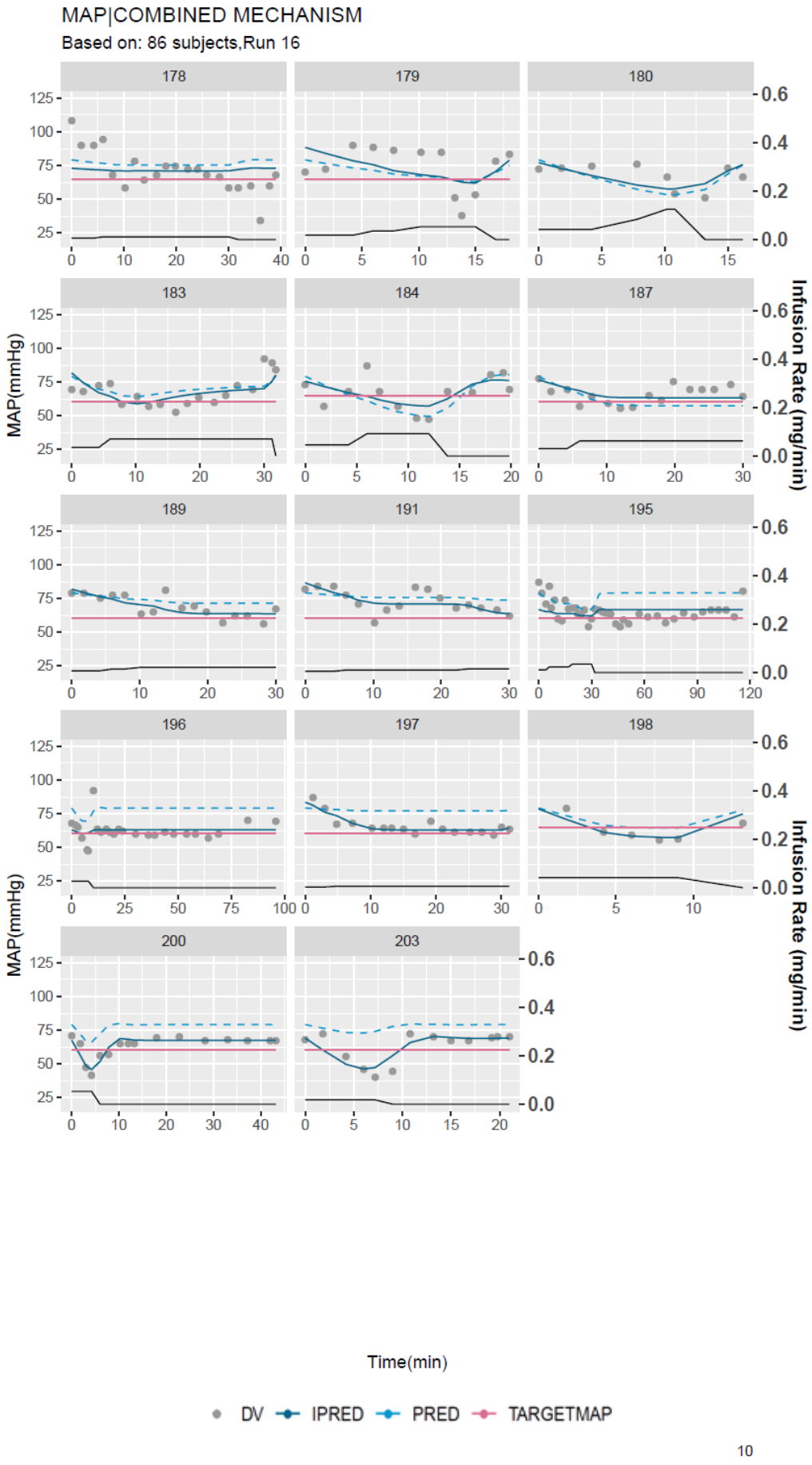
MAP|COMBINED MECHANISM
Based on: 86 subjects,Run 16
178
179
180
183
184
187
189
191
195
196
197
198
200
203
MAP(mmHg)
Infusion Rate (mg/min)
Time(min)
DV
IPRED
PRED
TARGETMAP

10

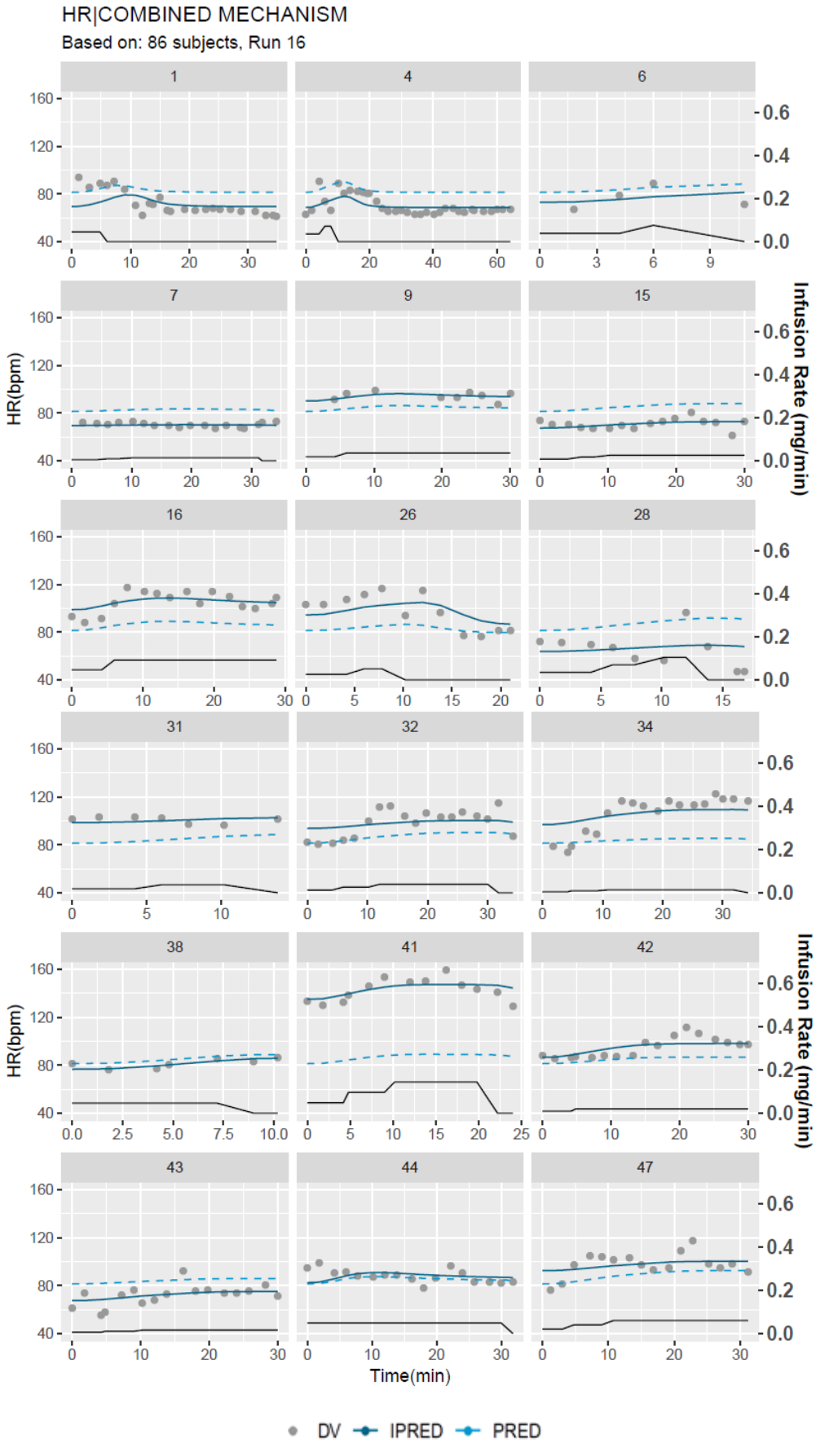
HR|COMBINED MECHANISM
Based on: 86 subjects, Run 16
1
4
6
7
9
15
16
26
28
31
32
34
38
41
42
43
44
47
HR(bpm)
Infusion Rate (mg/min)
Time(min)
DV
IPRED
PRED
2

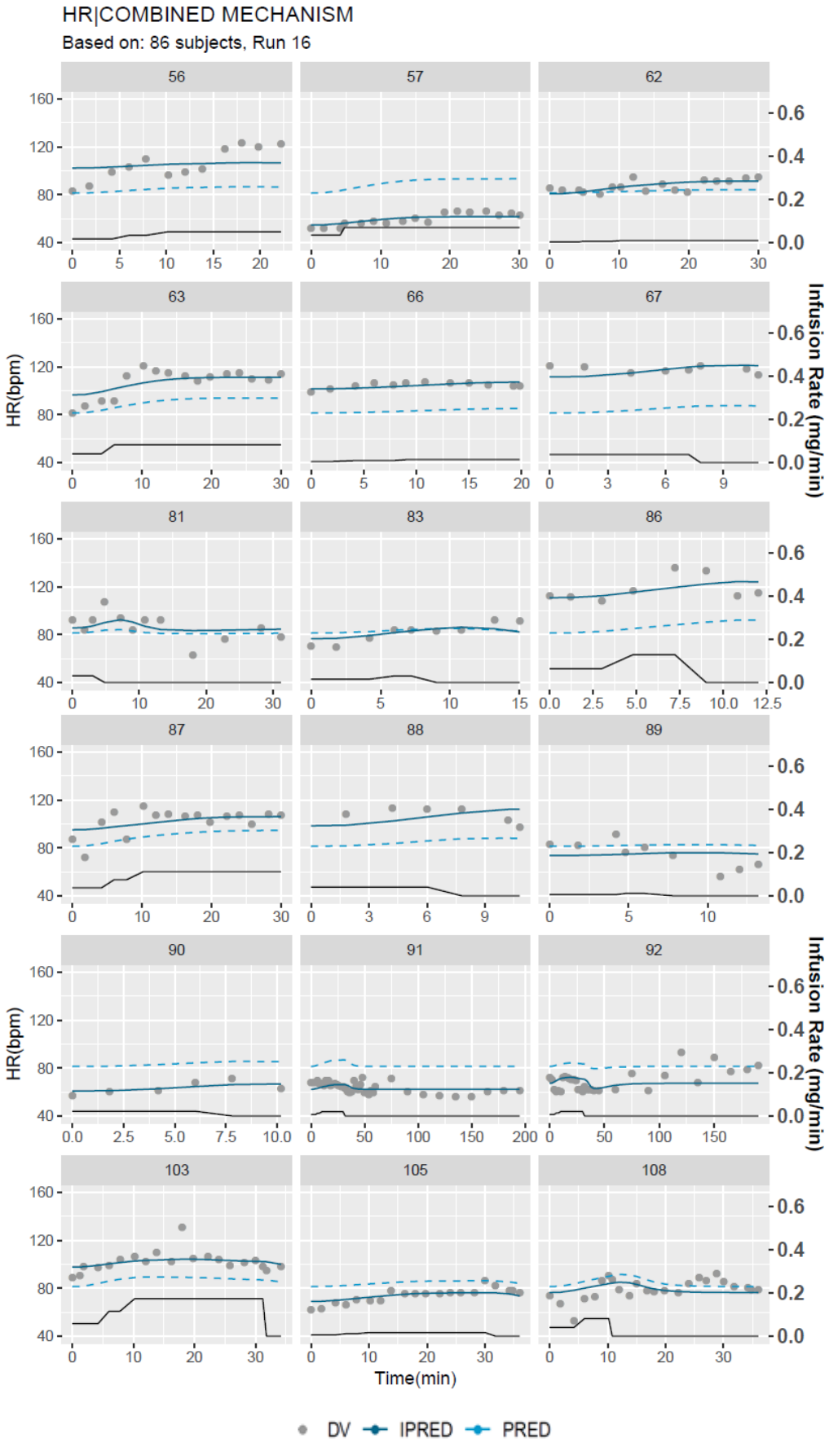
HR|COMBINED MECHANISM
Based on: 86 subjects, Run 16
56
57
62
63
66
67
81
83
86
87
88
89
90
91
92
103
105
108
HR(bpm)
Infusion Rate (mg/min)
Time(min)
DV
IPRED
PRED
4

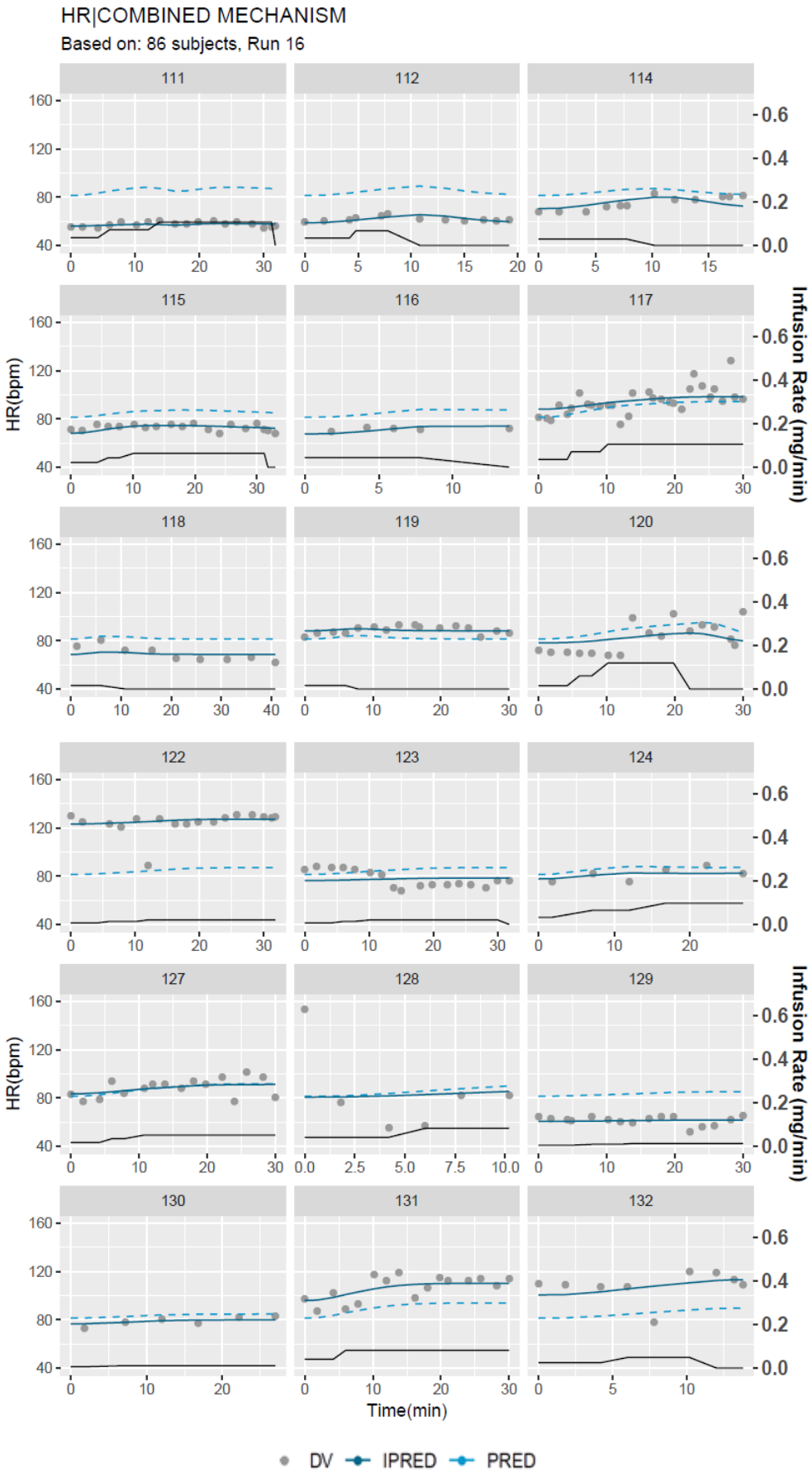
HR|COMBINED MECHANISM
Based on: 86 subjects, Run 16
111
112
114
115
116
117
118
119
120
122
123
124
127
128
129
130
131
132
HR(bpm)
Infusion Rate (mg/min)
Time(min)
DV
IPRED
PRED
6

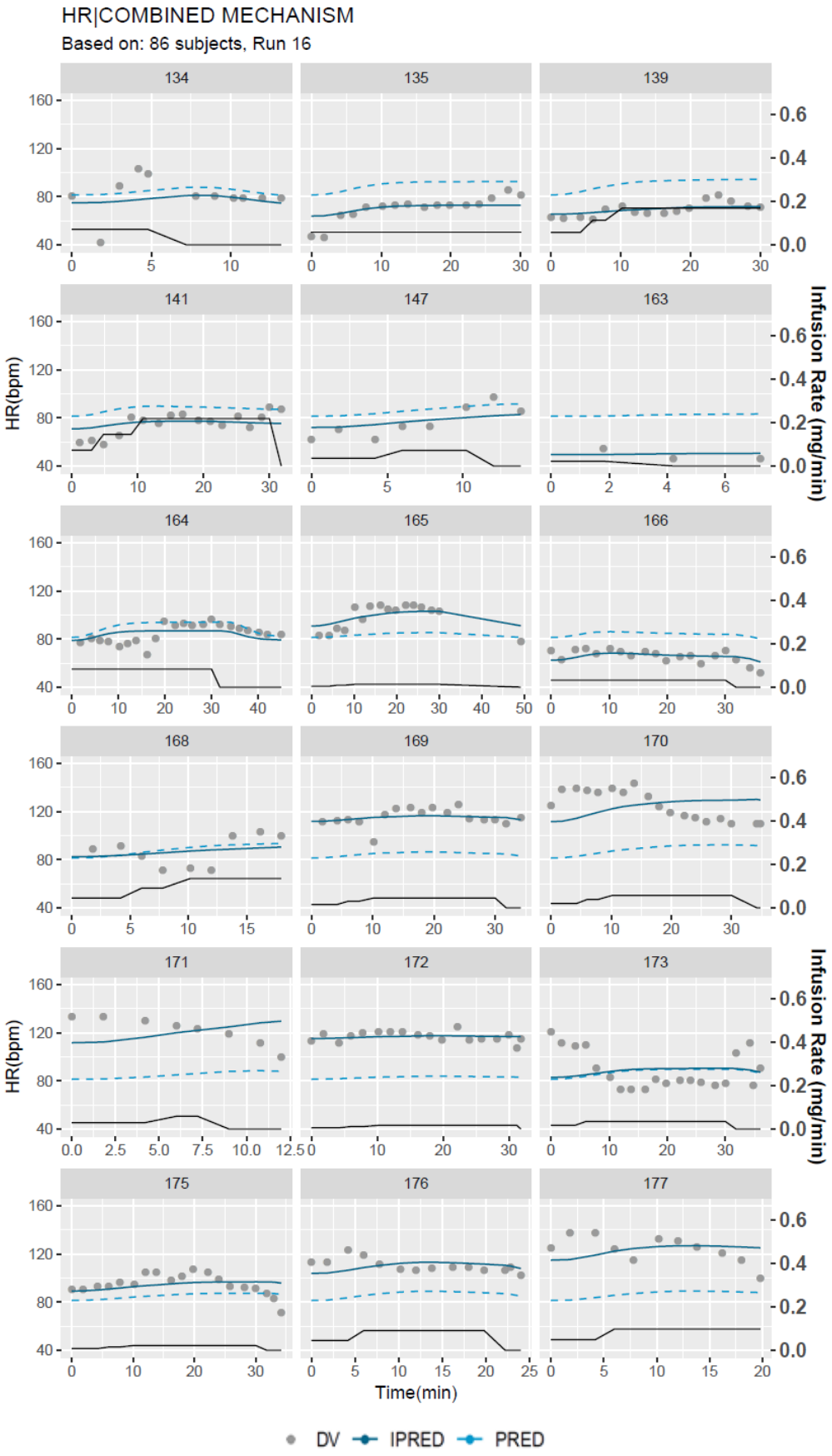
HR|COMBINED MECHANISM
Based on: 86 subjects, Run 16
134
135
139
141
147
163
164
165
166
168
169
170
171
172
173
175
176
177
HR(bpm)
Infusion Rate (mg/min)
Time(min)
DV
IPRED
PRED

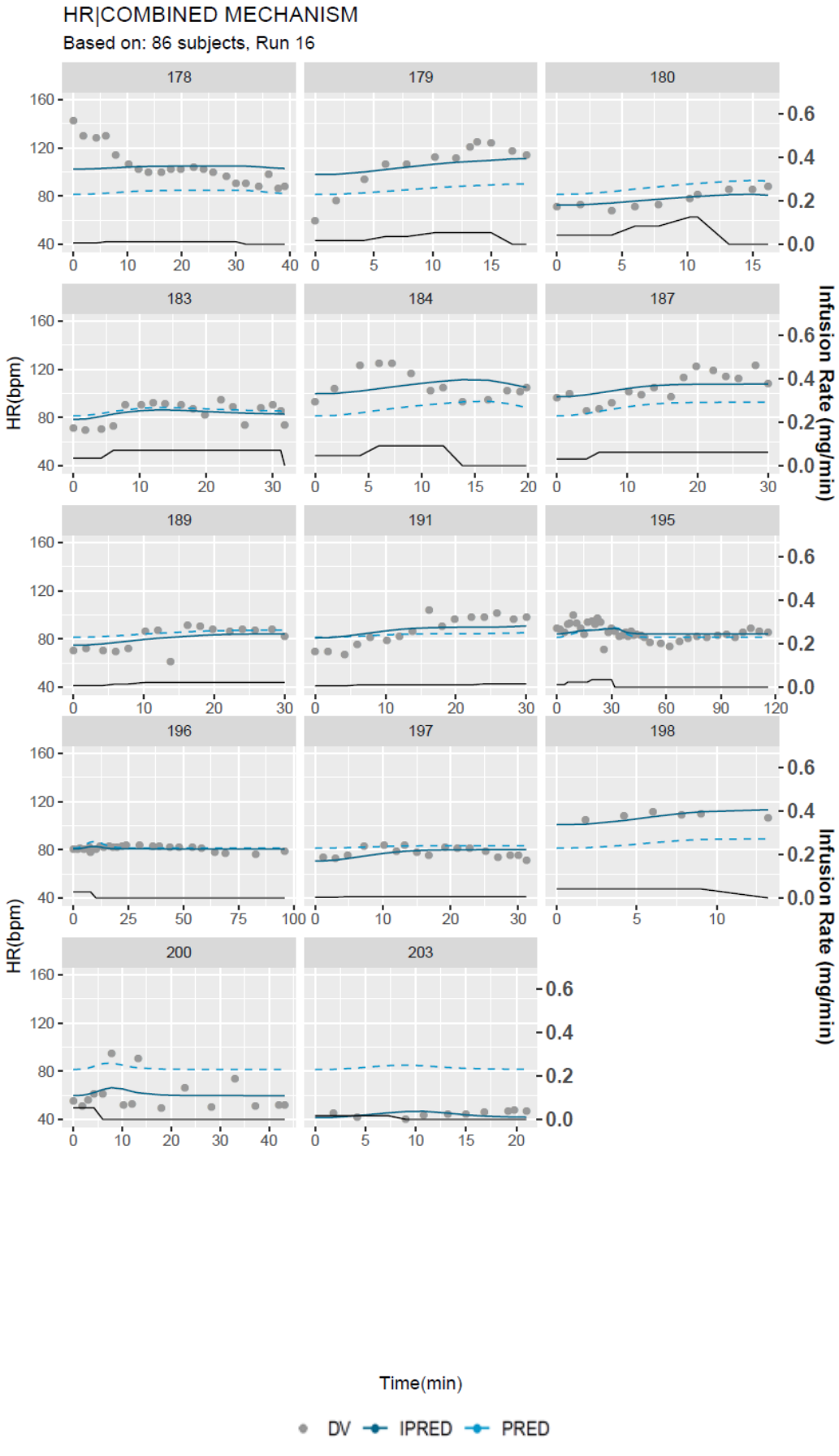
HR|COMBINED MECHANISM
Based on: 86 subjects, Run 16
178
179
180
183
184
187
189
191
195
196
197
198
200
203
HR(bpm)
Infusion Rate (mg/min)
Time(min)
DV
IPRED
PRED

A.2.4 pcVPC of final SNP model

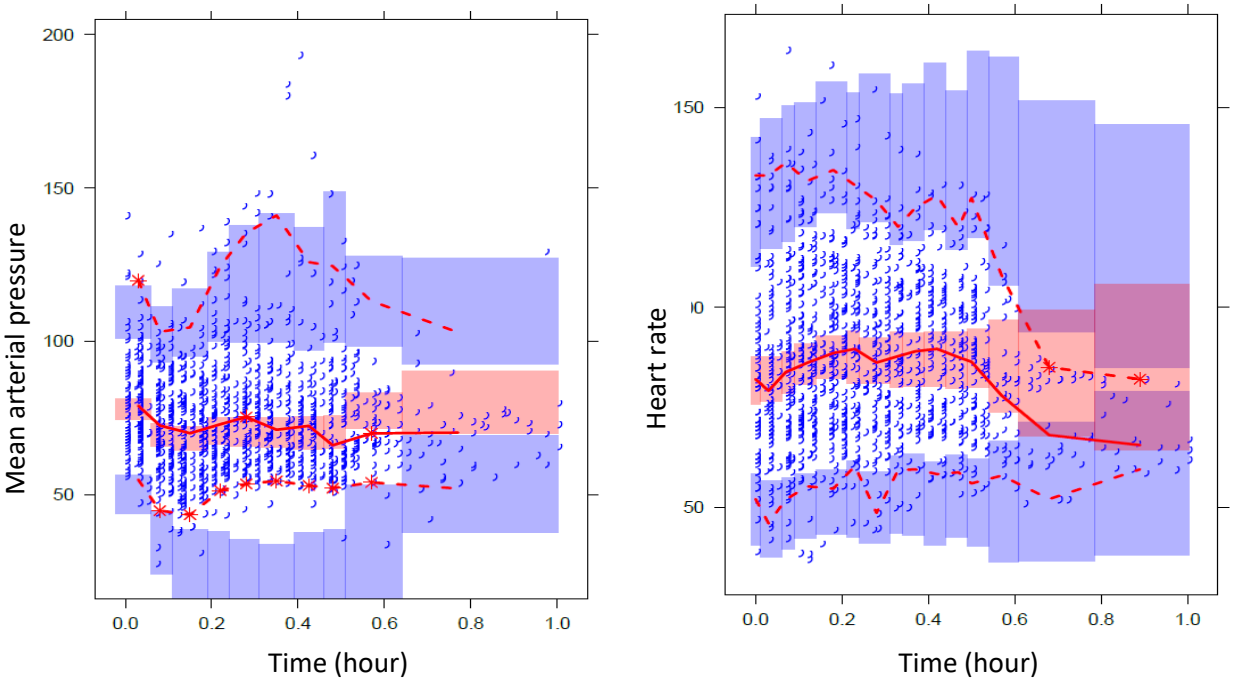

REFERENCES

ABUKHRES, M. M., ERTEL, R. J., DIXIT, B. N. & VOLLMER, R. R. 1979. Role of the Renin-Angiotensin System in the Blood-Pressure Rebound to Sodium-Nitroprusside in the Conscious Rat. *European Journal of Pharmacology,* 58**,** 247-254.

ADELMANN, G. A. 2011. Cardiology essentials in clinical practice. New York: Springer.

AMARANATH, L. & KELLERMEYER, W. F. 1976. Tachyphylaxis to Sodium Nitroprusside. *Anesthesiology,* 44**,** 345-347.

ARMSTRONG M, M. R. *Physiology, Baroreceptors [Updated 2019 Feb 20]. In:StatPearls [Internet].* Treasure Island (FL): StatPearls Publishing; 2020 Jan-.

BARRETT, J. S., HIRANKARN, S., HOLFORD, N., HAMMER, G. B., DROVER, D. R., COHANE, C., ANDERSON, B., DOMBROWSKI, E., REECE, T., ZAJICEK, A. & SCHULMAN, S. R. 2015. A hemodynamic model to guide blood pressure control during deliberate hypotension with sodium nitroprusside in children. *Frontiers in Pharmacology,* 6.

BENGTSSON, C., JOHNSSON, G. & REGARDH, C. G. 1975. Plasma levels and effects of metoprolol on blood pressure and heart rate in hypertensive patients after an acute dose and between two doses during long-term treatment. *Clinical Pharmacology & Therapeutics,* 17**,** 400-8.

BERGSTRAND, M., HOOKER, A. C., WALLIN, J. E. & KARLSSON, M. O. 2011. Prediction-corrected visual predictive checks for diagnosing nonlinear mixed-effects models. *AAPS J,* 13**,** 143-51.

BIGHAMIAN, R. & HAHN, J. O. 2014. Relationship between Stroke Volume and Pulse Pressure during Blood Volume Perturbation: A Mathematical Analysis. *Biomed Research International*.

BOX, G. E. P. & DRAPER, N. R. 1987. *Empirical model-building and response surfaces,* New York, Wiley.

BRAUNWALD, E., LIBBY, P. & MD CONSULT LLC. 2011. Braunwald's heart disease a textbook of cardiovascular medicine. *MD consult - reference books.* 9th ed. Philadelphia

St. Louis: Saunders ;

MD Consult LLC.

BUSH, E. N. & VOLLMER, R. R. 1984. Contribution of Beta-Adrenergic-Receptor Mediated Renin Release to the Maintenance of Blood-Pressure during Nitroprusside Infusion in Conscious Rats. *Clinical and Experimental Hypertension Part a-Theory and Practice,* 6**,** 2161-2172.

CARUSO, A., FRANCES, N., MEILLE, C., GREITER-WILKE, A., HILLEBRECHT, A. & LAVE, T. 2014. Translational PK/PD modeling for cardiovascular safety assessment of drug candidates: Methods and examples in drug development. *J Pharmacol Toxicol Methods,* 70**,** 73-85.

CHAE, D., SON, M., KIM, Y., SON, H. & PARK, K. 2018. Mechanistic Model for Blood Pressure and Heart Rate Changes Produced by Telmisartan in Human Beings. *Basic & Clinical Pharmacology & Toxicology,* 122**,** 139-148.

CHENG, H. M. & JUSOF, F. 2018. *Defining Physiology: Principles, Themes, Concepts : Cardiovascular, Respiratory and Renal Physiology,* Singapore, Springer Singapore Springer.

CHEUNG, S. Y. A., MAJID, O., YATES, J. W. T. & AARONS, L. 2012. Structural identifiability analysis and reparameterisation (parameter reduction) of a cardiovascular feedback model. *European Journal of Pharmaceutical Sciences,* 46**,** 259-271.

COLEMAN, T. G. & HALL, J. E. 1992. A mathematical model of renal hemodynamics and excretory function. *Structuring Biological Systems: A Computer Modelling Approach***,** 89-124.

COLLINS, T. A., BERGENHOLM, L., ABDULLA, T., YATES, J. W. T., EVANS, N., CHAPPELL, M. J. & METTETAL, J. T. 2015. Modeling and Simulation Approaches for Cardiovascular Function and Their Role in Safety Assessment. *Cpt-Pharmacometrics & Systems Pharmacology,* 4**,** 175-188.

COSTANZO, L. S. 2018. *Physiology*.

COTTRELL, J. E., ILLNER, P., KITTAY, M. J., STEELE, J. M., JR., LOWENSTEIN, J. & TURNDORF, H. 1980. Rebound hypertension

after sodium nitroprusside-induced hypotension. *Clin Pharmacol Ther,* 27**,** 32-6.

COTTRELL, J. E., PATEL, K., CASTHELY, P., KLEIN, A. & TURNDORF, H. 1978. Nitroprusside Tachyphylaxis without Acidosis. *Anesthesiology,* 49**,** 141-142.

DE SIMONE, G., DEVEREUX, R. B., DANIELS, S. R., MUREDDU, G., ROMAN, M. J., KIMBALL, T. R., GRECO, R., WITT, S. & CONTALDO, F. 1997. Stroke volume and cardiac output in normotensive children and adults. Assessment of relations with body size and impact of overweight. *Circulation,* 95**,** 1837-43.

DEABREU, G. R. & SALGADO, H. C. 1990. Antihypertensive Drugs Distinctly Modulate the Rapid Resetting of the Baroreceptors. *Hypertension,* 15**,** I63-I67.

DEGOUTE, C. S. 2007. Controlled hypotension: a guide to drug choice. *Drugs,* 67**,** 1053-76.

DELANEY, T. J. & MILLER, E. D., JR. 1980. Rebound hypertensive after sodium nitroprusside prevented by saralasin in rats. *Anesthesiology,* 52**,** 154-6.

DEWEY, F. E., ROSENTHAL, D., MURPHY, D. J., JR., FROELICHER, V. F. & ASHLEY, E. A. 2008. Does size matter? Clinical applications of scaling cardiac size and function for body size. *Circulation,* 117**,** 2279-87.

DIPIRO, J. T. 2011. *Pharmacotherapy: a pathophysiologic approach,* New York, McGraw-Hill Medical.

DORWARD, P. K., ANDRESEN, M. C., BURKE, S. L., OLIVER, J. R. & KORNER, P. I. 1982. Rapid Resetting of the Aortic Baroreceptors in the Rabbit and Its Implications for Short-Term and Longer Term Reflex Control. *Circulation Research,* 50**,** 428-439.

DROVER, D. R., HAMMER, G. B., BARRETT, J. S., COHANE, C. A., REECE, T., ZAJICEK, A. & SCHULMAN, S. R. 2015. Evaluation of sodium nitroprusside for controlled hypotension in children during surgery. *Frontiers in Pharmacology,* 6.

ETTE, E. E. I. & WILLIAMS, E. P. J. 2007. *Pharmacometrics: The Science of Quantitative Pharmacology*, John Wiley & Sons.

FLYNN, J. T. & FALKNER, B. E. 2017. New Clinical Practice Guideline for the Management of High Blood Pressure in Children and Adolescents. *Hypertension,* 70**,** 683-686.

FLYNN, J. T., KAELBER, D. C., BAKER-SMITH, C. M., BLOWEY, D., CARROLL, A. E., DANIELS, S. R., DE FERRANTI, S. D., DIONNE, J. M., FALKNER, B., FLINN, S. K., GIDDING, S. S., GOODWIN, C., LEU, M. G., POWERS, M. E., REA, C., SAMUELS, J., SIMASEK, M., THAKER, V. V., URBINA, E. M., SUBCOMMITTEE ON, S. & MANAGEMENT OF HIGH BLOOD PRESSURE IN, C. 2017. Clinical Practice Guideline for Screening and Management of High Blood Pressure in Children and Adolescents. *Pediatrics,* 140.

FOOD AND DRUG ADMINISTRATION, H. 2014. Pediatric Studies of Sodium Nitroprusside Conducted in Accordance With the Public Health Service Act; Availability of Summary Report and Requested Labeling Changes. *Federal Register Volume 79, Issue 16 (January 24, 2014).* Federal Register.

FRANCHETEAU, P., STEIMER, J. L., MERDJAN, H., GUERRET, M. & DUBRAY, C. 1993. A Mathematical-Model for Dynamics of Cardiovascular Drug-Action - Application to Intravenous Dihydropyridines in Healthy-Volunteers. *Journal of Pharmacokinetics and Biopharmaceutics,* 21**,** 489-514.

FRANKLIN, S. S. & WONG, N. D. 2016. Pulse Pressure How Valuable as a Diagnostic and Therapeutic Tool? *Journal of the American College of Cardiology,* 67**,** 404-406.

FRITSCH, J. M., REA, R. F. & ECKBERG, D. L. 1989. Carotid baroreflex resetting during drug-induced arterial pressure changes in humans. *Am J Physiol,* 256**,** R549-53.

GILLUM, R. F., PRINEAS, R. J. & HORIBE, H. 1982. Maturation vs age: assessing blood pressure by height. *J Natl Med Assoc,* 74**,** 43-6.

GUYTON, A. C. 1990. Long-Term Arterial-Pressure Control - an Analysis from Animal-Experiments and Computer and Graphic Models. *American Journal of Physiology,* 259**,** R865-R877.

GUYTON, A. C., GRANGER, H. J. & COLEMAN, T. G. 1972. Circulation - Overall Regulation. *Annual Review of Physiology,* 34**,** 13-+.

HAKIM, T. S., SUGIMORI, K., CAMPORESI, E. M. & ANDERSON, G. 1996. Half-life of nitric oxide in aqueous solutions with and without haemoglobin. *Physiological Measurement,* 17**,** 267-277.

HALLOW, K. M. & GEBREMICHAEL, Y. 2017. A Quantitative Systems Physiology Model of Renal Function and Blood Pressure Regulation: Model Description. *Cpt-Pharmacometrics & Systems Pharmacology,* 6**,** 383-392.

HALLOW, K. M., LO, A., BEH, J., RODRIGO, M., ERMAKOV, S., FRIEDMAN, S., DE LEON, H., SARKAR, A., XIONG, Y., SARANGAPANI, R., SCHMIDT, H., WEBB, R. & KONDIC, A. G. 2014. A model-based approach to investigating the pathophysiological mechanisms of hypertension and response to antihypertensive therapies: extending the Guyton model. *American Journal of Physiology-Regulatory Integrative and Comparative Physiology,* 306**,** R647-R662.

HAMMER, G. B., LEWANDOWSKI, A., DROVER, D. R., ROSEN, D. A., COHANE, C., ANAND, R., MITCHELL, J., REECE, T. & SCHULMAN, S. R. 2015. Safety and efficacy of sodium nitroprusside during prolonged infusion in pediatric patients. *Pediatr Crit Care Med,* 16**,** 397-403.

HEUSER, D., MCDOWALL, D. G. & HEMPEL, V. 1985. *Controlled hypotension in neuroanaesthesia,* New York, Plenum Press.

HILL, L. K., SOLLERS III, J. J. & THAYER, J. F. 2013. Resistance reconstructed estimation of total peripheral resistance from computationally derived cardiac output - biomed 2013. *Biomed Sci Instrum,* 49**,** 216-23.

HOCHT, C., BERTERA, F. M., DEL MAURO, J. S. & TAIRA, C. A. 2014. Models for evaluating the pharmacokinetics and pharmacodynamics for beta-blockers. *Expert Opinion on Drug Metabolism & Toxicology,* 10**,** 525-541.

HOTTINGER, D. G., BEEBE, D. S., KOZHIMANNIL, T., PRIELIPP, R. C. & BELANI, K. G. 2014. Sodium nitroprusside in 2014: A clinical concepts review. *J Anaesthesiol Clin Pharmacol,* 30**,** 462-71.

IVANKOVICH, A. D., MILETICH, D. J. & TINKER, J. H. 1978. Sodium nitroprusside: metabolism and general considerations. *Int Anesthesiol Clin,* 16**,** 1-29.

KARAASLAN, F., DENIZHAN, Y., KAYSERILIOGLU, A. & GULCUR, H. O. 2005. Long-term mathematical model involving renal sympathetic nerve activity, arterial pressure, and sodium excretion. *Annals of Biomedical Engineering,* 33**,** 1607-1630.

KHAMBATTA, H. J., STONE, J. G. & KHAN, E. 1979. Hypertension during Anesthesia on Discontinuation of Sodium Nitroprusside-Induced Hypotension. *Anesthesiology,* 51**,** 127-130.

KLABUNDE, R. E. 2012. *Cardiovascular physiology concepts,* Philadelphia, PA, Lippincott Williams & Wilkins/Wolters Kluwer.

KLOFT, C., TRAME, M. N. & RITTER, C. A. 2016. Systems pharmacology in drug development and therapeutic use - A forthcoming paradigm shift. *European Journal of Pharmaceutical Sciences,* 94**,** 1-3.

LAGERKRANSER, M., SOLLEVI, A., IRESTEDT, L., TIDGREN, B. & ANDREEN, M. 1985. Renin Release during Controlled Hypotension with Sodium-Nitroprusside, Nitroglycerin and Adenosine - a Comparative-Study in the Dog. *Acta Anaesthesiologica Scandinavica,* 29**,** 45-49.

LEVICK, J. R. 2009. An Introduction to Cardiovascular Physiology. 5th ed. London: Hodder Education.

LEVICK, J. R. 2013. Introduction to Cardiovascular Physiology. Oxford: Elsevier Science.

MA, J., WANG, Z., DONG, B., SONG, Y., HU, P. & ZHANG, B. 2012. Quantifying the relationships of blood pressure with weight, height and body mass index in Chinese children and adolescents. *J Paediatr Child Health,* 48**,** 413-8.

MAGER, D. E., KIMKO, H. H. C., SINHA, V., HUANG, S.-M., ABERNETHY, D. R., WANG, Y., ZHAO, P., ZINEH, I., RAMANUJAN, S., GADKAR, K., KADAMBI, A., BIRTWISTLE, M. R., HANSEN, J., GALLO, J. M., MUPPIRISETTY, S., UNG, P. M.-U., IYENGAR, R., SCHLESSINGER, A., STEINWAY, S. N., WANG, R.-S., ALBERT, R. E., BOUHADDOU, M., KHOO, M. C. K., HU, W.-H., CHALACHEVA, P., JUSKO, W. J.,

KRZYZANSKI, W., RUSSU, A., POGGESI, I., ZHANG, Y., D'ARGENIO, D. Z., BONATE, P. L., DESAI, A., RIZWAN, A., LU, Z., TANNENBAUM, S., KNIGHTS, J., RAMANATHAN, M., GEERTS, H., ROBERTS, P., SPIROS, A., CARR, R., SCHEFF, J. D., KAMISOGLU, K., ANDROULAKIS, I. P., KARIYA, Y., HONMA, M., SUZUKI, H., RAO, G. G., LY, N. S., TSUJI, B. T., BULITTA, J. U. B., FORREST, A., HASELTINE, E. L., KIROUAC, D. C., BOSLEY, J. R., MAURER, T. S., MUSANTE, C. J., SPRINGER (FIRM) & AMERICAN ASSOCIATION OF PHARMACEUTICAL SCIENTISTS *Systems pharmacology and pharmacodynamics*.

MATLAB 2017. MATLAB version 9.2.0.538062 (R2017a). Natick, Massachusetts: The MathWorks Inc.

MILLER, E. D., JR., ACKERLY, J. A., VAUGHAN, E. D., JR., PEACH, M. J. & EPSTEIN, R. M. 1977. The renin-angiotensin system during controlled hypotension with sodium nitroprusside. *Anesthesiology,* 47**,** 257-62.

MOHRMAN, D. E. & HELLER, L. J. 2014. *Cardiovascular physiology,* New York, McGraw-Hill Education Medical.

MONTANI, J. P., ADAI, T. H. & VAN VLIET, B. N. 2009. The Contribution of Guyton's Large Circulatory Model to Our Understanding of Long-Term Arterial Pressure Control. *Journal of Physiological Sciences,* 59**,** 132-132.

MORACA, P. P., BITTE, E. M., HALE, D. E., WASMUTH, C. E. & POUTASSE, E. F. 1962. Clinical evaluation of sodium nitroprusside as a hypotensive agent. *Anesthesiology,* 23**,** 193-9.

MORAN, D., Y, E., G, K., A, L., J, S. & Y, S. 1995. Calculation of mean arterial pressure during exercise as a function of heart rate. *Applied human science : journal of physiological anthropology,* 14**,** 293-295.

MOULD, D., R, U., EMAIL MOULD, D., PRI-HOME, D. & NET 2012. Basic concepts in population modeling, simulation, and model-based drug development. *CPT: Pharmacometrics and Systems Pharmacology,* 1**,** no pagination.

MOULD, D., R, U., EMAIL MOULD, D., PRI-HOME, D. & NET 2013. Basic concepts in population modeling, simulation, and model-based

drug development - Part 2: Introduction to pharmacokinetic modeling methods. *CPT: Pharmacometrics and Systems Pharmacology,* 2**,** no pagination.

PAGE, I. H., CORCORAN, A. C., DUSTAN, H. P. & KOPPANYI, T. 1955. Cardiovascular actions of sodium nitroprusside in animals and hypertensive patients. *Circulation,* 11**,** 188-98.

PEDERSEN, O. L. & MIKKELSEN, E. 1978. Acute and Chronic Effects of Nifedipine in Arterial-Hypertension. *European Journal of Clinical Pharmacology,* 14**,** 375-381.

PETERSON, M. C. & RIGGS, M. M. 2015. FDA Advisory Meeting Clinical Pharmacology Review Utilizes a Quantitative Systems Pharmacology (QSP) Model: A Watershed Moment? *Cpt-Pharmacometrics & Systems Pharmacology,* 4**,** 189-192.

PLAYFAIR, L. On the nitroprussides, a new class of salts. Abstracts of the Papers Communicated to the Royal Society of London, 1851. The Royal Society London, 846-847.

RAJ, T. D. 2017. *Data Interpretation in Anesthesia : a Clinical Guide,* Cham, Springer International Publishing Imprint : Springer.

RAVEN, P. B. & CHAPLEAU, M. W. 2014. Blood pressure regulation XI: overview and future research directions. *European Journal of Applied Physiology,* 114**,** 579-586.

RAZMINIA, M., TRIVEDI, A., MOLNAR, J., ELBZOUR, M., GUERRERO, M., SALEM, Y., AHMED, A., KHOSLA, S. & LUBELL, D. L. 2004. Validation of a new formula for mean arterial pressure calculation: The new formula is superior to the standard formula. *Catheterization and Cardiovascular Interventions,* 63**,** 419-425.

RIBBA, B., GRIMM, H. P., AGORAM, B., DAVIES, M. R., GADKAR, K., NIEDERER, S., VAN RIEL, N., TIMMIS, J. & VAN DER GRAAF, P. H. 2017. Methodologies for Quantitative Systems Pharmacology (QSP) Models: Design and Estimation. *Cpt-Pharmacometrics & Systems Pharmacology,* 6**,** 496-498.

ROHATGI, A. *WebPlotDigitizer* [Online]. San Francisco, California, USA. Available: https://automeris.io/WebPlotDigitizer [Accessed April, 2019].

SALGADO, H. C. & KRIEGER, E. M. 1988. Extent of Baroreceptor Resetting in Response to Sodium-Nitroprusside and Verapamil. *Hypertension,* 11**,** 121-125.

SCHADT, J. C. & LUDBROOK, J. 1991. Hemodynamic and Neurohumoral Responses to Acute Hypovolemia in Conscious Mammals. *American Journal of Physiology,* 260**,** H305-H318.

SECOMB, T. W. 2016. Hemodynamics. *Comprehensive Physiology,* 6**,** 975-1003.

SELVARAJ, S., STEG, P. G., ELBEZ, Y., SORBETS, E., FELDMAN, L. J., EAGLE, K. A., OHMAN, E. M., BLACHER, J., BHATT, D. L. & INVESTIGATORS, R. R. 2016. Pulse Pressure and Risk for Cardiovascular Events in Patients With Atherothrombosis From the REACH Registry. *Journal of the American College of Cardiology,* 67**,** 392-403.

SHERWOOD, L. 2015. *Human physiology : from cells to systems,* Australia, Brooks/Cole.

SHIVVA, V., KORELL, J., TUCKER, I. G. & DUFFULL, S. B. 2013. An approach for identifiability of population pharmacokinetic-pharmacodynamic models. *CPT Pharmacometrics Syst Pharmacol,* 2**,** e49.

SIMMONDS, M., J, D., P, C., EMAIL CONNES, P., YAHOO, P. & FR 2014. Nitric oxide, vasodilation and the red blood cell. *Biorheology,* 51**,** 121-134.

SNELDER, N., PLOEGER, B. A., LUTTRINGER, O., RIGEL, D. F., FU, F., BEIL, M., STANSKI, D. R. & DANHOF, M. 2014. Drug effects on the CVS in conscious rats: separating cardiac output into heart rate and stroke volume using PKPD modelling. *Br J Pharmacol,* 171**,** 5076-92.

SNELDER, N., PLOEGER, B. A., LUTTRINGER, O., RIGEL, D. F., WEBB, R. L., FELDMAN, D., FU, F., BEIL, M., JIN, L., STANSKI, D. R. & DANHOF, M. 2013. PKPD modelling of the interrelationship between mean arterial BP, cardiac output and total peripheral resistance in conscious rats. *British Journal of Pharmacology,* 169**,** 1510-1524.

SOLTESZ, K. 2018. Robust computation of pulse pressure variations. *Biomedical Signal Processing and Control,* 39**,** 197-203.

SPARKS, H. V. & ROOKE, T. W. 1987. *Essentials of cardiovascular physiology,* Minneapolis, University of Minnesota Press.

SPIELBERG, D. R., BARRETT, J. S., HAMMER, G. B., DROVER, D. R., REECE, T., COHANE, C. A. & SCHULMAN, S. R. 2014. Predictors of Arterial Blood Pressure Control During Deliberate Hypotension with Sodium Nitroprusside in Children. *Anesthesia and Analgesia,* 119**,** 867-874.

STANFIELD, C. L. 2013. *Principles of human physiology,* Boston, Pearson Education.

SVED, A. F. 2009. Blood Pressure: Baroreceptors. *In:* SQUIRE, L. R. (ed.) *Encyclopedia of Neuroscience.* Oxford: Academic Press.

TARAZI, R. C., SAFAR, M. & FOUAD-TARAZI, F. 1989. *The Heart in hypertension : a tribute to Robert Tarazi (1925-1986),* Dordrecht ; Boston

Norwell, MA, U.S.A., Kluwer Academic ;

Sold and distributed in the U.S.A. and Canada by Kluwer Academic.

THE FOOD AND DRUG ADMINISTRATION (FDA). 2017a. *HIGHLIGHTS OF PRESCRIBING INFORMATION* [Online]. Available: https://www.accessdata.fda.gov/drugsatfda_docs/label/2017/209387s000lbl.pdf [Accessed].

THE FOOD AND DRUG ADMINISTRATION (FDA). 2017b. *Pediatric Focused Safety Review: Sodium Nitroprusside (Nitropress)* [Online]. Available: https://www.fda.gov/media/103569/download [Accessed].

TINKER, J. H. & MICHENFELDER, J. D. 1976. Sodium nitroprusside: pharmacology, toxicology and therapeutics. *Anesthesiology,* 45**,** 340-54.

TOBIAS, J. D. 2002. Controlled hypotension in children: a critical review of available agents. *Paediatr Drugs,* 4**,** 439-53.

TYLUTKI, Z., POLAK, S. & WISNIOWSKA, B. 2016. Top-down, Bottom-up and Middle-out Strategies for Drug Cardiac Safety Assessment via Modeling and Simulations. *Curr Pharmacol Rep,* 2**,** 171-177.

UPTON, R. & D, M. 2014. Basic concepts in population modeling, simulation, and model-based drug development: Part 3-introduction to pharmacodynamic modeling methods. *CPT: Pharmacometrics and Systems Pharmacology,* 3**,** no pagination.

VENKATASUBRAMANIAN R , TERESA A. COLLINS , LAWRENCE J. LESKO , JAY T. METTETAL & TRAME, M. N. 2016. Development of a Mechanism Based Platform to Predict Cardiac Contractility and Hemodynamics in Conscious Dogs. *PAGE meeting*.

VILLAVERDE, A. F., BARREIRO, A. & PAPACHRISTODOULOU, A. 2016. Structural Identifiability of Dynamic Systems Biology Models. *Plos Computational Biology,* 12.

VINCENT, J. L. 2008. Understanding cardiac output. *Critical Care,* 12.

WALKER HK, HALL WD & JW, H. 1990. Clinical Methods: The History, Physical, and Laboratory Examinations. Butterworths.

WIDMAIER, E. P., VANDER, A. J., RAFF, H. & STRANG, K. T. 2019. *Vander's human physiology : the mechanisms of body function,* New York, NY, McGraw-Hill Education.

ZHANG, W. G. & WANG, Z. Y. 2001. Resetting baroreceptors to a lower arterial pressure level by enalapril avoids baroreflex mediated activation of sympathetic nervous system by nifedipine. *Life Sciences,* 68**,** 2769-2779.